

**ULTRASONOGRAPHIC EVALUATION OF THE HEPATOBILIARY SYSTEM
AND THE PANCREAS OF NIGERIAN INDIGENOUS DOGS**

BY

ABDULLAHI ALIYU

(P14VTSR8009)

DEPARTMENT OF VETERINARY SURGERY AND RADIOLOGY,

FACULTY OF VETERINARY MEDICINE

AHMADU BELLO UNIVERSITY,

ZARIA, NIGERIA

JULY, 2018

**ULTRASONOGRAPHIC EVALUATION OF THE HEPATOBILIARY SYSTEM
AND THE PANCREAS OF NIGERIAN INDIGENOUS DOGS**

BY

Abdullahi ALIYU DVM (ABU) 2010

(P14VTSR8009)

**A DISSERTATION SUBMITTED TO THE SCHOOL OF POSTGRADUATE
STUDIES, AHMADU BELLO UNIVERSITY, ZARIA IN PARTIAL
FULFILLMENT OF THE REQUIREMENTS FOR THE AWARD OF MASTER OF
SCIENCE IN VETERINARY DIAGNOSTIC IMAGING**

DEPARTMENT OF VETERINARY SURGERY AND RADIOLOGY,

AHMADU BELLO UNIVERSITY,

ZARIA, NIGERIA

JULY, 2018

Declaration

I declare that the work in this dissertation entitled “**Ultrasonographic Evaluation of the Hepatobiliary System and the Pancreas of Nigerian Indigenous dogs**” has been performed by me in the Department of Veterinary Surgery and Radiology, Ahmadu Bello University, Zaria, under the supervision of Prof. C.A. Awasum and Dr. J.B Igashi. The information derived from the literature has been duly acknowledged in the text and a list of references provided. No part of this dissertation was previously presented for another degree or diploma at this or any other Institution.

ABDULLAHI ALIYU

Name of Student

Signature

Date

Certification

This dissertation entitled “**ULTRASONOGRAPHIC EVALUATION OF THE HEPATOBILIARY SYSTEM AND THE PANCREAS OF NIGERIAN INDIGENOUS DOGS**” by **Abdullahi ALIYU**, meets the regulations governing the award of the degree of Masters of Science of Ahmadu Bello University, Zaria and is approved for its contribution to knowledge and literary presentation.

Prof. C. A. Awasum	_____	_____
Chairman Supervisory committee	Signature	Date
Dr. J.B. Igashi	_____	_____
Member, Supervisory committee	Signature	Date
Dr. S. T. Fadason	_____	_____
Head of Department	Signature	Date
Prof. S.Z. Abubakar	_____	_____
Dean, School of Postgraduate Studies, A.B.U. Zaria	Signature	Date

Dedication

This work is dedicated to the Almighty Allah and my parents for giving me the strength, health and Knowledge to get to this stage of my academic pursuit.

Acknowledgments

The process of earning an M.sc in Veterinary Diagnostic Imaging through series of research and writing of thesis is very tasking and certainly not done single handedly. First and foremost, I would like to thank Almighty Allah for giving me health, wisdom, knowledge, patience and strength to get to this stage of my academic pursuit.

My gratitude goes to Dr. S. T. Fadason (Head of Department), Department of Veterinary Surgery and Radiology, May the Almighty Lord be with you as you steer the ship to the Promised Land. Also to the director of Distance Learning Prof. A. Z. Hassan, may Almighty Allah bless you and your family.

A special appreciation is due to my supervisor; Prof. C.A. Awasum of the Department of Surgery and Radiology for his guidance, commitments and patience in supervising this work and the time taken to make necessary corrections. I would also like to express my sincere appreciation to Dr. J. B. Igashi (Consultant) from the Radiology unit of the Ahmadu Bello University Teaching Hospital Shika for his technical support, guidance and suggestions in the course of supervising this work in spite of his tight schedule.

My gratitude also goes to Dr. Maruf Lawal of the Department of Veterinary Surgery and Radiology Ahmadu Bello University Zaria for his priceless support and encouragement in the course of this research work. I wish to express my appreciation to all the staff of the department of Veterinary Surgery and Radiology, Ahmadu Bello University Zaria, Dr. E. O. Abidoeye, Drs B. Usman, G. E. Ochube, A. Andrew, S. Tanko, A. A. Bada, M. N. Bappah, M. A. Sani to count but few including Mrs. W. Ajibade, Mr S. A. Obed, Mr. I. Abdullahi, Mr. J. O. Momodu and Mr H. Yau. I thank all of them for all their contributions towards my successful stay in the faculty for my studies. And to all my fellow Post Graduate students, Drs Obalowu, D. O. Avazi, L. O. Oladimeji, O. Bojuwoye, O. Iskiil to count but few you are all dear to me and am very grateful to have a wonderful stay with you.

Special gratitude goes to my parents; Alh. J. Aliyu and Haj. Ladi Aliyu for their moral, spiritual and emotional support throughout my academic pursuit and also to my brothers and sisters; Kamal, Kabir, Amina and Aisha for their love and encouragement all through this vigorous moments.

A special appreciation is also due to my former Head of Department (Veterinary Surgery and Radiology University of Ilorin) Prof. J. B. Adeyanju; the present HOD Dr. F.M. Lawal; and other members of staff of the Department of Veterinary Surgery and Radiology University of Ilorin for their support, understanding and encouragement in the course of this research work.

I honestly consider myself to be blessed based on the fact that I'm been surrounded in my entire life by family and friends who have never failed to love, support and encourage me to live up to my potentials in order to achieve my dream. My prayer to Almighty Allah is to give me the will to pass these kind gestures to others as I continue my journey through life.

Abstract

This study was carried out to establish the normal ultrasonographic parameters for the hepatobiliary system and the pancreas of Nigerian Indigenous puppies and their correlation with the demographic data (age, sex, body weight (WT), length (BL), height (HT), mass index (BMI)). Six (6) clinically healthy Nigerian Indigenous puppies (from the same bitch) were obtained at eight (8) weeks of age from the owner at Hayin dogo, Samaru, Zaria. B-mode Sonoster ultrasound scanner was used to scan the hepatobiliary system and the pancreas at 2 week intervals to evaluate their echotexture and dimensions. Three millilitres (3mls) of blood samples were collected for serum at two months interval. The serum was assayed for alanine aminotransferase (ALT), aspartate aminotransferase (AST) and alkaline phosphatase (ALP) to ensure that the liver is apparently normal. The mean values and standard error of mean (\pm SEM) of the ultrasound measurements of the hepatic length (HL), hepatic width (HW) and hepatic volume (HV) of puppies ranged from 65 ± 4.7 to 134 ± 3.6 mm, 28 ± 1.4 to 81 ± 3 mm and 176 ± 16 to 1358 ± 71 mm³ respectively. The mean values \pm SEM for the gall bladder length (GBL), width (GBW), wall thickness (GBWT) and volume (GBV) of puppies ranged from 11 ± 0.9 to 21 ± 2.9 mm, 5.6 ± 0.63 to 15 ± 1.5 mm, 0.71 ± 0.063 to 0.67 ± 0.088 mm and 0.18 ± 0.025 to 2.2 ± 0.54 mm³ respectively. The mean \pm SEM for portal vein diameter (PVD) ranged from 2.3 ± 0.1 to 4.8 ± 0.07 mm while the cross sectional area (CSA) of the portal vein ranged from 4.25 ± 0.37 to 17.99 ± 0.53 mm². The liver parenchyma of Nigerian Indigenous puppies was seen as an isoechoic structure which appeared as loosely granular structure with homogenous and uniform echo texture, and interrupted by short, highly echogenic paired parallel lines surrounding an anechoic lumen that represents the portal veins. The gallbladder was observed as an anechoic, round to oval structure to the left of the midline of the puppies (right of the scanner). The HL, HW and HV correlated significantly and positively with all the demographic data with the HT, BL and WT being the best predictor of the HL, HW and HV respectively. The GBL, GBW and GBV correlated significantly and positively with all the demographic data with the weight being the best predictor of GBL and GBV while the height was the best predictor of GBW. The GBWT correlated significantly and negatively with the age ($r = -0.57$), weight ($r = -0.5$) and HV ($r = -0.52$). PVD neither correlate with

demographic data nor the hepatobiliary dimensions studied. The pancreas was not visualized with the ultrasound machine. It was concluded that normal parameters for the hepatic and gall bladder dimension could be determined from the WT, HT and BL of puppies hence, this can serve as a baseline in clinical examination of puppies towards diagnosis of hepatobiliary pathologic conditions.

Table of Contents

Declaration	iii
Certification.....	iv
Dedication.....	vi
Acknowledgments.....	vii
Abstract	viii
Table of Contents	x
Lists of Figures	xv
List of Plates	xvii
List of Appendices	xviii
List of Abbreviations.....	xix
1.0 INTRODUCTION	1
1.1 Background of the Study.....	1
1.2 Statement of Research Problem	5
1.3 Justification of the Study.....	6
1.4 Aim of the Study	8
1.5 Objectives of the Study.....	9
1.6 Research Questions.....	9
2.0 LITERATURE REVIEW.....	10
2.1 Anatomy of Canine Hepatobiliary System	10
2.1.1 The hepatobiliary system	10
2.1.2 Liver.....	10
2.1.3 Hepatic vasculature.....	12
2.1.4 Biliary system.....	13
2.1.5 Function of the biliary system.....	14

2.2 Nigerian Indigenous Dogs	15
2.3 Ultrasound and Ultrasonography	16
2.3.1 Historical overview of ultrasonography	17
2.3.2 General principles of ultrasonography.....	18
2.3.3 Transducers	19
2.3.4 Transducer types.....	20
2.3.5 Transducer frequencies	22
2.3.6 Ultrasound image formation	22
2.3.7 Artifacts.....	23
2.4 Normal Ultrasonography Appearance of the Liver	28
2.4.1 Echogenicity and ecotexture of the liver	28
2.4.2 Evaluation of the liver size.....	31
2.4.3 Hepatic vasculature.....	31
2.4.4 Mean portal flow velocity	32
2.4.5 Factors affecting the visibility of hepatic portal vein	33
2.4.6 Gall bladder	33
2.4.7 Gall bladder volume	33
2.5 Ultrasonographic Features of Hepatic Disorders	34
2.5.1 Diffuse hepatic parenchymal disease.....	34
2.5.2 Focal hepatic parenchymal disorders.....	37
2.5.3 Disorders of the biliary system.....	40
2.5.4 Disorders of the hepatic and portal vasculature	43
2.6 Imaging Modalities for Evaluating the Hepatobiliary System.....	46
2.6.1 Radiography	46
2.6.2 Ultrasonography	47

2.6.3 Computed tomography	48
2.6.4 Magnetic resonance imaging.....	49
2.6.5 Laparoscopy	50
2.6.6 Hepatobiliary scintigraphy	51
2.7 Anatomy of the Canine Pancreas	52
2.7.1 Pancreas	52
2.7.2 Anatomic landmarks for identifying the pancreas.....	54
2.7.3 Normal ultrasonographic appearance of the pancreas and pancreatic duct in dogs	54
2.7.4 Size of the pancreas	54
2.7.5 Factors affecting the visualization of the pancreas by ultrasonography	55
2.7.6 Ultrasonographic features of pancreatic disorders	55
2.8 Imaging Modalities for Evaluating the Pancreas	58
2.8.1 Radiography	58
2.8.2 Ultrasonography	59
2.8.3 Computed tomography	60
3.0 MATERIALS AND METHODS.....	61
3.1 Location of Research	61
3.2 Materials	61
3.2.1 Equipment	61
3.2.2 Consumables	61
3.2.3 Source and type of study animals	62
3.3 Methodology	62
3.3.1 Ethical committee permission	62
3.3.2 Inclusion and exclusion factors	62
3.3.3 Study design	62

3.3.4 Demographic data collection.....	64
3.3.5 Experimental animal distribution	64
3.3.6 Pre-ultrasound scanning consideration	68
3.3.7 Ultrasonographic techniques and measurements	68
3.3.8 Measurements of the organs.....	68
3.4 Data Analysis	74
4.0 RESULT.....	75
4.1 Biometry of the Hepatobiliary System of the 6 (six) Puppies and their Correlations	75
4.1.1 Biometry of the liver.....	75
4.1.2 Biometry of the gallbladder	80
4.1.3 Echotexture of the liver and gall bladder	86
4.1.4 The correlation between the age and other demographic data and ultrasound hepatobiliary dimensions in the six puppies	90
4.1.5 The correlation between the hepatic length (HL) with the demographic data and other ultrasound hepatobiliary dimensions.....	90
4.1.6 The correlation between the hepatic width (HW) with the demographic data and other ultrasound hepatobiliary dimensions.....	90
4.1.7 Correlation between the hepatic volume (HV), demographic data and other ultrasound hepatobiliary dimensions.....	94
4.1.8 Correlation between the gallbladder length (GBL), demographic data and other ultrasound hepatobiliary dimensions.....	94
4.1.9 Correlation between the gallbladder width (GBW), demographic data and other ultrasound hepatobiliary dimensions.....	94
4.1.10 Correlation between the gallbladder wall thickness (GBWT), demographic data and other ultrasound hepatobiliary dimensions.....	94
4.1.11 Correlation between the gallbladder volume (GBV), demographic data and other ultrasound hepatobiliary dimensions.....	100
4.2 Evaluation of the Portal Vein in Six (6) Nigerian Indigenous Puppies.....	100

4.2.1 Biometry of the portal vein.	100
4.2.2 Correlation between the portal vein diameter (PVD), demographic data and ultrasound hepatobiliary dimensions.	100
4.3 Biometry of the Pancreas	106
4.4 The Biochemical Assay of Alanine Aminotransferase (ALT), Aspartate Aminotransferase (AST) and Alkaline Phosphatase (ALP).....	106
CHAPTER FIVE	108
5.0 DISCUSSION	108
CHAPTER SIX	115
6.0 CONCLUSION AND RECOMMENDATION	115
6.1 Conclusion	115
6.2 Recommendations	116
6.3 Limitations	117
REFERENCES	118
APPENDICES	137

Lists of Figures

Figure 4.1: Mean values and SEM of the hepatic length ultrasound dimension in male and female puppies.	76
Figure 4.2: Mean values and SEM of the hepatic width ultrasound dimension in male and female puppies.	77
Figure 4.3: Mean values and SEM of the hepatic volume ultrasound dimension in male and female puppies.	78
Figure 4.4: Variation of the hepatic ultrasound dimension with age.	79
Figure 4.5: Mean values and SEM of the ultrasound gall bladder length dimension in male and female puppies.....	81
Figure 4.6: Mean values and SEM of the ultrasound gall bladder width dimension in male and female puppies.....	82
Figure 4.7: Mean values and SEM of the ultrasound gall bladder wall thickness dimension in male and female puppies	83
Figure 4.8: Mean values and SEM of the ultrasound gall bladder volume dimension in male and female puppies.....	84
Figure 4.9 Variation of the ultrasound gall bladder dimension with age.	85
Figure 4.10: The mean and SEM of the portal vein diameter (PVD) and in male and female Nigerian Indigenous puppies	102
Figure 4.11: The mean and SEM of the cross sectional area (CSA) in male and female Nigerian Indigenous puppies	103

List of Tables

Table 2.1 Depth and axial resolutions obtained by different transducer frequencies	21
Table 3.1. Illustration of the format for presentation of the obtained demographic data of the puppies under study	67
Table. 4.1 The correlation between the age other demographic data and ultrasound hepatobiliary dimensions in the six puppies (n = 6).....	91
Table. 4.2 The correlation between the hepatic length with demographic data and other ultrasound hepatobiliary dimensions in the six puppies. (n = 6)	92
Table. 4.3 The correlation between the hepatic width with demographic data and other ultrasound hepatobiliary dimensions in the six puppies. (n = 6)	93
Table. 4.4 The correlations between the hepatic volume, demographic data and other ultrasound hepatobiliary dimensions in the six puppies. (n = 6)	95
Table. 4.5 The correlation between the gall bladder length, demographic data and other ultrasound hepatobiliary dimensions in the six puppies. (n = 6)	96
Table. 4.6 The correlation between the gall bladder width, demographic data and other ultrasound hepatobiliary dimensions in the six puppies. (n = 6)	98
Table. 4.7 The correlation between the gall bladder wall thickness, demographic data and other ultrasound hepatobiliary dimensions in the six puppies. (n = 6)	99
Table. 4.8 The correlation between the gall bladder volume, demographic data and other ultrasound hepatobiliary dimensions in the six puppies. (n = 6)	101
Table 4.9 Correlation between the portal vein diameter, demographic data and ultrasound hepatobiliary dimensions in the six puppies. (n = 6)	104
Table 4.10 The correlation between the cross sectional area of the portal vein diameter, demographic data and ultrasound hepatobiliary dimensions in the six puppies. (n = 6) ...	105
Table 4.11. Mean values of the ALT, AST and ALP from the Nigerian Indigenous puppies. (n = 6).	107

List of Plates

Plate 2.1. Anatomy of the canine liver (caudal or visceral aspect), with the lobes, portal hepatis, caudal vena cava, and gallbladder identified. Illustration by Pamella Boutilier (Small Animal Internal Medicine)	11
Plate 2.2. Long-axis image of a normal canine Liver. The hyperechoic line along the left side of the image, represents lung-diaphragm interphase; the arrows mark the hyperechoic portal vessels.	30
Plate 3.1: Six Nigerian Indigenous Puppies acquired for the research work.....	63
Plate 3.2: A male puppy from group A placed on a standing position with a Freeman’s tape placed from the neck to the first coccygeus to obtain the body length (BL).	65
Plate 3.3: A male puppy from group A placed on standing position with a Freeman’s tape placed from the highest point of the withers to the extreme 3 rd phalanx to obtain the withal height (HT)	66
Plate 3.4. A female puppy (Nigerian indigenous puppy) positioned on dorsal recumbency in preparation for scanning.	69
Plate 3.5. B-mode Sonoster C5 ultrasound scanner and a 7.5 MHz curvilinear transducer used for the abdominal ultrasound	70
KEY: Monitor (A); Keyboard or control panel (B); Mouse (C); Pulse control (D) and Transducer (E).....	70
Plate 3.6. Cranial abdominal scan of the puppy illustrating the echotexture of the hepatic parenchyma (HP), gallbladder (GB), diaphragm (DP) and hepatic portal vein (HPV)	71
Plate 3.7 Sonogram of the cranial abdomen indicating the horizontal and vertical dimensions of the liver (long arrow), gallbladder (short arrow) of the puppy.	72
Plate 4.1: Longitudinal sonograph of the Nigerian Indigenous Puppy with homogenous isoechoic hepatic parenchyma (HP), anechoic circular area representing the gall bladder (GB) and curved hyper echoic line that represents the diaphragm (DPH)	87
Plate 4.2: Measurements of the dimensions of the liver: hepatic length (HL), hepatic width (HW) and gallbladder volume (GBV) in Nigerian Indigenous Puppy.	88
Plate 4.3: Echogenic paired parallel lines surrounding an anechoic lumen that represents the portal veins (short arrow) and curved hyper echoic line that represents the diaphragm (long arrow).	89

List of Appendices

Appendix 1: Demographic data of 6 Nigerian Indigenous Puppies.....	137
Appendix 2: Biometry of the liver and the Hepatic portal vein diameter in six (6) Nigerian Indigenous Puppies	143
Appendix 3: Biometry of the gallbladder of six Nigerian Indigenous Puppies	151
Appendix 4a: The mean and SEM of the portal vein diameter (PVD) and cross sectional area (CSA) in male (n=3) and female (n=3) Nigerian Indigenous puppies.....	159
Appendix 4b: The overall mean values and standard error of mean (\pm SEM) of the portal vein diameter (PVD) and Cross sectional area (CSA) of six (6) Nigerian Indigenous puppies.....	160
Appendix 5. Assay of serum ALT, AST and ALP	161
Appendix 6: Ethical clearance certificate	165

List of Abbreviations

ALT	Alanine aminotransferase
AST	Aspartate aminotransferase
ALP	Alkaline phosphatase
GBL	Gall bladder length
GBV	Gall bladder volume
GBW	Gall bladder width
GBWT	Gall bladder wall thickness
HW	Hepatic width
HV	Hepatic volume
PVD	Portal vein diameter
HT	Height
BMI	Body mass index
CSA	Cross sectional area
WT	Weight
BL	Body length
NIDs	Nigerian Indigenous Dogs
SOD	Sphincter of Oddi

CHAPTER ONE

1.0 INTRODUCTION

1.1 Background of the Study

The liver and its associated structures is the most important organ and the largest parenchymal gland of the body with large reserves of function (70-80%), it has the capacity to regenerate and perform adequately despite often extensive damage to its integrity (Tantary *et al.*, 2014). It provides myriad of biochemical, synthetic, excretory and regulatory functions important to body mechanisms (Center, 1998). Hepatic disorders are one of the causes of death in dogs (Tantary *et al.*, 2014). It is associated with varied and often vague clinical signs and symptoms and thus frequently presents a diagnostic challenge to veterinary clinicians (Tantary *et al.*, 2014).

The liver is a large pyramidal shaped organ (Christoph *et al.*, 2012). It is located within the rib cage, just cranial to the stomach, with its cranial margin against the diaphragm and lung interface. Caudally, the liver is in contact with the spleen on the left, the stomach central with the kidney on the right side at the level of the renal fossa of the caudate lobe (Frances and Lorrie, 2011). It is made up of 6 lobes; right medial and lateral, left medial and lateral, caudate and quadrate lobes (Abby, 2010). Within the liver, the canaliculi drains bile into the interlobular ducts which converge to form the lobar ducts that becomes the hepatic duct as they exit the liver parenchyma and form part of the extrabiliary tract (Evans, 1993). The hepatic ducts converge to form the common bile ducts (CBD) which enters the duodenum at the duodenal papillae (Evans, 1993). Blood supply to the liver comes from the hepatic artery which is a branch of celiac artery and portal vein (Markowitz *et al.*,

1949). In dogs, the portal vein divides into right and left portal branches 0.5 to 1.0 cm beyond the entrance of its gastroduodenal tributary. The right portal vein is a short venous trunk that supplies the caudate process of the caudate lobe and the right medial liver lobe; at its bifurcation, it may be partially or completely surrounded by hepatic tissue (Tobias and Rawlings, 1996; Ursic *et al.*, 2007). The left portal vein is larger and longer than the right portal vein. It gives off a central branch to the right medial lobe and a small papillary branch to the papillary process of the caudate lobe before dividing into quadrate, left medial, and left lateral branches. (Tobias and Rawlings, 1996;Uršič,*et al.*, 2007).

The gall bladder is a pear-shaped structure which lies on the right ventral aspect of the liver and is located between the quadrate and right medial lobe (Abby, 2010).

The pancreas is primarily a glandular organ with both exocrine and endocrine functions (Tsai, 2011). They secrete enzymes responsible for the breakdown of proteins, carbohydrates and lipids (Tsai, 2011). Their function is also related to the control of blood glucose through the secretion of insulin and glucagon (Tsai, 2011). Anatomically, the pancreas is divided into the right limb, body and left limb (Tsai, 2011). Pancreatic disorders are recognised with increasing frequency (Hecht and Henry, 2007). The normal pancreas is a small, inconspicuous organ of similar echogenicity to the surrounding mesentery and may be difficult to identify (Hecht and Henry, 2007). Therefore the knowledge of anatomic landmark such as the portal vein, and contributing vessels, duodenum and stomach is necessary to facilitate identification and examination (Hecht and Henry, 2007).

The Nigerian Indigenous breeds of Dogs are dogs that have been domesticated, with their feeding pattern being majorly omnivorous as a consequence of their high level of domestication (Igado, 2011). Arowolo (1999) reported that the population of Nigerian Indigenous dogs was estimated to be about 4.5million (Arowolo, 1999). They are used locally for hunting in the rural areas, while in the urban cities they are used as guard dogs and pets. In recent years, there has been an increase in the acquisition of this breed of dogs probably due to the fact that they are more resistant to some haemoparasites causing diseases such as babesiosis and trypanosomosis that constantly plague the exotic breeds (Olayemi *et al.*, 2009).

The general process of diagnosis of hepatobiliary and pancreatic diseases in dogs consist of integrating patient's history, physical examination, biochemical analysis, radiography and ultrasonography (Murtaught *et al.*, 1985).

The knowledge of normal anatomical imaging is essential for the detection of conditions in the hepatobiliary system and the pancreas (Sullivan, 1976; Nyland *et al.*, 2005; Gunderman, 2007). The determination of liver size is an important procedure in detecting hepatomegaly, monitoring the progress of diseases and response of liver to treatments (Nyland and Hager, 1985; Nyland *et al.*, 1985; Rocha *et al.*, 2003). In cases of suspected hepatomegaly, invivo liver assessment can be carried out by means of clinical and/or imaging modalities such as radiography, scintigraphy, ultrasonography, computed tomography (CT) scan (Rocha *et al.*, 2003). The utilisation of a more reliable method for liver assessment is recommended as a large liver abnormality is easily detectable but smaller abnormalities may be underestimated (Sullivan *et al.*, 1976). In such situations, ultrasound is considered a simple

qualitative method for assessment of the liver size, being the first imaging study requested for such purpose (Rocha *et al.*, 2003; Chammas *et al.*, 2006).

Ultrasonography is a very important imaging modality for assessing the internal architecture of the liver (Lamb, 1978) allowing an elaborate study of the parenchyma, assessing the dimensions, shape, contour, borders, changes in echogenicity and appearance of vessels and hepatic structures as well as its relationship with adjacent structures (Zwiebel *et al.*, 1995; Rocha *et al.*, 2003; Nyland *et al.*, 2005). However, disease conditions such as fatty infiltration, steroid hepatopathy, diabetes mellitus, lymphoma and toxic hepatopathies normally cause increased echogenicity of the hepatic parenchyma without significant changes in liver dimension, while in cirrhosis and chronic cholangiohepatitis generally presents reduced dimensions and irregular contour (Contran *et al.*, 2005; Nyland *et al.*, 2005).

There is a wide variety of imaging modalities for assessment of the biliary tract of small animals (Franchi-Teixeira *et al.*, 1997; Sullivan and Fígado, 2000; Chammas *et al.*, 2006) this include; radio-isotope, cholescintigraphy, CT scan, Magnetic Resonance Imaging (MRI), ultrasonography, transhepatic cholangiography, endoscopic retrograde cholangio-pancreatography or even radiography, oral cholecystography, and hepatic-scintigraphy in some cases (Sullivan and Fígado, 2000; Dähnert, 2001; Chammas *et al.*, 2006). Among such techniques, ultrasonography is preferred by most professionals in the initial investigation of patients with suspected biliary conditions (Franchi- Teixeira *et al.*, 1997; Sullivan and Fígado, 2000; Chammas *et al.*, 2006; Gunderman, 2007). The utilisation of such technique is indicated in most abdominal diseases and is a totally non- invasive and essential for establishing diagnosis in many situations (Cerri and Vogueira, 2002 ; Rocha *et*

al., 2003; Nyland *et al.*, 2005). It has the advantage of being accessible, rapid and innocuous, besides capability (Nyland *et al.*, 2005). Furthermore, it is a less expensive method, does not rely on ionizing radiation or contrast utilisation and does not require patient sedation (Rocha *et al.*, 2003; Chammas *et al.*, 2006).

Real time ultrasonography is one of the methods that have been employed to assess gallbladder volume; it is accurate, reproducible, non-invasive, cheap, easy and widely available method for evaluating gallbladder volume variations (Marzio *et al.*, 1988; Jazrawi, 2003; Jankers *et al.*, 2003; Portincasa *et al.*, 2003). Two-Dimensional (2D) ultrasonography has been widely employed to measure gallbladder volume by ellipsoid method (Jonderko, *et al.*, 1994; Romanski and Siembieda, 2002; Aguirre *et al.*, 2007; Atalan *et al.*, 2007; Ramstedt,*et al.*, 2008; Tsukagoshi *et al.*, 2012). However, 2D ultrasonography is operator dependent and deviation from gallbladder shape could affect results. The 3-Dimensional ultrasonography is an emerging technology that has been developed to assess gall bladder volume. This method has been shown to be an exact and appropriate tool for the evaluation of organ volume in both dogs and human. (Hashimoto *et al.*, 1999; Scheffer *et al.*,2004 ; Mundt *et al.*,2005; Asadi *et al.*, 2011; Vasough *et al.*,2008; Vajhi *et al.*,2010; Mendonca *et al.*, 2012). Measuring a gallbladder volume using 3D-ultrasound has a potential advantage in that a sagittal section of the gallbladder at its maximal diameter is not required, which may be essential in patients with irregular gallbladder shape (Rahmani *et al.*, 2015).

1.2 Statement of Research Problem

There is dearth of information on the sonographic parameters of the hepatobiliary system and pancreas of Nigerian Indigenous Dogs. The ante mortem diagnosis of canine hepatobiliary and pancreatic diseases poses a significant challenge to clinicians. Clinical presentation and clinical pathologic findings are often nonspecific in these conditions (Murtaugh *et al.*, 1985; Saundres, 1991; Lee and Lee, 2014).

There are certain disease conditions of the hepatobiliary and pancreatic conditions that can result in alterations in the size of these organs (Larson *et al.*, 2005). In small animal clinical practice, several dimensional ultrasonographic association have been proposed among various anatomical structures of the body (Hasson *et al.*, 2002; Hetch *et al.*, 2006; Mareschal *et al.*, 2007; Barella *et al.*, 2012). However, evaluating the size of the hepatobiliary system and the pancreas is still challenging; largely because of the wide variations among breeds. Age, weight, sex and Body Mass Index (BMI) are reliable parameters to consider in avoiding false positive diagnosis of hepatobiliary and pancreatic conditions. To the best of our knowledge, there is no published information on the sonographic parameters of the hepatobiliary system and the pancreas of Nigerian Indigenous Dogs that can be correlated with the demographic factors such as age, sex, weight and Body Mass Index. Thus there is need to use the ultrasound to establish a baseline research data to evaluate the normal sonographic parameters of the hepatobiliary system of the Nigerian Indigenous dogs.

1.3 Justification of the Study

The Nigerian Indigenous Dogs are constantly presented to the Teaching Hospital Veterinary clinics for diagnosis and treatment of diseases that themselves affect the liver

such as babesiosis, ehrlichiosis, infectious canine hepatitis, and canine herpes virus. Even though hypertension, diabetes and related diseases are not routinely investigated in our laboratories, the incidence of weight loss, ocular defects and pathologies suggests that the pancreas and its related functions must be studied. Besides the extensive diagnostic kits made available for diagnosis of diseases that may affect the organs, it is equally important to substantiate these diagnoses with imaging evidence or findings. Hence the need to have a reference normal anatomical imaging indices which are important for detection of conditions of the Hepatobiliary system and pancreas (Sullivan *et al.*, 1976; Nyland *et al.*, 2005; Gunderman., 2007).

Though imaging modalities such as radiography, computed tomography (CT) scan, ultrasonography, magnetic resonance imaging (MRI), scintigraphy and cholangiography have been used for the assessment of the Hepatobiliary system and pancreas. Ultrasonography remains the preferred technique used in the initial investigation of patient with suspected Hepatobiliary and pancreatic conditions (Franchi-Teixeira *et al.*, 1997; Sullivan and Fígado, 2000; Rocha *et al.*, 2003; Chamas *et al.*, 2006 Hecht and Henry, 2007). This is largely due to the fact that it does not rely on ionization radiation or contrast utilization and does not require patient sedation (Rocha *et al.*, 2003). It also has the advantage of being accessible, rapid innocuous besides capability (Nyland *et al.*, 2005). No in depth study has been done so far on the Nigerian Indigenous dogs. Arowolo (1999) estimated that there are about 4.5million Nigerian Indigenous Dogs, and as at today we have not access records that evaluated the sonographic parameters of the Hepatobiliary system and pancreas of Nigerian Indigenous Dogs that can be correlated with the demographic factors such as age, sex, weight and Body Mass Index (BMI).

The knowledge of the normal sonographic parameters with respect to the anthropometrical measurements will improve the accuracy of clinical assessment of the hepatobiliary and pancreatic conditions. There is insufficient information on normal liver dimension and its variant for the interpretation of the sonographic examination in NIDs. Details of anatomical structures in canine species vary tremendously from breed to breed more than in any animal species, wild or domesticated (Anonymous 5, 2005). Choi *et al.*, 2013 observed that the normal Pekingese had significantly small liver volume/ body weight ratio than normal non Pekingese brachycephalic breeds of dogs and normal non-brachycephalic breeds of Dogs (Choi *et al.*, 2013). Also the liver length /T11 vertebral length ratio in normal Pekingese was significantly smaller than normal non-Pekingese brachycephalic breeds of dogs and normal non-brachycephalic breeds of dogs (Choi *et al.*, 2013). That is Pekingese breed of dogs have smaller liver size than other breeds of dogs. Similarly in humans, racial differences in the normal liver dimension has been shown to exist by El Sharkawy *et al.*, (1997). There is need to establish a breed specific baseline data on sonographic parameters of the hepatobiliary system of NIDs. More so, Breed-specific differences in haematological and biochemical variables have been reported by several authors such as in Alaskan malamutes, Siberian huskies, golden retrievers, English setters (Sharkey *et al.*, 2009), Bernese mountain dogs (Nielsen *et al.*, 2010), dachshunds (Torres *et al.*, 2014) and dogues de Bordeaux (Lavoue *et al.*, 2014). Therefore, it is important to extensively study the ultrasonographic anatomical parameters of the hepatobiliary system and the pancreas to establish a baseline data in Nigerian Indigenous Dogs.

1.4 Aim of the Study

The aim of this study is to evaluate the hepatobiliary system and the pancreas of the Nigerian Indigenous Dogs for the purpose of setting a sonographic baseline data for clinical use.

1.5 Objectives of the Study

- i. Determine the sonographic parameters of the hepatobiliary system and their correlation with age, sex, weight and Body Mass Index (BMI) of Nigerian Indigenous Dogs.
- ii. Evaluate the portal vein of Nigerian Indigenous Dogs
- iii. Determine the sonographic parameters of the pancreas and their correlation with age, sex, weight and Body Mass Index (BMI) of Nigerian Indigenous Dogs

1.6 Research Questions

- i. Will the sonographic parameters of the Hepatobiliary system of the Nigerian Indigenous Dogs show any correlations with age, sex, weight and BMI?
- ii. Are there sonographic differences in the portal vein of the Nigerian Indigenous Dogs with respect to age, sex, weight and BMI?
- iii. Will the sonographic parameters of the Pancreas of the Nigerian Indigenous Dogs show any correlation with age, sex, weight and BMI?

CHAPTER TWO

2.0 LITERATURE REVIEW

2.1 Anatomy of Canine Hepatobiliary System

2.1.1 The hepatobiliary system

The hepatobiliary system comprise of the liver, hepatic vasculature and the biliary system (Center, 2009).

2.1.2 Liver

The liver is the large pyramidal shaped organ (Christoph *et al.*, 2012) which is made up of 6 lobes; right medial and lateral, left medial and lateral, caudate and quadrate lobes (Abby, 2010).

*2.1.2.1 Topography of the liver:*The liver is located inside the intraperitoneal cavity and under the right hemi diaphragm, but can also extend across the midline reach to the left hemi diaphragm and to the spleen in some dogs. The greater proportion of the liver's mass lies to the right of the median plane, with a right-to-left proportion of approximately 3: 2 in dogs. (Dyce *et al.*, 1987). It lies just cranial to the stomach with its cranial margin against the diaphragm and lung interphase. Caudally, the liver is in contact with the spleen on the left, the stomach central with the kidney on the right side at the level of the renal fossa of the caudate lobe (Francis and Lorrie, 2012).

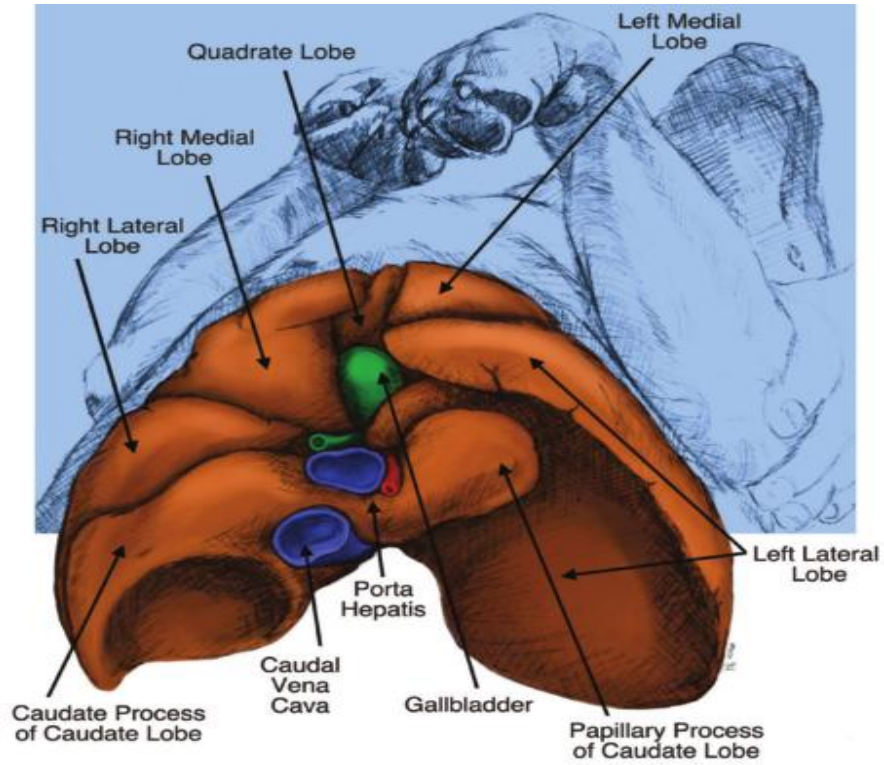


Plate 2.1. Anatomy of the canine liver (caudal or visceral aspect), with the lobes, portal hepatis, caudal vena cava, and gallbladder identified. Illustration by Pamella Boutilier (Small Animal Internal Medicine).

2.1.2.2 Liver lobulations: In dogs, the liver is composed of 6 lobes; right medial and lateral, left medial and lateral caudate and quadrate lobes (Evans 1993; Hudson and Hamilton 1993; Abby, 2010) – which are separated by fissures and cannot be easily distinguished unless separated by peritoneal effusion.

*Left lobe:*The left lobe is the largest and is subdivided into the left lateral and left medial lobes. A substantial cleft separates the two portions of the left lobe, making access to the bases of the left lateral and medial lobes less technically demanding compared with right side approaches (Evans, 1993; Covey *et al.*, 2009).

*Quadrate lobe:*The quadrate lobe lies almost on the midline, and its lateral aspect forms one side of the gallbladder fossa. Its attachment to the right medial lobe is substantial, with often only a small fissure separating these two lobes, which makes surgical separation of these two lobes more challenging (Covey *et al.*, 2009).

*Right lobe:*The right lateral lobe is usually fused at its base with the caudate lobe, which is subdivided into the caudate and papillary processes. The caudate process is the most caudal part of the liver, usually extending to the level of the twelfth intercostal space. The papillary process extends toward the left side, crossing the midline, and is loosely covered by the lesser omentum (Evans, 1993).

2.1.3 Hepatic vasculature

Blood supply to the liver comes from the hepatic artery which is a branch of celiac artery and portal vein (Markowitz *et al.*, 1949). In dogs, the portal vein divides into right and left portal branches 0.5 to 1.0 cm beyond the entrance of its gastroduodenal tributary.

*2.1.3.1 Right portal vein:*The right portal vein is a short venous trunk that supplies the caudate process of the caudate lobe and the right medial liver lobe; at its bifurcation, it may be partially or completely surrounded by hepatic tissue (Tobias and Rawlings, 1996; Uršičet *al.*, 2007).

*2.1.3.2 Left portal vein:*The left portal vein is larger and longer than the right portal vein. It gives off a central branch to the right medial lobe and a small papillary branch to the papillary process of the caudate lobe before dividing into quadrate, left medial, and left lateral branches (Tobias and Rawlings, 1996; Ursic *et al.*, 2007).

2.1.4 Biliary system

The biliary system is comprised of the bile canaliculi, bile ductules, intralobular ducts, interlobular ducts, hepatic ducts, gallbladder (GB), cystic duct, and bile duct (BD) (Center, 2009).

*2.1.4.1 Gallbladder:*The GB is a pear-shaped organ that lies in a fossa between the right medial and quadrate liver lobes and is attached to the hepatic visceral surface (Neer, 1992; Mehler and Bennet, 2009; Center, 2009; Aguirre, 2010). The apical aspect of the GB is called the fundus, the middle portion is called the body, and the tapered portion that is confluent with the cystic duct is called the neck (Aguirre, 2010) Gallbladder (GB) volume can be estimated using the ellipsoid method (Penninck *et al.*,2010). It can vary distinctly in size and become quite large in anorexic patients, so that GB volume alone cannot be used as a reliable sign of biliary obstruction. Yet, monitoring its reduction postprandially may help to rule out outflow obstruction. Gallbladder (GB) width can be used to predict its postprandial change in volume (Diana *et al.*, 2012). Parasympathetic and sympathetic

innervation of the GB is via the vagus nerve and splanchnic nerves respectively (Neer, 1992; Mehler and Bennet, 2009; Center, 2009; Aguirre, 2010). The cystic artery, which is the left branch of the hepatic artery, is the sole source of blood supply to the GB (Neer, 1992; Mehler and Bennel, 2006; Center, 2009).

2.1.4.2 Gallbladder contractions: Gallbladder contractions and delivery of bile to the duodenum occurs in both the interdigestive and postprandial states. In the fasted state, gastrointestinal contractions occur in response to a periodic motor activity called the migrating motor complex.

2.1.5 Function of the biliary system

The biliary system transports bile from liver to its eventual destination in the duodenal lumen. Bile serves as a source of bile acids for fat digestion and absorption, a source of bicarbonate to buffer hydrogen ions in the duodenal contents, and an elimination route for lipophilic metabolic products and xenobiotics (Center, 2009; Washabau, 2013). The majority of bile is stored, concentrated, and modified in the GB during the interdigestive phase. During this phase, bile is continuously delivered into the relaxed GB (Center, 2009).

Gallbladder contractions and delivery of bile to the duodenum occurs in both the interdigestive and postprandial states. In the fasted state, gastrointestinal contractions occur in response to a periodic motor activity called the migrating motor complex. The GB responds to the migrating motor complex via motilin, which induces “bellows-like” contractions during the interdigestive phase. (Matsumoto *et al.*, 1988; Center, 2009). Rhythmic relaxation of the Sphincter of Oddi(SOD) delivers the GB bile into the duodenum in spurts instead of a continuous flow. (Neer, 1992; Mehler and Bennel, 2009;

Center, 2009). In the postprandial state, GB contraction and secretion is mediated via neurohormonal stimulation to coordinate GB contraction with meal ingestion. Gastric distension, free fatty acids, and amino acids lead to vagal stimulation and cholecystokinin (CCK) release from duodenal enteroendocrine cells (I cells). Cholecystokinin stimulates GB contraction and relaxation of the Sphincter of Oddi (SOD) (Neer, 1992; Aguirre, 2010). Cholecystokinin is the most potent stimulus for GB contraction whereas acetylcholine is a weak stimulant. Sphincter of Oddi (SOD) relaxation is enhanced by secretin. Acidic chyme entering the duodenum stimulates release of secretin from the S cells in the duodenum and vagal stimulation results in release of vasoactive intestinal polypeptide. Secretin and vasoactive intestinal polypeptide stimulate secretion of mucin and bicarbonate from the GB mucosa. This bicarbonate-rich fluid mixes with the stored bile prior to expulsion into the duodenum (Center, 2009). Bile acids are delivered back to the liver via enterohepatic circulation and inhibit further release of CCK (Neer, 1992; Center, 2009; Aguirre, 2010). As fatty acids enter the small intestines, the release of somatostatin and gastrointestinal epithelium inhibits GB contraction (Aguirre, 2010). The GB relaxes and SOD tone increases to facilitate the delivery of hepatic bile into the GB (Center, 2009; Aguirre, 2010).

2.2 Nigerian Indigenous Dogs

The Nigeria, indigenous Dogs are dogs that have not been classified or recognized as a breed and are commonly referred to as “locals” or indigenous dogs. They are dogs that have been domesticated, with their feeding pattern being majorly omnivorous as a consequence of their high level of domestication (Igado, 2011). Arowolo (1999) reported that the population of Nigerian Indigenous dogs was estimated to be about 4.5million. They are used locally for hunting in the rural areas, while in the urban cities they are used as guard

dogs and pets. They are medium sized dogs and appear in various coat colours and patterns (Bukar-Kolo *et al.*, 2016).

Some of the dogs have distinct coat colors while others appear in mixture of colours. This could most likely be due to uncontrolled breeding (Lipinski *et al.*, 2008) as these dogs move about freely and thus mating at random. A higher percentage of the Nigerian indigenous dogs are classified as thin based on their Body Condition Score (BCS) (Bukar-Kolo *et al.*, 2016) This may most likely be due to inadequate nutrition in terms of quantity and quality and also based on the fact that most dogs in households go without food if there are no leftovers. In recent years, there has been an increase in the acquisition of this breed of dogs probably due to the fact that they are more resistant to some haemoparasites causing diseases such as babesiosis and trypanosomosis that constantly plague the exotic breeds (Olayemi *et al.*, 2009).

2.3 Ultrasound and Ultrasonography

Ultrasonography is a non-invasive diagnostic imaging modality and the examination can be carried out quickly and easily (Peteret *et al.*, 1992). The principle in which it works is based on the ability to reflect transmitted high-frequency sound waves by tissue (Kumari *et al.*, 2016). Ultrasound waves are generated by the piezoelectric effect in a suitable medium such as lead zirconate (Kumari *et al.*, 2016). Echoes produced by ultrasound depend on relative density of tissue (Pierson and Adams, 1995). A, B, and M modes are the three basic forms of ultrasound used in soft tissue imaging. A-mode ultrasonic imaging is a one-dimensional display of echo amplitudes versus distance; B-mode ultrasonic imaging produces an accurate two-dimensional (2D) cross-sectional image of soft tissues while the

M-mode ultrasonic imaging is an adaptation of B-modes to evaluate moving structure of the heart (Kumari *et al.*, 2016). Diagnostic ultrasound frequencies range from 2 to 15 MHz and are inaudible to the human ear (Kumari *et al.*, 2016). The ultrasonogram is essentially an image of a thin slice of tissue, and therefore, enables serial examinations to monitor the progression of the condition, response to treatment and to practice scanning techniques (Hornbuckle and Kleine, 1980). One of the drawbacks of diagnostic ultrasound however is that it has a steep learning curve and requires a great deal of skill and experience (Kumari *et al.*, 2016). Ultrasonography is one of the most widely used diagnostic tools in modern medicine used to visualize many internal organs, their size, structure and any pathological lesions with real time sonographic images (Ahmed *et al.*, 2012). A complete ultrasonographic assessment of the liver can provide detailed information about the size, position and the parenchymal pattern of the liver. Ultrasonography has become an essential imaging tool for identifying abnormalities of the liver parenchyma, biliary tract and vascular system (Braun *et al.*, 2005).

2.3.1 Historical overview of ultrasonography

World War I saw the first practical use of the piezoelectric effect in the development of sonar using a separate sound generator and detectors (Coltera, 2010). In 1880, the French Physicist; Pierre Currie discovered the Piezoelectric property of certain crystals which upon application of electricity resulted in the deformation and production of sound with a frequency greater than 20KHz known as Ultrasound (Vignoli and Saunders, 2011). Thereafter, in 1940, The American acoustical physicist; Floyd Firestone, devised the first ultrasonic imaging devise, the supersonic reflectoscope, to detect the internal flaws in metal casting. In 1941, the Austrian Neurologist; Karl Theo Dussik and a physicist; Friedrich

are the first to use the ultrasound to image the human body (Siddharth, 2007; Levine, 2010). In the 1940s, Dr. George Ludwig was the first person to apply the ultrasonic energy to the human body for medical purposes at the Naval Medical Research Institute, Bethesda, Maryland (Anon 3, 2015; Anon 1, 2006). Douglass Howry with the help of Joseph Holmes, an American nephrologist, develops a *B-mode linear compound ultrasound scanner* to include superior transducers, amplifiers, and display imaging. Howry and his team introduced compound scanning in order to eliminate ‘false’ echoes. Compound scanning allowed Howry to differentiate between structures and tissues which ultimately produced better imaging and were referred to as ‘*sonagrams*’ (Anon 3, 2015). Today, the applications of ultrasound are diverse and include use as a therapeutic aid to stimulate tissue healing (Porter 1991; Steiss, 2000), food sterilization (Piyasena *et al.*, 2003) and vaccination of fish (Zhou *et al.*, 2002).

2.3.2 General principles of ultrasonography

2.3.2.1 Resolution: Resolution is the ability of an ultrasound machine to distinguish echoes on the basis of space, time, and strength (Kremkau, 2011b). The better the resolution, the more likely an abnormality can be identified. As the frequency of an ultrasound wave increases, the resolution increases. There are three types of resolution found in ultrasound imaging; axial resolution, lateral resolution and elevation resolution.

Axial resolution: Axial resolution is the resolution of two separate reflectors along the direction of the ultrasound beam (Kremkau, 2011b). It is determined by the ability of the transducer to detect two reflecting echoes separately without an overlap in the returning echoes, therefore both echoes have to be separated by half the spatial pulse length (SPL) (

Daniela, 2011). SPL is the length of space in one pulse of ultrasound. When two reflectors are separated by a distance that is greater than half the SPL, the echoes from these two reflectors do not overlap as they return to the transducer and are interpreted as separate echoes (Daniela, 2011) The shorter the transmitted pulse and likewise its returning echo pulse, the better the axial resolution. The pulse length is determined by the number of cycles emitted multiplied by the wave-length.

Lateral resolution:Lateral resolution is the ability separate two adjacent reflectors perpendicular to the beam direction in (Kremkau, 2011b) .This is determined by the width of the ultrasound beam which must be narrower than the space separating the reflectors (Daniela, 2011). The width of an ultrasound beam decreases with increasing frequency. In a focused ultrasound beam, where the width of the beam is restricted, the lateral resolution is best at the focal point of the ultrasound beam because this is the narrowest part of the beam (Kremkau, 2011b).

*2.3.2.2 Focusing:*Focusing the beam results in reduced beam diameter and improved lateral resolution (Powis, 1986). Focusing of the beam can occur only in the near field of the ultrasound beam (Kremkau 1993). Beam focusing characteristics are variable for each transducer and frequency and should be obtained from the manufacturer at the time ultrasound equipment is purchased. The focal distance and focal zone can be verified with an ultrasound test object. A number of devices are available commercially for testing imaging performance. Focusing can be performed dynamically or manually.

2.3.3 Transducers

A transducer is a very important part of an ultrasound imaging system. A typical ultrasound machine uses a wide variety of transducers optimized for specific diagnostic applications (Scampini, 2017). Each transducer is comprised of an array of piezoelectric materials that sends focused energy into the body and receives the resulting reflections. Each transducer is connected to the ultrasound imaging system with fine coaxial cables. Typical transducers have up to 32 to as many as 512 piezoelectric elements that operates at frequencies from 1MHz to 15MHz (Scampini, 2017). Most ultrasound systems provide two to as many as four switchable transducer connections to allow the clinician to easily switch among the various transducer for each examination type (Scampini, 2017).

2.3.4 Transducer types

2.3.4.1 Array transducers: The array transducers are either linear or curved in shape and their piezoelectric crystals are arranged in a line along the surface of the transducer (Patrick, 2010). They have the advantage of allowing a wide superficial field of view. The linear array is particularly important in viewing superficial tissues. They are used for the examination of the musculoskeletal system, abdominal organs, eyes, body wall and non-cardiac thoracic structures (Patrick, 2010).

2.3.4.2 Phased array transducers: Phased array (sector) transducers are composed of only small number of crystals in rectangular format that are electronically excited as a group with small time difference (phasing), which results in the sound pulse being sent out in a specific direction that is constantly changing.

They have the advantage of working with small foot prints and creating pie-shape images, which allow deep structures to be view clearly (Patrick, 2010). These transducers have a

limited near field visibility compared with the linear array or curvilinear array transducer and are not a good choice for imaging superficial structures (Powis 1993; Patrick, 2010).

Table 2.1 Depth and axial resolutions obtained by different transducer frequencies

Frequency	Image depth (cm)	Axial Resolution (mm)
2.0	20	0.77
3.5	17	0.44
5.0	12	0.31
7.5	8	0.20
10.0	6	0.15

Reference: (Nyland and Matton, 1995)

Phased array transducers are used for echocardiography and for scanning structures that are deeply located such as the abdominal or thoracic structures in large breeds of dogs (Patrick, 2010).

2.3.5 Transducer frequencies

The ultrasound wave frequency produced by the transducer is a function of the crystals within it (Patrick, 2010). A wide range of transducer frequencies is currently available from low frequency transducers imaging at 2.0 MHz to high frequency transducers imaging at 10.0 MHz. Ultra high frequency transducers exist for specialty imaging. The lower the transducer frequency the deeper the penetration, but less resolution. Routinely, 7.5 MHz penetrates a depth of 4-6 cm, 5 MHz penetrates 10-12 cm, 3.5MHz penetrates 15-20 cm and 2.5 MHz penetrates 25-30 cm. To reach superficial structures a standoff pad can be used to transfer the focal zone to a higher level (Allen and Stone, 1990). The selection of the appropriate transducer for an examination depends upon the structure being evaluated, and the depth of the area from the transducer surface and the acoustic properties of the intervening tissues (Powis, 1986).

2.3.6 Ultrasound image formation

The formation of image in ultrasonography is based on the principle of pulse echo (Hangiandreou, 2003; Kremkau, 2011c). As pulse transmits through the patient, sound waves are reflected back to the transducer from each tissue interface. In between, the transducer is dampened to stop the piezoelectric crystal from vibrating. The electric signals generated from the returning echoes are amplified to form the final image. Two modes of echo display are commonly used in ultrasonography: brightness mode (B-mode, B scan, or

gray scale) and motion mode (M-mode). B-mode is used commonly in both abdominal and cardiac imaging. M-mode is used only for echocardiography (Kremkau, 2011c).

2.3.6.1 B-Mode: B-mode displays a static image of a section of a tissue (Daniela, 2011). They are made up of collection of dots that corresponds to the amplitude and strength of the returning echo (Kremkau, 2011e). These dots are displayed on a black background, and the brightness of the dot is highest (whitest) for the strongest returning echoes. The greater the amplitude the, the brighter the dot on the image.

2.3.6.2 M-mode: M-mode is a time motion displayed on the ultrasound wave along a chosen ultrasound line (Anon 4, 2017). It displays a static image of a section of a tissue. The echo generated from a single ultrasound wave passes through a moving structure and are acquired and displayed as a function of time on the horizontal axis. The motion pattern allows functional evaluation of moving structures such as the heart (Daniela, 2011). M-mode provides a monodimensional view of the heart and thus used only for echocardiography (Kremkau, 2011c). It has an advantage of very high sampling rate, which results in a high time resolution so that even very rapid motions can be recorded, displayed, and measured (Anon 4, 2017). The disadvantage is that the ultrasound line is fixed to the tip of the ultrasound sector.

2.3.7 Artifacts

Artifacts are present in ultrasound, they are often part of the images, and may lead to misinterpretations (Kirberger 1995; Feldman *et al.*, 2009; Hindi *et al.*, 2013).

In medical ultrasound, it is assumed that:

- Ultrasound waves always travel in straight lines from their emitting point.
- The lateral width and depth of the beam are narrow and constant.
- Each interface generates a single reflection.
- The intensity and location of echoes displayed as pixels on the monitor truly correspond to the reflecting power and anatomical location of structures being scanned.
- The speed of the ultrasound waves and the coefficient of attenuation are constant within tissues.
- Each echo seen on the screen comes from the most recently transmitted wave.

In reality, these assumptions are theoretical, and the sound interaction with biological tissues is complex and responsible for many explained and unexplained artifacts. Additionally, the understanding of physical properties of artifacts has been studied *in vitro* by several authors (Barthez *et al.*, 1997; Heng and Widmer 2010).

2.3.7.1 Acoustic shadows: Acoustic shadows are areas of decreased echogenicity below a dense object with high reflectivity (Park *et al.*, 1981; Penninck, 2002). It occurs if the primary beam is almost completely reflected or absorbed. An insufficient quantity of echoes returned from the location distal to the strong reflector makes these regions appear anechoic (black). This type of artifact is useful because it gives information about the composition of the structure causing the shadowing. Bone, air, foreign bodies and calcification stops the transmission of sound waves producing a ‘sonic shadow’ which is a

dark region distal to the echogenic obstructing region. Acoustic shadowing artifacts are minimized with spatial compounding (Heng and Widmer, 2010; Kremkau, 2011a). This may allow a lesion hidden by a shadowing artifact to be identified. Conversely, the composition of a structure may be misinterpreted because it is not shadowing (Hangiandreou, 2003).

2.3.7.2 Acoustic enhancement: This is an area of increased echogenicity behind structures of low attenuation (Kirberger, 1995; Penninck, 2002; Kremkau, 2011a). It mostly occurs at sites distal to cysts, gallbladder and urinary bladder and appears as a hyper intense (hyperechoic) signal. The attenuation of ultrasound wave in fluid is much lower compared to other tissues; therefore tissues distal to the fluid are enhanced. Artificial enhancement may also be found distal to a homogenous solid tumor surrounded by adipose fat (Kremkau, 2011a).

2.3.7.3 Reverberation artifacts: They occur when the sound waves encounter an area of high reflectivity such as bowel gas and the sound is reflected towards the transducer. They are produced from multiple reflections of sound wave, if the acoustic impedances of tissue layers are too much different and the detected echo does not run the shortest sound path because it bounces back and forth between the object and transducer (Park *et al.*, 1981; Feldman *et al.*, 2009). They appear as multiple hyperechoic foci that occur at regular intervals.

2.3.7.4 Comet tail artifacts: This is another form of reverberation artifact that appears as a series of short, very closely spaced successive echoes that are typically decrease in intensity and width in depth. They are caused by two closely spaced, discrete highly

reflective surfaces (Feldman *et al.*, 2009; Kremkau, 2011a). When gas bubbles form thin layers separated by liquid just as in the digestive tract, the waves rebound between the layers, resulting in many echoes that return to the probe at regular intervals, making a trail of echoes in the form of a shadow looking like a comet's tail.

2.3.7.5 Ring-down artifacts: This is also a variation of reverberation artifact that appears as a series of short parallel reflective lines that extends behind a gas collection. It occurs when ultrasound wave reverberates within fluid trapped between collections of air bubbles (Feldman *et al.*, 2009; Kirberger, 1995).

2.3.7.6 Mirror-image artifacts: This type of artifact occurs when a highly reflective and obliquely oriented surface reflect sound beam distally instead of returning it to the transducer (Daniela, 2011). It appears as a duplication of a normal structure on the opposite side of a strong reflector (Kremkau, 2011a). This goes against the assumption that echoes return to the transducer after a single reflection and that sound wave travel in a straight line (Feldman *et al.*, 2009). This is most commonly encountered when the liver is imaged with the diaphragm/lung interface is acting as a strong reflective surface.

2.3.7.7 Side lobes and grating lobe artifacts: Side lobes and grating lobes are different types of secondary lobes present on the side of the primary sound beam. Side lobes are present in all transducers and originate from additional mode vibrations of the piezoelectric crystal. They are usually of low intensity and can create spurious echoes in the near field. Grating lobes are associated with the geometric construction of linear probes (Barthez *et al.*, 1997). The artifacts created by secondary lobes result in misplacement of reflected echoes. The side or grating lobes are weaker than the primary sound beam. These lobes must encounter

a highly reflective surface and be of sufficient intensity to be noticed. In clinical situations, secondary lobe artifacts are difficult to differentiate from volume-averaging artifacts.

2.3.7.8 Slice thickness artifacts: These occur when the ultrasound beam is wider than the diameter of the cystic structure being scanned and include normal structures which lie immediately close to the cystic structure, the echoes from the tissues are displayed within the cystic structure mimicking the presence of a pseudo-sludge (Daniela, 2011). This does not occur when the entire beam width includes the cystic structure alone. Thus slice thickness artifacts are avoided when the beam width is narrowed, such as in the focal zone of the beam. The surface of a pseudo-sludge is curved while the surface of a real sludge is flat (Penninck, 2002).

2.3.7.9 Refraction: This occurs when a sound wave changes in direction on passing from one medium to the other. It occurs when sound waves travel from one tissue of different acoustic velocities, its frequency remains the same but its wavelength changes (Daniela, 2011). As the sound wave moves to the new medium it deviates resulting in display of organs in incorrect locations, usually to the side of their actual location (Feldman *et al.*, 2009; Kremkau, 2011a). Refraction artifacts may lead to measurement errors because organs may appear wider than normal (Kremkau, 2011a).

2.3.7.10 Edge-shadowing artifacts: They are a form of refraction artifacts that are produced when sound waves deviate as they encounter a curved surface tangentially (Kirberger, 1995). As a result of the sound waves that have been deviated by the curved surfaces, areas of anechoic regions are seen distal to the curved surface. This type of artifact is most

commonly encountered when the kidneys, urinary bladder, or gallbladder is imaged and can be eliminated with spatial compounding (Heng and Widmer, 2010).

2.4 Normal Ultrasonography Appearance of the Liver

The canine liver is made up of four lobes, four sub lobes, and two processes – left lobe (lateral and medial), quadrate lobe, right lobe (lateral and medial), and caudate lobe (caudate and papillary processes) (Evans 1993; Hudson and Hamilton 1993). Ultrasonographically, it is difficult to distinguish the division between the liver lobes except in the presence of peritoneal effusion (Larson, 2013). The liver is located within the ribcage just cranial to the stomach, with its cranial margins against the diaphragm and lung interface. Sonographically, the diaphragm appears as a curved hyper echoic line which is the interface of the diaphragm and the bright reflector of air in lung in the far field (Nathalie, 2010; Larson, 2013). This hyper echoic line is sometimes associated with a ‘mirror image’ artifact caused by multiple echoes at the strongly reflective interface with air filled lungs thus giving the false impression of liver on both sides of the diaphragm (Nathalie, 2010; Larson, 2013).

2.4.1 Echogenicity and ecotexture of the liver

Normal hepatic parenchyma is homogeneous and uniform in echogenicity with uniform texture (coarser echo texture than spleen) (Nyland *et al.*, 2002; Ivancic and Mai, 2008). Echogenicity is usually evaluated in comparison with adjacent structures such as the falciform fat, the right renal cortex, and spleen. Falciform fat is generally isoechoic (same as) or hyper echoic (brighter than) when compared to normal hepatic parenchyma. The

echo texture of falciform fat is coarser than hepatic parenchyma. The liver is generally hypo echoic when compared to normal spleen and this comparison should be done at the head of the spleen where depth is similar and allows for better comparison. When in comparison with

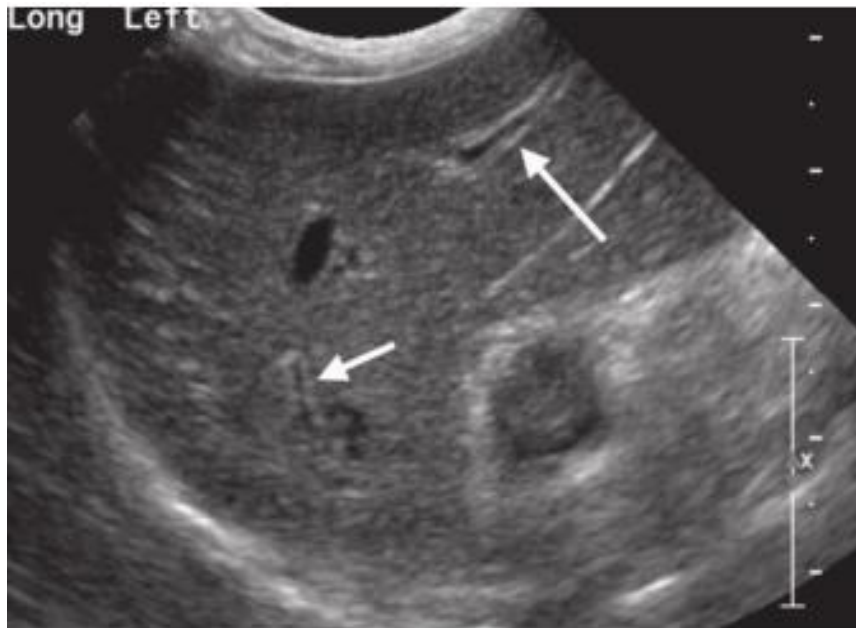


Plate 2.2. Long-axis image of a normal canine Liver. The hyperechoic line along the left side of the image, represents lung-diaphragm interphase; the arrows mark the hyperechoic portal vessels.

the renal cortex the liver may be isoechoic (same as) or mildly hypoechoic (darker than) (Nyland *et al.*, 2002; Ivancic and Mai, 2008).

2.4.2 Evaluation of the liver size

The ultrasound evaluation of liver size/volume is subjective and based on operator experience (Godshalk *et al.*, 1988). A small liver is not easy to assess sonographically because of cranial displacement of the stomach, limiting the imaging window (Larson, 2013). Liver size may appear decreased in dogs with a deep thoracic cavity wherein liver location is more completely within the costal arch and the stomach may interfere with its evaluation (Larson, 2013). Intercostal ultrasound windows may be needed in these patients. Conversely, in small dog breeds, the liver normally extends to the costal arch. It may also extend beyond that point in some small breeds of dogs, particularly in puppies (d' Anjou and Penninck, 2015). The enlarged liver can be examined relatively easily with ultrasound because it extends well beyond the xiphoid cartilage and covers the right kidney more completely.

2.4.3 Hepatic vasculature

The hepatic and portal veins (PVs) of each of these hepatic lobe divisions are relatively constant in dogs and can represent useful ultrasonographic landmarks (Carlisle *et al.*, 1995). Hepatic and portal veins are routinely visualized sonographically within hepatic parenchyma. Portal veins are smoothly tapering anechoic tubular structures characterized by bright, echogenic borders (Nyland *et al.*, 2002). The larger left and smaller right branch originate from the main portal vein near the porta hepatis, although they branch in different imaging planes (Wu and Carlisle, 1995). Hepatic veins are anechoic linear structures

extending through the parenchyma. Hepatic vein borders are not echogenic with the exception of their confluence with the caudal vena cava, immediately adjacent to the diaphragm. The right lateral dorsal intercostal window provides an excellent window to the aorta, caudal vena cava, and main portal vein. The main PV is more convoluted than the CVC and aorta, and curves a little to the right side before entering the liver. When measured at the level of the porta hepatis, its luminal diameter ranges between 3.4mm and 5.0mm in normal cats and between 3.3mm and 10.5mm in normal dogs. When comparing the maximal luminal diameter of the PV and the aorta, PV/aorta ratios of 0.71–1.25 are normally expected in these two species (d'Anjou *et al.*, 2004). Normal hepatic arteries are not visualized easily without color Doppler examination (Larson, 2013). The caudal vena cava can be visualized coursing through the liver in the right lateral abdominal quadrant.

2.4.4 Mean portal flow velocity

Portal flow mean velocity can be measured with spectral Doppler, after the use of an insonation angle correction of less than 60°. Portal flow mean velocity can be calculated by the ultrasound system by using the consistent insonation technique, which requires the application of a sample gate volume that fills the entire width of the main PV. On the other hand, a sample gate volume that fills approximately half of the vessel lumen placed in its center can be used to obtain maximal flow velocity. Because of the parabolic pattern of the portal flow, mean portal flow velocity can then be estimated by multiplying this result by 0.57. Mean portal flow velocities have been reported to range between 15 ± 3 and 18 ± 8 cm/s in normal dogs and 10–18 cm/s in normal cats (Nyland and Fisher 1990; Lamb and Mahoney 1994; Lamb 1996; d'Anjou *et al.*, 2004). However, these measurements are

prone to imprecise estimations, especially with higher correction angles (more than 60°), and must as a result be used cautiously.

2.4.5 Factors affecting the visibility of hepatic portal vein

The visibility of the larger and smaller branches of these veins is influenced by patient size, vascular luminal diameter, portal flow, pressure in the caudal vena cava (CVC), hepatic parenchymal echogenicity, and image quality and resolution (d' Anjou and Penninck, 2015). When measured at the same depth, the hepatic and portal branches should be relatively similar in diameter. The use of color Doppler facilitates the identification and distinction of hepatic vessels (d' Anjou and Penninck, 2015).

2.4.6 Gall bladder

The gallbladder (GB) is seen ultrasonographically as an oval, anechoic structure in the right cranio-ventral portion of the liver. It has a thin uniform echogenic wall. The normal canine gallbladder wall typically measures 2 to 3 mm (Spaulding, 1993 and Hittmair *et al.*, 2001). Echogenic gravity dependent material within the lumen is common in dogs and generally a benign finding in the absence of other significant ultrasonographic and clinical findings (Tsukagoshi *et al.*, 2012). GB sludge in can be prognostic of rise in liver enzymes and total bilirubin (Harran *et al.*, 2011), but it may also be encountered without evidence of biliary disease.

2.4.7 Gall bladder volume

Gallbladder (GB) volume can be estimated using the ellipsoid method (Penninck *et al.*, 2010). It can vary markedly in size and become quite large in anorexic patients, so that GB

volume alone cannot be used as a reliable sign of biliary obstruction. Yet, monitoring its reduction postprandially may help to rule out outflow obstruction. In cats, GB width can be used to predict its postprandial change in volume (Diana *et al.*, 2012).

2.5 Ultrasonographic Features of Hepatic Disorders

There are quite a number of hepatic disorders that are found in dogs and causes focal, multifocal or diffuse hepatic disorders. When evaluating the liver for these disorders, several parameters must be taken into account which includes liver size, contour, parenchyma ecogenicity, ultrasound beam attenuation as well as distribution of abnormalities. Although some of these parenchymal alterations have characteristic ultrasonographic features, most changes are not pathognomonic of one process. Therefore a more specific diagnosis is usually based on the combination of clinical presentation, laboratory analysis such as biochemical tests, histopathology and ultrasonographic findings.

2.5.1 Diffuse hepatic parenchymal disease

Diffuse parenchymal diseases can be difficult to differentiate from poorly defined multifocal diseases. Typically, these disorders affect all lobes and may appear as isoechoic, hypoechoic or hyperechoic to the expected appearance (Nathalie, 2010). These disorders can also affect the parenchymal uniformity and distort the hepatic margin. The evaluation of the liver contour is facilitated by the presence of peritoneal effusion.

2.5.1.1 Hepatitis, cholangitis/cholangiohepatitis, and cirrhosis: Diffuse hepatic inflammatory conditions can exhibit variable ultrasonographic features. In cases of dogs with acute cholangitis/cholangiohepatitis, the liver is commonly associated with a decrease

in parenchymal echogenicity and an increased visibility of the portal vasculature (Newell *et al.*, 1998), although the liver may appear normal, hyper echoic or heterogeneous (Penninck and Berry, 1997; Marolf *et al.*, 2012). Additionally, this process is often associated with biliary anomalies, such as biliary sludge, cholelithiasis, or wall thickening, and with pancreatitis (Nathalie, 2010). In dogs, acute hepatitis also tends to cause diffuse liver hypo echogenicity, as seen with leptospirosis. Chronic liver inflammatory processes, on the other hand, tend to be associated with fibrosis, which typically results in increased echogenicity. The presence of chronic active inflammation, consisting of a mixture of inflammatory cells, edema, fibrosis, necrosis, as well as regenerative nodules (hyperplasia) can cause a markedly heterogeneous liver with variable echogenicity. Although cirrhosis classically causes the liver to appear small, hyperechoic, and irregular in contour, its appearance can vary and sometimes mimic neoplasia.

2.5.1.2 Metabolic conditions: Metabolic conditions that most commonly causes diffuse parenchymal disorders in dogs include hepatic lipidosis, steroid induced and vacuolar hepatopathy. These hepatoopathies usually causes hepatomegally and are associated with diffuse increase in parenchymal ecogenicity, making vessel walls indistinct and difficult to detect (Nathalie, 2010). Degenerative vacuolar hepatopathy is often present with other primary disorders in dogs (Wang *et al.*, 2004). The parenchyma can also appear hyper attenuating, i.e., result in excessive sound-beam attenuation. Consequently, the far gain must be increased (or bottom time gain compensation causes liver to appear small, hyperechoic, and irregular in contour, its appearance can vary and sometimes mimic neoplasia. However, chronic hepatitis and its ultimate outcome, cirrhosis, usually do not cause hepatic enlargement, as opposed to massive neoplastic infiltration.

2.5.1.3 Hepatic neoplasia: Hepatic neoplasia can occur as diffuse, multi-focal or focal disease. The most common neoplasms that may lead to diffuse changes and remain ultrasonographically undetectable include mast cell tumor, lymphoma, and histiocytic sarcoma. These conditions are usually characterized with generalized hepatomegally and have variable echogenicity (Whiteley *et al.*, 1989; Lamb *et al.*, 1991; Nathalie, 2010). Histiocytic neoplasms are more commonly associated with hypoechoic nodules and masses, although diffuse hepatic hypoechogenicity has been reported (Cruz-Arambulo *et al.*, 2004). Conversely, mast cell infiltration of the liver tends to cause diffuse hyperechogenicity (Sato and Solano 2004), although, as for other round-cell infiltrations, several manifestations are possible. Hepatic carcinomas can also be diffuse, or involve multiple lobes, with a variable ultrasonographic appearance that depends on the presence of necrosis, inflammation, hemorrhage, or cavitation. A mixed pattern of echogenicity is common with these malignant tumors.

2.5.1.4 Miscellaneous diffuse hepatic disorders: Other types of hepatopathies can be encountered in small animals, although less commonly. Amyloidosis can cause hepatic enlargement and parenchymal ultrasonographic changes. The liver tends to become diffusely heterogeneous with mixed hyperechoic and hypoechoic foci (Beatty *et al.*, 2002). Spontaneous hepatic rupture and hemoabdomen can also be caused by massive hepatic amyloidosis. In dogs with hepatocutaneous syndrome (superficial necrolytic dermatitis), the liver can become highly hyperechoic with diffusely distributed 0.5–1.5 cm-wide hypoechoic regions, producing a honeycomb pattern (Nyland *et al.*, 1996).

2.5.2 Focal hepatic parenchymal disorders

Focal or multifocal hepatic changes are easily visualized sonographically due to the uniform background of the liver parenchyma and the sensitivity of the ultrasonography in detecting focal hepatic lesions. Nyman *et al.*, 2004, suggested that well-differentiated carcinomas exceeding 5mm can be identified in an ideal imaging condition in humans. Focal hepatic disorders can be caused by conditions which include primary or metastatic neoplastic disease, cyst, haematomas, abscesses, granulomas, lobar torsion, and thrombosis (Nathalie, 2010). These hepatic conditions may appear as isoechoic, hypoechoic, hyperechoic or mixed echogenicity. The conspicuity of a focal lesion is also greatly influenced by its imaging characteristics. Hence, for a given size, an anechoic cyst is more likely to be detected than a soft-tissue nodule of echogenicity similar to one of adjacent normal parenchyma. Although many different types of focal lesions can be detected with ultrasonography, the appearance of several of these processes is quite variable, resulting in limited diagnostic specificity. The advances in contrast harmonic ultrasonography have helped to increase the overall diagnostic accuracy and may prove to be useful in clinical settings (Nyman *et al.*, 2004; O'Brien *et al.*, 2004). Although some trends in ultrasonographic appearance have been reported for some of these processes, a definitive diagnosis usually requires fine-needle aspiration or biopsy.

2.5.2.1 Benign hyperplasia and neoplasia: Benign nodular hyperplasia is common, particularly in dogs, and accounts for many focal hepatic lesions identified with ultrasonography. Although these regenerative nodules can vary in echogenicity and size, they tend to appear as hypoechoic nodules measuring less than 5–15mm wide (Stonewater *et al.*, 1990; O'Brien *et al.*, 2004). As for most other types of focal lesions, their margin can

be well or poorly defined. Benign hepatic adenomas cannot be differentiated from carcinomas or hepatomas appear as masses of variable size and are usually isoechoic to hyperechoic, although they may also present cavities (O'Brien *et al.*, 2004).

2.5.2.2 Malignant neoplasia: Hepatocellular carcinoma is the most common hepatic malignant neoplasia in dogs, although other malignant hepatic neoplasia includes carcinoids, sarcomas, carcinomas and bile duct carcinomas (Liptak *et al.*, 2004). The liver is the primary target for metastasis, mainly through the portal system which drains most abdominal structures. The neoplasm originates mainly from spleen, pancreas and gastrointestinal tract (Nathalie, 2010). Metastatic neoplastic processes have variable tissue characteristics such as tissue density, vascular pattern, necrosis, liquefaction and calcification which all cause variable ultrasonographic appearances (Whiteley *et al.*, 1989; O' Brein *et al.*, 2004). Focal hypoechoic lesions with hyperechoic center also termed target lesions are usually predictive of metastasia although benign processes such as nodular hyperplasia can cause a similar pattern (Cuccovillo and Lamb, 2002; O' Brein *et al.*, 2004). Other features supportive of malignancy include lesion size (<3cm) and presence of peritoneal effusion (Guillot *et al.*, 2009; Mukarami *et al.*, 2012). Additional features differentiating malignant from benign hepatic masses may be found with triple- phased computed tomography (CT) (Katura *et al.*, 2013).

2.5.2.3 Cavitory lesions: Necrosis, neoplasms, Hepatic and biliary cysts are the main cause of cavitory lesions in in Dogs. They appear as well defined regular or irregular anechoic structures, typically associated with distal acoustic enhancement. Cysts are localized lesions surrounded by normal parenchyma. These cavitory lesions must be differentiated from cystic tumours such as cystadenocarcinomas, cystadenomas commonly demonstrating a

multilobular pattern and a change in tissue appearance around the anechoic cavitation (Nyland *et al.*, 1999). Hepatic abscess in dogs appears poorly margined, round to oval, regular or irregular, hypoechoic lesions which are often cavitated (Schwarz *et al.*, 1998). Parasitic cyst occurring with liver flukes or hydatid disease can look similar to abscess with addition of mineralization (Nyland *et al.*, 1990).

2.5.2.4 Granulomas, hematomas, and mineralization: Hepatic granulomas or pyogranulomas can sometimes be found in dogs and associated with fungal diseases, feline infectious peritonitis or with feline eosinophilic fibroplasia (Weissman *et al.*, 2012). In humans, granulomatous lesions tend to appear ultrasonographically as hyperechoic and non-homogeneous (Mills *et al.*, 1990). Hepatic hemorrhage is rare condition in dogs and is usually associated with hemangiosarcoma or trauma (Whiteley *et al.*, 1989). Ultrasound-guided procedures such as biopsies can also cause hepatic hematomas and has variable ultrasonographic changes related to clot organization and resorption. With time, hematomas tend to develop a cystic component following clot lysis. This feature, as well as the progressive reduction in size on follow-up exams, should help in differentiating spontaneous hematomas from neoplastic processes. Hepatic mineralization other than cholelithiasis can accompany benign processes (such as hematoma or granuloma) or malignant processes. Mineralization typically appears as strongly hyperechoic foci associated with acoustic shadowing.

2.5.2.5 Hepatic lobe torsion, infarction, and gas: Liver lobe torsion is a rare condition in dogs and can cause acute or abdominal effusion (Nathalie, 2010). The torsion leads to lobar congestion, hemorrhage, necrosis, can show variable signs that can mimic neoplasia or abscess formation. Ultrasonographically, the affected lobe was commonly hypoechoic or

mixed in echogenicity, and Doppler assessment of the lobe revealed reduced vascularity in many dogs (Hinkle Schwartz *et al.*, 2006). Infarction is less common in the liver when compared with the spleen, but can show a similar pattern of an irregular and poorly echogenic area with reduced flow on color Doppler or power Doppler. Hyperechoic foci associated with reverberating artifact, consistent with gas, can be seen in the liver, most often in the biliary tract, following surgery. Gas can also form because of bacterial infection. Metallic clips used with surgical biopsies appear as short, strongly hyperechoic lines with reverberation, mimicking gas. A radiograph can be used, if needed, to differentiate gas from metal.

2.5.2.6 Peliosis hepatis: Peliosis hepatis is a condition that is characterized by random distribution of dilated vascular spaces in the hepatic parenchyma; it occurs in old dogs and can be mistaken for a vascular tumor, haemangioma or haemangiosarcoma (Cullen *et al.*, 2006; Cullen, 2009).

2.5.3 Disorders of the biliary system

2.5.3.1 Congenital cystic anomalies of the biliary tree: Congenital cystic anomalies of the biliary tree originate from malformation of the ductal plate (Santiago *et al.*, 2012). They can affect any part of the biliary tree including the intra and extra biliary ducts. The lesions may be located on the larger bile ducts and extra hepatic ducts and as such categorized as Caroli's disease (Last *et al.*, 2006) or cholangiocyst if they affect the pancreato-biliary ductal junction (Best *et al.*, 2010). The anatomical complexity of these lesions makes it difficult to differentiate them from obstructive biliary disease, but clinically they have no evidence of obstructive biliary disorders. Identification of a GB and the connection of the

extrahepatic bile ducts to the common bile duct (CBD) are paramount in diagnosing these anomalies. Commonly, these segmental dilations are associated with inflammation or infection. Thickening of the biliary duct walls and echogenic bile are then noted. Congenital polycystic disease involving the kidneys, liver and pancreas is well reported in cats (Bosje *et al.*, 1998). The concurrent presence of multiple cysts in the kidneys assists in the diagnosis of this condition. Agenesis of the GB is rare and the segmentally dilated CBD is often confused for the GB, but identifying the extrahepatic ducts' connection to the dilated CBD is useful. At times, CT or magnetic resonance imaging (MRI) may assist in further characterizing the distribution of these lesions.

2.5.3.2 Biliary obstruction and other causes of biliary ectasia: Biliary obstruction is common in dogs and usually results in icterus. It is routinely assessed with ultrasonography which is an important imaging modality for assessing the icteric dog (Nathalie, 2010). After complete obstruction of the Common bile duct, retrograde dilatation is expected that initially affects the common bile ducts and gallbladder, followed by the extra- and intrahepatic ducts (Nyland and Gillett 1982). With extra hepatic biliary obstruction, the cystic duct and common bile ducts dilate and often become tortuous proximal to the site of obstruction. A common bile duct more than 4–5mm wide is usually predictive of obstruction in small animal (Léveillé *et al.*, 1996; Gaillot *et al.*, 2007). Ultrasonographically within 5–7 days, irregular and tortuous anechoic tubes with hyperechoic walls can be found in the liver, following the more linear portal veins and unassociated with color flow, indicating dilated hepatic ducts. This sign, also referred to as the “too many tubes” sign, is usually indicative of complete obstruction. Additionally, these

anechoic tubes can be associated with acoustic far enhancement, which is not expected with vessels that contain a more attenuating cellular fluid (Nyland and Gillett 1982).

Although the GB can be dilated with biliary obstruction, wall contraction or inflammation possibly associated with fibrosis can limit its capacity to distend. Furthermore, reduced compliance of the peripheral liver parenchyma may limit GB dilatation. Gallbladder dilatation was in fact seen in <50% of cats with extra hepatic biliary obstruction (Gaillot *et al.*, 2007). Thus, the absence of GB distension should not be used to rule out biliary obstruction.

2.5.3.3 Biliary sludge and cholelithiasis: Sludge is routinely identified in dogs and is composed of a complex mixture of cholesterol crystals, precipitated bile pigment, mucin and bile salts. Sonographically it appears as echogenic debris which is mobile and changes with body position, causing swirling and redistribution. It is usually considered non-significant especially in dogs. In cats it has been associated with elevated serum liver parameters and could predict hepatobiliary disease (Harran *et al.*, 2009). Sludge balls are accumulation of thick bile and can be found in the gallbladder lumen or within the bile duct. They are round and non-shadowing structures of moderate echogenicity (Nathalie, 2010). Mineralized and non-mineralized materials can also be found in the bile ducts. Choleliths can occur more commonly in dogs, and appear as hyperechoic structures of variable size, number and shape which can produce acoustic shadowing.

2.5.3.4 Thickening of the gallbladder: Gallbladder wall thickening (>1mm) can be caused by inflammation (cholecystitis/cholangitis/cholangiohepatitis), edema (portal hypertension, hypoalbuminemia, biliary obstruction, or inflammation), cystic mucosal hyperplasia, or,

rarely, neoplasia (Spaulding 1993; Hittmair *et al.*, 2001). In case of gallbladder inflammation, the chronicity and severity of the process influence the appearance of the wall. The thickened wall may have a double-rim pattern (particularly in acute cases) or diffuse wall hyperechogenicity. Gallbladder wall thickening is also seen with right-sided congestive heart failure and sepsis, and neoplasia (Nyland and Hager, 1985; Rivers *et al.*, 1997; Nyland *et al.*, 2002; d'Anjou, 2008). Peritoneal fluid surrounding the gallbladder can result in a false impression of wall thickening. Gallbladder thickening may be permanent as a result of inflammation and fibrosis despite resolution of the underlying disease. In dogs, the normal GBW (<2mm) is either poorly visualized or appears as thin hyperechoic line, and the ability to accurately measure GBW depends on the angulation of the sound beam and degree of GB distension (Aguirre, 2010).

2.5.4 Disorders of the hepatic and portal vasculature

2.5.4.1 Congenital portosystemic shunt (PSSs): Congenital PSSs are single large calibre connections between the portal vein and systemic veins that allow blood from the intestine to bypass the liver. It is one of the most common vascular anomalies in dogs. The use of ultrasonography in the detection and characterization of these anomalies has been well described (Lamb 1996; Lamb *et al.*, 1996a; d'Anjou *et al.*, 2004; Szatmari *et al.* 2004; d'Anjou 2007). Congenital PSSs are most often single. Double shunting loops anastomosing before entering the systemic circulation were reported to be more common with shunts originating from the right gastric vein in dogs (Szatmari *et al.*, 2004). A congenital shunt can be intrahepatic or extrahepatic in location. Intrahepatic congenital shunts occur predominantly in large-breed dogs and are often attributable to a patent ductus venosus, originating from the left branch of the portal vein. If originating from the right

branch of the portal vein, they drain directly into the caudal vena cava. Extrahepatic congenital PSSs occur more commonly in small-breed dogs (e.g. Yorkshire, Maltese and Cairn Terriers, Miniature Schnauzers) and connect the portal vein to the caudal vena cava or to another vein. Acoustic windows include the subxiphoid as well as a high right dorsal one. For the latter, the dog is placed in left lateral recumbency with the limbs positioned either toward or away from the ultrasonographer. A window is found in the intercostal spaces of the last three ribs, relatively close to the spine, until the liver is visualized cranial to the right kidney. In cross-section, the aorta, caudal vena cava and portal vein can be identified adjacent to one another. (Nathalie, 2010). The shunting vessel can be identified coursing between the vena cava and portal vein. Furthermore, measurement of portal vein size can also be made in this window. The size of the portal vein cranial to the shunt is generally reduced in diameter. A portal vein: aortic ratio of ≤ 0.65 is predictive for the presence of an extrahepatic shunt, and a value of ≥ 0.8 excludes it (Nathalie, 2010). If the ratio is ≥ 0.80 , other types of disease, such as microvascular dysplasia, intrahepatic shunt and portal hypertension attributable to chronic liver disease with secondary shunting, could still be present (Nathalie, 2010). The sensitivity and specificity of ultrasonography for the detection of extra hepatic PSSs have been reported to be 80.5% and 66.7%, respectively. A greater sensitivity of 100% was seen for intrahepatic PSSs alone (Nathalie, 2010).

2.5.4.2 Acquired: Multiple acquired PSSs occurs secondary to chronic portal hypertension and result in reduced blood flow to the liver. Causes of portal hypertension are many and include chronic liver disease, diffuse nodular regeneration, infiltrative neoplasia, congenital hypoplasia of the portal vein, arteriovenous fistula and portal vein thrombosis or extra luminal compression (Nathalie, 2010). Multiple small collateral tortuous vessels form

connecting the portal vein or its tributaries to the caudal vena cava. Screening of the mid-abdomen is recommended to evaluate these vessels. The vessels may develop collateral circulation by way of the renal vein and lead to clinical signs of PSS. Ascites is commonly found on ultrasonography in association with portal hypertension and the blood flow is reduced, seen on spectral Doppler ultrasonography, to mean velocities of 10 cm/s (Nathalie, 2010).

Portal hypertension:Chronic liver disease, particularly involving fibrosis and diffuse nodular regeneration (cirrhosis) or infiltrative neoplasia, can cause reduced portal vein compliance and increased pressure. Portal hypertension can also be caused by congenital or developmental portal hypoplasia (also termed non-cirrhotic portal hypertension), arterioportal fistula, portal thrombosis, or portal vein compression from an extra luminal mass. Ultrasonographically, portal hypertension can be manifested by the presence of ascites and signs of edema involving several structures, such as the gallbladder wall and pancreas. Portal hypertension is suspected when the portal flow is significantly reduced in velocity (mean <10 cm/s) or reversed (hepatofugal), especially if the vein is normal in size or dilated (Nyland and Fisher 1990; d'Anjou *et al.*, 2004). However, flow reduction or reversal may not be observed at the time of the exam. Sustained portal hypertension leads to the opening of pre-existing collateral vessels that connect the portal system to the systemic circulation.

Arteriovenous fistula:This condition can be congenital or acquired and causes a linkage between the portal veins and the hepatic arteries. The resulting high pressure over loads the venous side and hypertension occurs. Acquired portosystemic shunt is formed because of the portal hypertension and clinical signs of shunting occur. Ultrasonographically, the

portal vein can become markedly enlarged and flow reversal can be observed with Doppler (Zsatmari *et al.*, 2004). Intrahepatic tortuous and dilated branches may be difficult to visualize ultrasonographically (Zwingenberger *et al.*, 2005).

Portal vein thrombosis:Thrombosis of the portal vein occurs with many diseases that are associated with the development of coagulopathies. They are recognized ultrasonographically as intraluminal structures of moderate to high echogenicity and the absence of colour Doppler signals within the lumen (Nathalie, 2010). Thrombosis can be focal or diffuses into all branches of the portal venous system and cause acquired shunting. Free peritoneal fluid may develop.

2.6 Imaging Modalities for Evaluating the Hepatobiliary System

2.6.1 Radiography

Routine abdominal radiographs are useful to determine liver size and may detect irregular liver borders. Mineralized densities that involve parenchyma or the biliary tree can reflect stasis of bile flow, dystrophic mineralization associated with congenital malformations, acquired duct “sacculation,” chronic duct inflammation, or choleliths. (Sharon and Center, 2016). Choleliths that contain enough calcium bilirubinate or calcium carbonate are radiographically visible. (Sharon and Center, 2016) A mass effect in the right cranial quadrant in suspected EHBDO may represent an engorged gallbladder, pancreatitis, neoplasia, or focal bile peritonitis. Radiographic suspicion of abdominal effusion (poor abdominal detail) may prompt diagnosis of bile peritonitis and ascitic effusion. (Sharon and Center, 2016) Gas within hepatic parenchyma or biliary structures indicates an emphysematous process (eg, cholecystitis, choledochitis, infected biliary cyst, hepatic

abscess, necrotic tumor mass) and warrants prompt antimicrobial therapy and either surgical intervention or percutaneous, ultrasound-guided aspiration/lavage. (Sharon and Center, 2016) Contrast studies of the portal vasculature are the gold standard for confirmation of a congenital portosystemic shunt. Radiographs should be taken in right and left lateral and ventrodorsal positions for best test sensitivity. (Sharon and Center, 2016).

2.6.2 Ultrasonography

Ultrasound (US) is frequently the first imaging modality used during the evaluation of suspected liver disease. The role of ultrasound in cirrhosis includes screening for hepatocellular carcinoma (HCC) and diagnosis of cirrhosis, portal hypertension, and HCC. Ultrasound is readily available, relatively inexpensive, radiation-free, and offers real time evaluation of the liver parenchyma, border, vascular architecture, and vascular flow (Tchelepi *et al.*, 2002; Elbagir *et al.*, 2014). Ultrasound with linear array transducers can offer high-resolution images of the capsule of the liver, picking up even subtle cases of nodularity. Ultrasound can detect cirrhosis with an accuracy of 64-79%, sensitivity of 52-69%, and specificity of 74-89% (Huber *et al.*, 2015). The ability to additionally evaluate for other signs and complications of cirrhosis, such as dilated portal vein/portosystemic collaterals, splenomegaly and ascites indicating portal hypertension, makes ultrasound an even stronger method for evaluation (Heller and Tublin, 2014). Color Doppler, a modality used in US, can show portal vein flow, flow reversal, and collateral flow, which help evaluate for portal hypertension. It has been noted that reversal of flow (hepatofugal flow) and/or collateral flow may be the only findings of cirrhosis in otherwise asymptomatic patients, showing the importance of color doppler in the evaluation of liver conditions like cirrhosis (Tchelepi *et al.*, 2002). Other findings on color Doppler include enlarged, tortuous

hepatic arteries (corkscrew appearance) suggesting increased flow velocity (Tchelepi *et al.*, 2002). There may also be stasis in the hepatic veins as in the case of thrombosis (Heller and Tublin, 2014). The limitations of ultrasound include operator dependence, and difficulty visualizing the entire liver. The main advantage of ultrasound is that it has a high negative predictive value for cirrhosis (Choong *et al.*, 2012).

2.6.3 Computed tomography

Abdominal computed tomography (CT) is a frequently used study obtained because of its wide range of utility. As a part of routine evaluation of the CT images, the liver is screened for fibrosis and parenchymal changes. Findings of liver conditions like cirrhosis on CT include an irregular/nodular surface, blunt liver edge, parenchymal and morphological changes, and signs of portal hypertension. The diagnostic accuracy, sensitivity, and specificity have been shown to be 67–86%, 77–84% and 53–68% (Kudo *et al.*, 2008; Huber *et al.*, 2015). Using a cirrhosis scoring criteria developed by Harbin *et al.* (1980) with the ratio of transverse caudate lobe width to transverse right lobe width, cirrhotic livers could be separated from non-cirrhotic livers with an accuracy, sensitivity, and specificity of 94%, 84%, and 100% (Harbin *et al.*, 1980). Limitations of diagnostic CT include cost and radiation exposure, making the radiation free and inexpensive ultrasound more appealing as an initial test. The advantage of CT imaging over ultrasound is its ability to detect HCC and perform staging post contrast injection (Huber *et al.*, 2015). The best predictive signs of liver cirrhosis on CT and MRI were liver parenchymal abnormalities, manifestation of portal hypertension, and morphological changes (Kudo *et al.*, 2008). In a multicenter study review by Kudo *et al.* (2008), MRI and CT were deemed superior in sensitivity to US in predicting cirrhosis since they evaluate the hepatic parenchyma and morphology better than

radiopharmaceutical is detected in the gall bladder or intestine. Another application of scintigraphy is used in the diagnosis of PSS in canines.

2.6.4 Magnetic resonance imaging

Magnetic resonance imaging (MRI) is another modality that can detect features of hepatic abnormality, including surface irregularity, heterogenous enhancement, and caudate lobe enlargement, splenomegaly, decreased right to left lobe volume ratio, varices, expanding gallbladder fossa, and ascites (Huber *et al.*, 2015). The sensitivity and specificity of contrast enhanced MRI for cirrhosis is similar to that of CT. However, by measuring the diameter of hepatic veins, particularly for a right hepatic vein $<7\text{mm}$, Zhang *et al.* (2009) shows an increase in detecting cirrhosis with a sensitivity and specificity of 88% and 85%. Through the use of MR elastography (MRE), double contrast enhanced MRI, diffusion-weighted MRI, susceptibility-weighted MRI, and T1rho, the detection of liver fibrosis in pre-cirrhotic stage was detected with great accuracy. MR elastography (MRE) may be the most reliable of these newer MRI based methods, as it appears to be more accurate for detecting fibrosis early and measuring the stiffness of the liver as a whole, with a sensitivity and specificity of 98% and 99% (Yin *et al.*, 2007). MRE is a magnetic resonance imaging (MRI) technique. It is the most precise noninvasive imaging technique for detection and staging of liver fibrosis. MRE of the liver is performed using an MRI safe passive driver that is applied to the right upper abdomen and lower chest overlying the right lobe of the liver while the patient is being scanned in the MRI scanner. The accuracy of MRE is better than routine serum liver function tests (Huwart *et al.*, 2007; Venkatesh *et al.*, 2014) for detection of significant and advanced fibrosis. In 2008, Huwart *et al.*, carried out a study and reported that the diagnostic accuracy of MRE (0.994 for $F >2$, 0.985 for $F >3$, and

0.998 for F >4) was higher than transient elastography (TE), serum aspartate aminotransferase to platelets ratio index (APRI) and the combination of TE with APRI (0.837, 0.709, and 0.849 for F >2; 0.906, 0.816, and 0.936 for F >3; 0.930, 0.820, and 0.944 for F >4, respectively). In the systematic review of 153 studies by Bonekamp *et al.*(2009), it was reported that MRE was the only noninvasive technique that was able to stage liver fibrosis or diagnose mild hepatic fibrosis with reasonable accuracy. Several more recent studies have attested to the ability of MRE to reliably differentiate between early and late stages of hepatic fibrosis. Compared to the standard anatomic evaluation of liver morphology, MRE performs significantly better for both significant fibrosis (0.989 in MRE vs 0.71 to 0.82 in MRI) and cirrhosis (0.935 in MRE vs 0.61 to 0.80 in MRI). (Venkatesh *et al.*, 2015). Using a 3.7-kPa cutoff value, the study by Venkatesh *et al.* (2014) found that MRE yielded a sensitivity of 91% and specificity of 80% for differentiating F0–F2 from F3–F4 grades of fibrosis. With a slightly lower threshold of 3.6 kPa on MRE, Loomba *et al.* (2014), showed similar results (sensitivity, 86%; specificity, 91%).The limitations of MRE are the cost and limitations in patients with hepatitis and congestive heart failure (Yin *et al.*, 2007).

2.6.5 Laparoscopy

Laparoscopy offers tremendous advantage of direct visceral visualization (three-dimensional) of the liver and adjacent structures such as the pancreas and extrahepatic biliary tract. Laparoscopy may reveal very small (0.5 cm or less) metastatic lesions that are not easily observed by other diagnostic techniques. Laparoscopy may also provide accurate, definitive and staging information that otherwise would have been obtained only through a surgical laparotomy. It also provides minimal invasive method to obtain cytology, biopsy,

and cultural samples from focal hepatic lesions or generalized disease condition/carcinomatous growth (Monnet and Twedt, 2003). It is seen that laparoscopy provides better liver biopsy tissues than any other traditional percutaneous methods especially when the liver is small (Hall and German, 2005). It also provides the advantage of procuring biopsy from areas visually that are less vascular and to monitor the extent of bleeding after a biopsy (Monnet and Twedt, 2003). It is preferred to percutaneous techniques when excess bleeding is expected and to laparotomy when delayed wound healing (hypoalbuminaemia) is anticipated. The minimal invasiveness of the procedure, rapid patient recovery, and diagnostic accuracy make laparoscopy an ideal technique compared with more invasive procedures. Despite the advent of newer laboratory tests, imaging techniques, and ultrasound-directed fine-needle biopsy or aspiration, laparoscopy remains a valuable tool when appropriately applied in a diagnostic plan. Ascites, abnormal clotting times, small body size (<2 kg of body weight), and poor patient condition are the only relative contraindications to laparoscopy. This technique requires heavy sedation or anaesthesia and is subject to equipment availability and clinician expertise.

2.6.6 Hepatobiliary scintigraphy

Cholescintigraphy with ^{99m}Tc -hepatobiliary radiopharmaceuticals has been an important, clinically useful diagnostic imaging study for almost 4 decades (Zeissman, 2014). Its strength lies in the fact that the diagnostic information provided defines pathophysiology rather than anatomy (Zeissman, 2014). It is capable of quantifying liver function but has mainly been evaluated in small animals for diagnosis of cholestasis and extrahepatic biliary obstruction (Boothe *et al.*, 1992; Newell *et al.*, 1996; Head and Daniel, 2005). Radiopharmaceutical agents used for hepatobiliary scintigraphy in dogs and cats are

usually derivatives of ^{99m}technetium iminodiacetic acid (mebrofenin or disofenin) (Bootheet *al.*, 1992; Newell *et al.*, 1996; Head and Daniel, 2005). After intravenous injection in normal animals, these compounds accumulate within the biliary tract and then pass into the intestines through the major duodenal papilla. If the intestines cannot be visualized within 3 hours of the injection of the agent, extrahepatic biliary obstruction is generally considered to be present. (Bootheet *al.*, 1992; Newell *et al.*, 1996; Head and Daniel, 2005). Scintigraphy shows prompt hepatic uptake and secretion into the biliary ducts but poor ductal clearance. It is best visualized in the common duct and seen at 1h after injection of the ^{99m}Tc-HIDA radiopharmaceutical. At 2h no further ductal clearance occurs or retention may be greater than at 1h (Zeissman, 2014). The main disadvantage of scintigraphy is that it is incapable of giving accurate information as to the exact site or cause of obstruction or of differentiating functional obstruction (e.g., from a thickened gallbladder wall or hepatic adhesions) from mechanical. Radiation safety issues, including patient isolation, must also be addressed.

2.7 Anatomy of the Canine Pancreas

2.7.1 Pancreas

The pancreas is a thin, elongated organ made up of the right and left lobes, which join to form a small, central body. It is located along the greater curvature of the stomach and the mesenteric border of the descending duodenum (Penninck and d'Anjou, 2015).

2.7.1.1 Right pancreatic lobe: The right lobe lies in the mesoduodenum, dorsomedial to the descending duodenum, ventral to the right kidney, and ventrolateral to the portal vein (Penninck and d'Anjou, 2015).

*2.7.1.2 Left Pancreatic lobe:*The left lobe originates at the pancreatic body, lies dorsocaudal to the gastric antrum, and continues across the midline between the stomach and the transverse colon. The normal left lobe is occasionally seen in the triangular region defined by the spleen, stomach, and left kidney (Penninck and d'Anjou, 2015).

*2.7.1.3 Body of the Pancreas:*The body of the pancreas lies caudal to the pyloric region, in the right cranial abdomen, and craniomedial to the right kidney and ventral to the portal vein (Penninck and d'Anjou, 2015).

*2.7.1.4 Pancreatic vasculature:*Blood supply to the pancreas originates from the celiac artery and is supplied via the splenic and hepatic arteries. The splenic artery is the primary blood supply to the left limb of the pancreas (Cornell, 2012). The hepatic artery terminates as the cranial pancreaticoduodenal artery, which enters the body of the pancreas and courses through the proximal portion of the right limb of the pancreas. Caudal pancreaticoduodenal artery, a branch of the cranial mesenteric artery, supplies and courses through the distal portion of the right limb of the pancreas. The cranial and caudal pancreaticoduodenal arteries anastomose within the right limb of the pancreas (Cornell, 2012).

*2.7.1.5 Pancreatic duct:*The pancreatic duct is a duct from each of the pancreatic limb connecting the pancreas to the bile duct to supply the pancreatic juice provided for the exocrine pancreas which aids in digestion (Goel, 2015). These ducts come together to form a Y shape. The tail of the Y forms the accessory pancreatic duct, or duct of Santorini, which empties into the duodenum at the minor duodenal papilla (Cornell, 2012). A second duct, the pancreatic duct or duct of Wirsung, emerges from the main duct of either the right or

left lobe and enters the duodenum adjacent to the bile duct at the major duodenal papilla (Cornell, 2012). The accessory pancreatic duct is the larger of the two ducts and transports the majority of pancreatic secretions to the duodenum. Anatomic variations in the canine pancreatic duct include the presence of an accessory pancreatic duct alone and the presence of three duodenal openings (Cornell, 2012).

2.7.2 Anatomic landmarks for identifying the pancreas

The anatomical landmarks used to locate the right pancreatic lobe are the right kidney; the descending duodenum, with its straight course along the right abdominal wall; and the pancreaticoduodenal vein paralleling the descending duodenum (Penninck and d'Anjou, 2015).

2.7.3 Normal ultrasonographic appearance of the pancreas and pancreatic duct in dogs

The normal pancreas is slightly ill defined, homogeneous and is isoechoic to the surrounding mesentery, isoechoic to slightly hyperechoic to the liver and hypoechoic to the spleen (Hetch and Baron, 2011). The pancreaticoduodenal vein is seen clearly in the right lobe and can be traced into the gastroduodenal vein and portal vein. The pancreas can appear normal when examined ultrasonographically even when diseased. This can be encountered in cases of pancreatitis and certain neoplastic conditions. Thus, normal ultrasonographic appearance of the pancreas should not rule out the pancreatic pathology (Hetch and Baron, 2011).

2.7.4 Size of the pancreas

The size of a normal pancreas in medium -sized dog (15-30 kg) is variable and has been reported to range from 1-3 cm in width and up to 1cm in thickness (Penninck *et al.*, 2013). The pancreatic duct can be seen in normal dogs, especially in the right lobe. Penninck *et al.*, (2013) also found that pancreatic thickness and pancreatic duct diameter correlate with body weight, but not with age (Penninck and d'Ajou, 2015).

2.7.5 Factors affecting the visualization of the pancreas by ultrasonography

The normal pancreas is not easy to identify sonographically because of its small size, echogenicity comparable to that of adjacent fat, and lack of a well-defined capsule (Lamb, 1990; Saunders, 1991). In addition, gas in adjacent bowel frequently obscures the pancreatic region. Therefore identifiable landmarks are used to scan the pancreatic area. The pancreas is more likely to be identified in puppies, thin dogs, and dogs with peritoneal fluid (Saunders, 1991). In people, fatty infiltration of the pancreas is associated with obesity, and increased pancreatic echogenicity is associated with age, making the pancreas similar in echogenicity to surrounding fat and therefore difficult to identify (Worthen and Beabeau, 1982). In cats, the normal pancreas is isoechoic to the liver and hypoechoic to the surrounding mesentery, findings that do not appear to change with age, gender, body weight, or body condition (Etue *et al.*, 2001; Larson *et al.*, 2005).

2.7.6 Ultrasonographic features of pancreatic disorders

2.7.6.1 Inflammation:

Acute pancreatitis: Acute inflammation of the pancreas is a common pancreatic pathology in dogs (Hetch and Baron, 2015). It has various ultrasonographic appearances, depending

on the severity, duration, and extent of pancreatic and peripancreatic tissue inflammation (Penninck and d'Anjou, 2015).

Classic ultrasonographic features of acute pancreatitis include an enlarged pancreas, hypoechoic pancreatic parenchyma, surrounding hyperechoic mesentery, focal peritoneal fluid accumulation, corrugated duodenum, and focal mild intestinal dilatation with decreased intestinal motility (indicative of focal ileus) (Hetch and Baron, 2015). In dogs, the right limb of the pancreas tends to be most commonly affected, whereas in cats, the changes tend to be more severe in the body and left limb (Penninck and d'Anjou, 2015). In severe hemorrhagic, necrotizing pancreatitis, irregular hypo to anechoic area(s) represents necrosis and hemorrhage of part of the pancreas and peripancreatic tissue. The pancreatic margins usually become ill-defined. The adjacent mesentery is hyperechoic and hyperattenuating because of regional inflammation and edema. In these cases, contrast enhanced computed tomography can complement ultrasound in better defining the extent of pancreatic necrosis (Jaeger, *et al.*, 2003).

Chronic pancreatitis: In dogs, chronic pancreatitis has variable ultrasonographic appearance. It is characterized by hypoechoic irregular pancreas, hyperechoic pancreatic parenchyma believed to represent pancreatic fibrosis, and hyperechoic mineralized foci with distal acoustic shadowing within and/or surrounding the pancreatic parenchyma, resulting from dystrophic mineralization of chronically inflamed pancreatic and peripancreatic tissue (Hetch and Baron, 2015). Most cases encountered have unclear clinical signs and non-specific laboratory values. In these cases, the pancreas can be within normal range for size, and the parenchyma is often inhomogeneous with hyperechoic non-shadowing foci or lines (Penninck and d'Anjou, 2015).

*2.7.6.2 Exocrine pancreatic insufficiency (EPI):*In dogs, exocrine pancreatic insufficiency (EPI) is usually caused by atrophy of the pancreatic acinar. There are limited publications on the sonographic appearance of EPI in dogs (Penninck and d'Anjou, 2015). Ultrasonographically, the pancreatic parenchyma appears as Hyperechogenic and inhomogeneous in dogs (Watson 2003; Hecht *et al.*, 2006). In confirmed cases of EPI, there is a reduced size of the pancreatic parenchyma, hyperechoic parenchyma and dilated pancreatic duct with or without calculi (Penninck and d'Anjou, 2015). It is also interesting that, at times, the intestinal tract is hypermotile and distended with echogenic contents, possibly related to the malabsorption encountered with EPI (Penninck and d'Anjou, 2015).

*2.7.6.3 Pancreatolithiasis and abnormal pancreatic duct:*Pancreatolithiasis is a condition that is characterized by the presence of calculi in the pancreatic ductal system or parenchyma. This unusual incidence can be diagnosed radiographically or sonographically (Penninck and d'Anjou, 2015). The size and number of calculi can vary widely and are usually associated with shadowing. They can also be associated with a variable degree of ductal dilation, or an anomaly such as pseudobladder and underlying chronic pancreatitis (Bailiff 2004). Pseudobladder is described as a dilated segment of the pancreatic duct of unknown etiology; this fluid-filled focal dilation can be confused with a pseudocyst or abscess. After surgical ligation of pancreatic duct in four dogs, a study showed endoscopic evidence of progressive dilation of the pancreatic ductal system and atrophy of the acinar tissue replaced by fibrosis and fat and resulting in increased echogenicity of the parenchyma (Morita *et al.*, 1998). In these uncommon cases, the pancreatic duct wall is mildly thickened, and mixed anechoic to echogenic fluid is noted in the lumen. The exact etiology of this severe distension is unknown (Penninck and d'Anjou, 2015).

2.7.6.4 Pancreatic nodular hyperplasia: Pancreatic nodular hyperplasia is infrequently seen in the pancreas of older dogs. It is characterized by a well-defined hypoechoic to nearly isoechoic nodules that can vary in size (Hecht and Henry 2007). These nodules may appear as neoplastic disorders, such as insulinomas. They may also look similar to cysts, although far acoustic enhancement is not usually associated with soft-tissue nodules. Therefore cytology or histopathology is required to establish a definitive diagnosis (Hetch and Baron, 2015).

2.7.6.5 Pancreatic Exocrine Tumors: Pancreatic exocrine tumors are rare in small animals. In spite of the fact that these tumors are rare, adenocarcinomas is the most common type of pancreatic neoplasm in small animals. They stem from arise acinar cells or ductal epithelium. They tend to develop in the central portion of the gland. As they grow, they may compress the CBD, invade the adjacent gastric and duodenal segments, and frequently metastasize to the liver (Lamb *et al.*, 1995). They are often poorly echogenic nodules or masses that can be associated with mineralized foci. Other common ultrasonographic features pancreatic enlargement, multifocal pancreatic nodules, abdominal effusion, and extra hepatic biliary obstruction (Hetch and Baron, 2015). The size of the pancreatic lesions varies greatly, but a majority of the lesions tend to be ≤ 2.5 cm and poorly echogenic (Lamb *et al.*, 1995). Ultrasonography is fairly sensitive in the diagnosis of exocrine pancreatic tumors; however, identification of endocrine pancreatic tumors is often limited to small size (Hetch and Baron, 2015).

2.8 Imaging Modalities for Evaluating the Pancreas

2.8.1 Radiography

Radiography is one of the diagnostic imaging modality used in working up abdominal disorders in small animals. Unfortunately, radiographs are of little value in the diagnosis of pancreatic disease. The normal pancreas is not observed in dogs on abdominal radiographs, and is only occasionally visible in cats, if they are obese(Hetch and Baron, 2015). Furthermore, the value of abdominal radiographs in diagnosing pancreatic diseases is limited; in dogs, their sensitivity for the diagnosis of severe pancreatitis is as low as 24% (Hess *et al.*, 1998). Whilst the sensitivity of abdominal radiography for the detection of pancreatic tumors in dogs has also been shown to be low (19%) (Lamb *et al.*, 1995), radiographic abnormalities were observed in 100% of cats with pancreatic malignancies and pancreatic nodular hyperplasias according to one study (Hecht and Henry, 2007). However, in no case were the radiographic abnormalities observed necessarily specific to the pancreas, and pancreatic nodular hyperplasia could not be distinguished from pancreatic malignancy based on radiographic findings(Hetch and Baron, 2015).

2.8.2 Ultrasonography

Abdominal ultrasonography enhances visualization of the normal pancreas in the majority of small animals, and has proven useful in the identification of various pancreatic disorders. In dogs, abdominal ultrasonography was reported to have a sensitivity of 68% for the detection of severe pancreatitis (Hess *et al.*, 1998), and a sensitivity of 75% was reported for the diagnosis of pancreatic neoplasia (Lamb *et al.*, 1995). Ultrasonography is of limited value in the detection of endocrine pancreatic tumours, likely due to their small size (Robben *et al.*, 2005). It may be inferred from one retrospective study that abdominal ultrasonography is not as helpful in the diagnosis of pancreatitis in cats as it is in dogs: most reports indicate a sensitivity of 11-35%(Gerhardt *et al.*, 2001;Saunders, 1991),

although one study reports a sensitivity of 80%(Forman *et al.*,2004). Abdominal ultrasonography fares well at identifying and characterizing lesions in cats with pancreatic neoplasia and nodular hyperplasia: in a retrospective study, ultrasonography revealed pancreatic abnormalities in 16 of 17 cats with pancreatic malignancy and 5 of 5 cats with nodular hyperplasia (Hecht and Henry, 2007). There was considerable overlap in ultrasonographic findings between the two diseases, although a solitary mass of >2 cm appeared to be specific for malignancy(Hetch and Baron, 2015).

2.8.3 Computed tomography

Contrast-enhanced computed tomography (CT) is considered the best imaging modality for the diagnosis of acute pancreatitis and other pancreatic disorders in human medicine. Disadvantages of CT in veterinary medicine in comparison with radiography and ultrasonography include cost and the need for general anaesthesia (Hetch and Baron, 2015). Initial case studies describing the use of CT in the diagnosis of canine pancreatitis yielded promising results (Jaeger *et al.*, 2003). Studies investigating the use of contrast-enhanced CT in the diagnosis of feline pancreatitis indicated that this modality was largely unhelpful, with a sensitivity as low as 20% (Gerhardt *et al.*, 2001; Forman *et al.*, 2004). Recent reports investigating the use of CT for diagnosing pancreatic neoplasms such as insulinoma in dogs (Robben *et al.*, 2005) yielded promising results.

CHAPTER THREE

3.0 MATERIALS AND METHODS

3.1 Location of Research

The experiment was conducted at the Department of Veterinary Surgery and Radiology, Faculty of Veterinary Medicine, Ahmadu Bello, Zaria. North-western Nigeria, with geographical coordinates, 11°4'0" North and 7° 42'0 "East (Anonymous 2).

3.2 Materials

3.2.1 Equipment

A Sonoster C5 (Guangzhou, China, 2015) ultrasound machine coupled with a 7.5 MHz curvilinear probe, a sony video graphic thermal printer, digital camera with 32 mega pixel, laptop computer, ultrasound table, measuring tape, mouth muzzle, weighing scale (Zhongshan, china, CP481CONVB5914KANMY), tiger electricity generator, electric plug, razor blade, electrical clipper, sample bottle, table centrifuge, deep freezer, needle and syringe.

3.2.2 Consumables

Consumables used are thermal printing paper, aquasonic gel, tissue papers, dettol antiseptic solution, disposable gloves, cotton wool, alcohol, shaving blade, toilet soap, feeding materials and petrol for fueling generator.

3.2.3 Source and type of study animals

The study animals were Nigerian Indigenous Dogs. Six puppies (from the same bitch) (Plate 3.1) were acquired from the owner at Hayin Dogo, Samaru, Zaria area of Kaduna state, Nigeria.

3.3 Methodology

3.3.1 Ethical committee permission

The animal care and handling was carried out according to the guidelines and principles in the care and use of experimental animals in Nigeria. The protocol used were approved by Ahmadu Bello University's Committee on Animal Use and Care (ABUCAU). Approval number (ABUCAUC/2018/007).

3.3.2 Inclusion and exclusion factors

Only clinically healthy puppies (8weeks old) from the same bitch were used for the study. Sick puppies were excluded from the study on the basis of survey ultrasonography.

3.3.3 Study design

Six (6) apparently healthy puppies of the same age (8weeks) group and equal sexes (3 males and 3 females) were used for this study. They were kept in their natural environment together with the bitch and were fed on rice, beans, fish, and some brisket bones. A thorough physical and clinical examination were also carried out on each puppy. Blood and fecal samples were collected and sent to the haematology (complete blood count) and parasitology laboratory (fecal egg count) respectively.



Plate 3.1: Six Nigerian Indigenous Puppies acquired for the research work

The study was carried out for a period of 8 months (between the months of November 2016 and June 2017) and the hepatobiliary system and the pancreas of the puppies were scanned at two (2) weeks interval using the C5 ultrasound machine coupled with a 7.5 MHz transducer. The demographic data which includes the age, sex, body weight, body length and Body mass index were obtained as shown in table (3.1). Blood samples (for serum) were collected once in every two months for biochemical analysis.

3.3.4 Demographic data collection

For reliability, all measurements were carried out by one person using Freeman's measuring tape and a weighing balance (kg)(Zhongshan, china, CP481CONVB5914KANMY). Puppies were physically restrained and measurements were taken with the animal in a standing position. Live body weight (LBW), wither height (HT), body length (BL) were measured. The body weight was measured with a weighing scale in (kg) and the value was obtained, recorded and presented in tables and graphs. The body length (BL) was measured with a Freeman's tape in centimeters as the distance from the point of the shoulder to the base of the tail (Plate II). The withal height (HT) was also measured with a freeman's tape in centimeters (cm) as the distance from the top of the withers to the digits (precisely extreme 3rd phalanx) (Plate III). After obtaining the values for height and weight, the body mass Index was calculated using the formula: weight/height^2 (kg/m²).

3.3.5 Experimental animal distribution

The experimental animals were distributed into 2 groups of 3 (male and female).



Plate 3.2: A male puppy from group A placed on a standing position with a Freeman's tape placed from the neck to the first coccygeus to obtain the body length (BL).



Plate 3.3: A male puppy from group A placed on standing position with a Freeman's tape placed from the highest point of the withers to the extreme 3rd phalanx to obtain the withal height (HT) .

Table 3.1. Illustration of the format for presentation of the obtained demographic data of the puppies under study

Dog no. (n)	Age (weeks)	Sex (M/F)	Weight (Kg)	Body length(cm)	Height (cm)	Body mass index (kg/m²)	Overall mean ±SEM
1							
2							
3							
4							
5							
6							

3.3.6 Pre-ultrasound scanning consideration

The cranial abdomen to be scanned was liberally shaved with a razor blade from the costal arch extending caudally to the umbilicus and laterally along the body wall at about 15cm towards the vertebrae. After shaving, the site was thoroughly cleaned and dried with a tissue paper (Plate IV). The puppies were restrained on a dorsal recumbency on the examination table for physical examination of the hepatobiliary system and on left lateral recumbency for examination of the pancreas.

3.3.7 Ultrasonographic techniques and measurements

Adopting the method used by Nyland *et al.*, (2002), an ultrasound examination of the puppies was done transcutaneously by means of 7.5 MHz curvilinear probe with the B-mode SonoStar C5 ultrasound scanner as shown in Plate V to examine the Hepatobiliary system (liver, gallbladder and portal vein) and the pancreas. The liver was scanned transcutaneously in a transverse and longitudinal plane (using the gallbladder as a point of reference) to examine the echotexture, echogenicity and liver dimensions as shown in Plate VI and VII respectively. The Pancreas and the pancreatic duct were also scanned between the 10-12th intercostal spaces in a transverse plain. The procedure was repeated thrice and the mean measurements were taken as the final values.

3.3.8 Measurements of the organs

3.3.8. *Liver*: The liver and associated structures were identified; as scanning proceeded to measure the liver as described by Nyland *et al.*, (2005) adopting the following:

- Cross-sectional length (L) of the Liver



Plate 3.4. A female puppy (Nigerian Indigenous Puppy) positioned on dorsal recumbency in preparation for scanning.



Plate 3.5. B-mode Sonostar C5 ultrasound scanner and a 7.5 MHz curvilinear transducer used for the abdominal ultrasound

KEY: Monitor (A); Keyboard or control panel (B); Mouse (C); Pulse control (D) and Transducer (E).

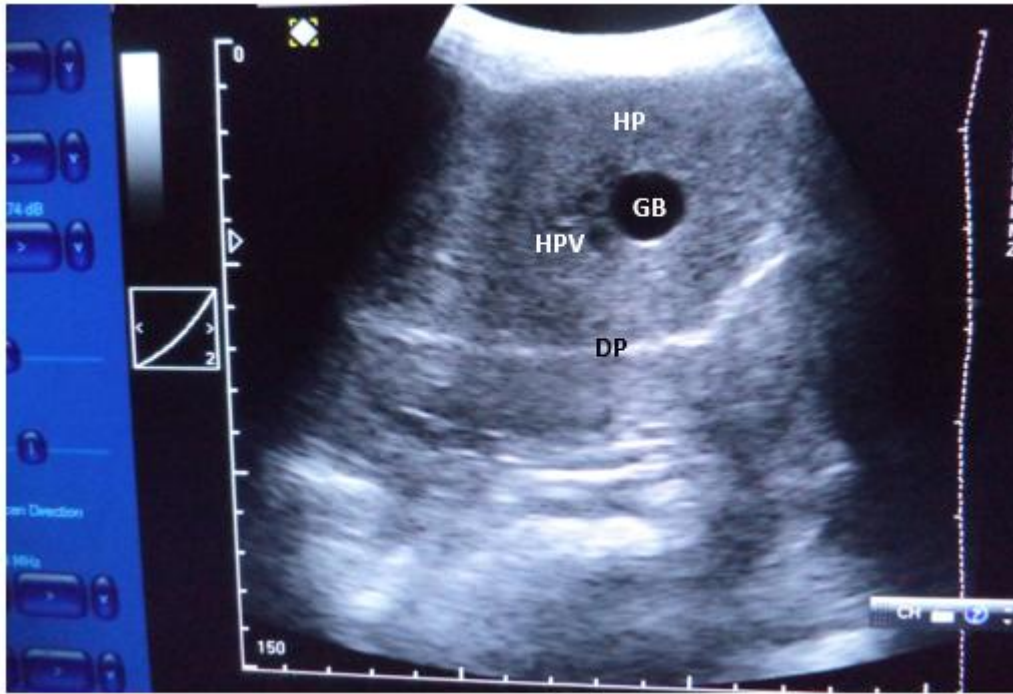


Plate 3.6. Cranial abdominal scan of the puppy illustrating the echotexture of the hepatic parenchyma (HP), gallbladder (GB), diaphragm (DP) and hepatic portal vein (HPV).

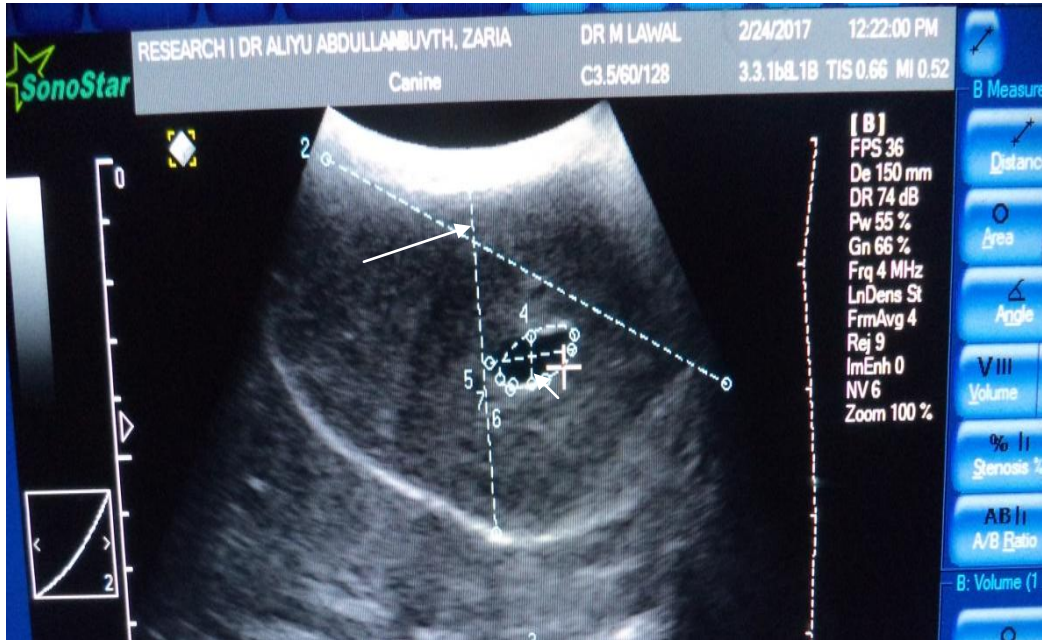


Plate 3.7 Sonogram of the cranial abdomen indicating the horizontal and vertical dimensions of the liver (long arrow), gallbladder (short arrow) of the puppy.

- Breadth of the liver
- Volume of the Liver
- Echogenicity and echo texture

3.3.8.2 *Portal vein*: The method of Nyland and Fisher, (1990) was adopted to scan and visualize the portal vein ventrally and the left of caudal vena cava. The cross sectional image of the portal vein was obtained and its diameter measured excluding the vessel walls i.e. the luminal diameter. After obtaining the diameter, the cross-sectional area was calculated using the formula:

$$A = \frac{(D)^2 \times \pi}{4}$$

Where A: portal vein area; D: portal vein diameter; π : 3.14

3.3.8.3 *Gall bladder*: The gallbladder was scanned both vertically (N-S) and horizontally (E-W). Measurements were undertaken such that the maximum vertical and horizontal lengths of the gallbladder were obtained in 3 trials and the mean recorded. The lengths and gallbladder wall thickness were taken in the longitudinal and axial planes while the width (W) was taken in transverse plane. Gallbladder volume was obtained using the Sonostar ultrasound machine.

3.3.8.4 *Pancreas and the pancreatic duct*: The method of Lim *et al.*, 2013, was adopted to sonographically measure the maximum pancreatic thickness and diameter of the pancreatic duct at the level of the left and right lobe of the pancreas. The duct of the right pancreatic

lobe was identified as a central tubular structure with a thick wall and the diameter was measured in millimeters (mm) as described by Penninck *et al.*, 2013.

3.4 Data Analysis

The mean values and standard error of mean (\pm SEM) of the body weight, body length, height, BMI and hepatobiliary and pancreatic measurements obtained were calculated. In order to observe the relationship between the ultrasound measurements of the hepatobiliary system and the demographic data, the correlation coefficient between these values were computed using Graph pad prism version 5.0. Two way ANOVA was used to compare the difference between the male and the female measurements using Bon ferroni as post hoc Analysis was considered significant at $P \leq 0.05$.

CHAPTER FOUR

4.0 RESULT

4.1 Biometry of the Hepatobiliary System of the 6 (six) Puppies and their Correlations

4.1.1 Biometry of the liver

The vertical axis (cross sectional length), horizontal axis (width) and the volume of the liver measured were represented in the (Appendix 2a-2h). The mean values and standard error of mean (\pm SEM) of the hepatic length (HL), the hepatic width (HW) and hepatic volume (HV) of the male puppies ranges from 55 ± 1.7 to 129 ± 4.4 mm, 28 ± 1.1 to 77 ± 3.3 mm and 151 ± 25 to 1275 ± 43 cm³ respectively (Figure 4.1; 4.2; and 4.3). The mean values \pm SEM of the hepatic length (HL), the hepatic width (HW) and hepatic volume (HV) of the female puppies ranges from 74 ± 2.9 to 140 ± 4.1 mm, 28 ± 3 to 85 ± 4.4 mm and 201 ± 9.5 to 1441 ± 130 cm³ respectively (Figure 4.1; Figure 4.2; Figure 4.3).

The overall mean values and standard error of mean (\pm SEM) of the hepatic length (HL), the hepatic width (HW) and hepatic volume (HV) ranges from 65 ± 4.7 to 134 ± 3.6 mm, 28 ± 1.4 to 81 ± 3 mm and 176 ± 16 to 1358 ± 71 cm³ respectively (Figure 4.4; Appendix 2h).

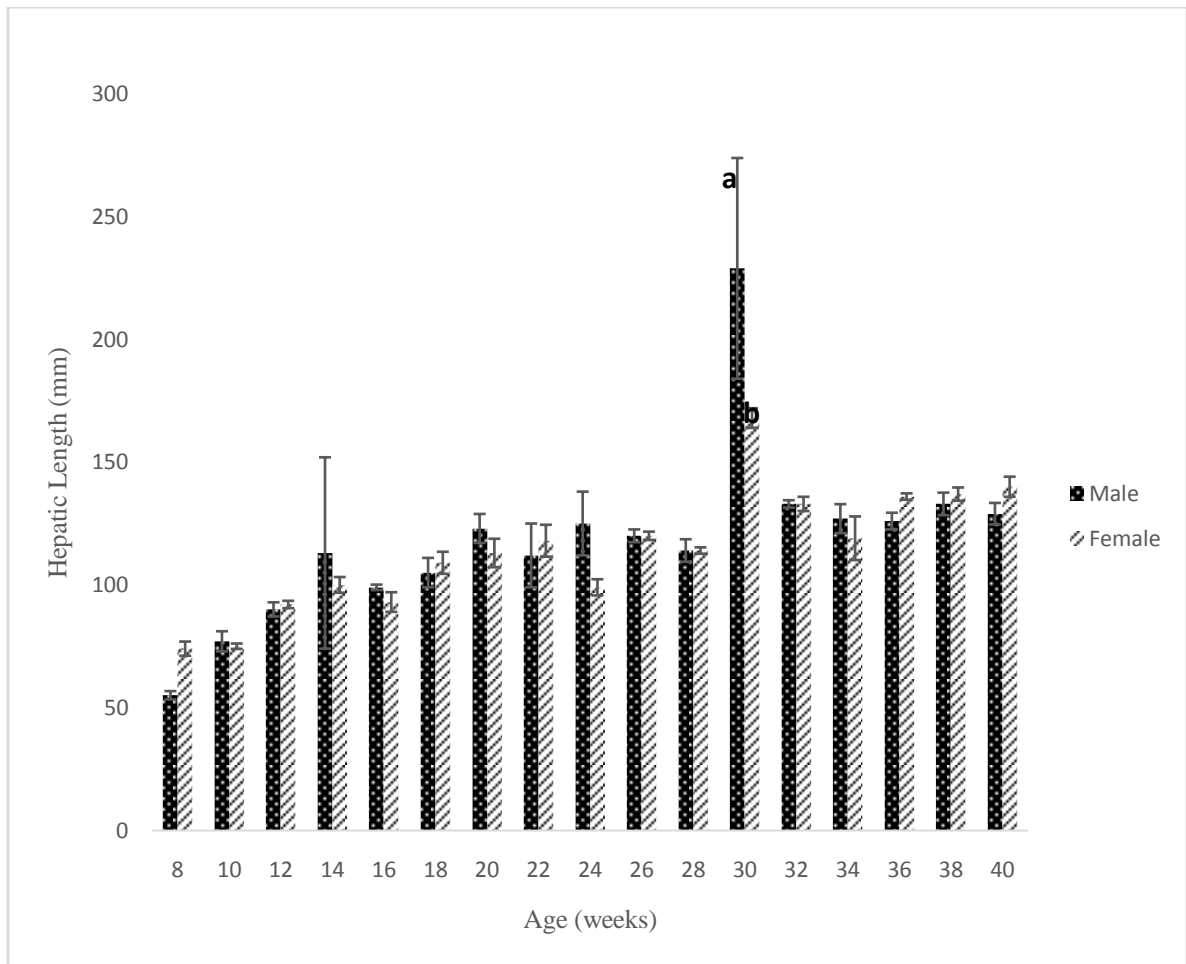


Figure 4.1: Mean values and SEM of the hepatic length ultrasound dimension in male and female puppies.

^{ab} Means in the same column with different superscript alphabets were significantly different ($p < 0.05$).

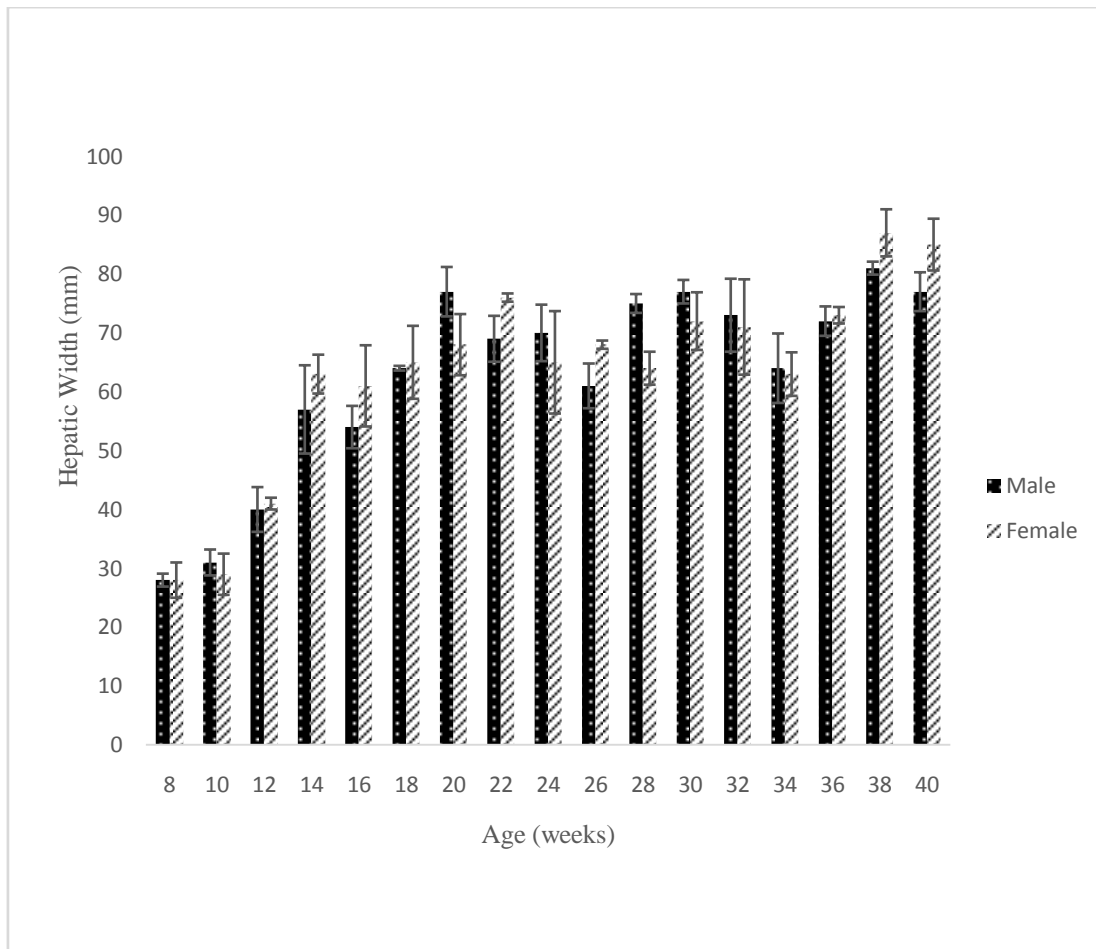


Figure 4.2: Mean values and SEM of the hepatic width ultrasound dimension in male and female puppies.

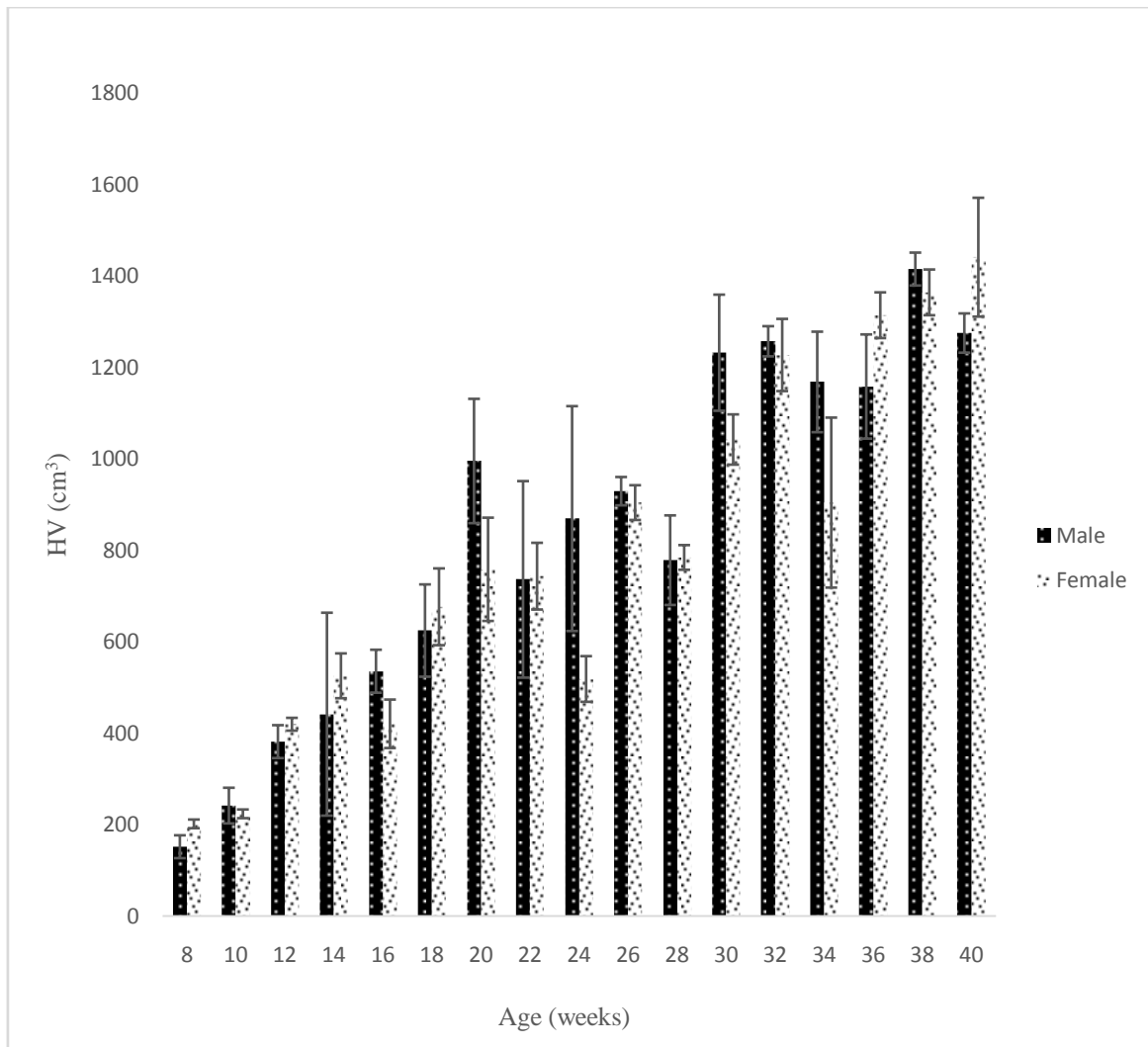


Figure 4.3: Mean values and SEM of the hepatic volume ultrasound dimension in male and female puppies.

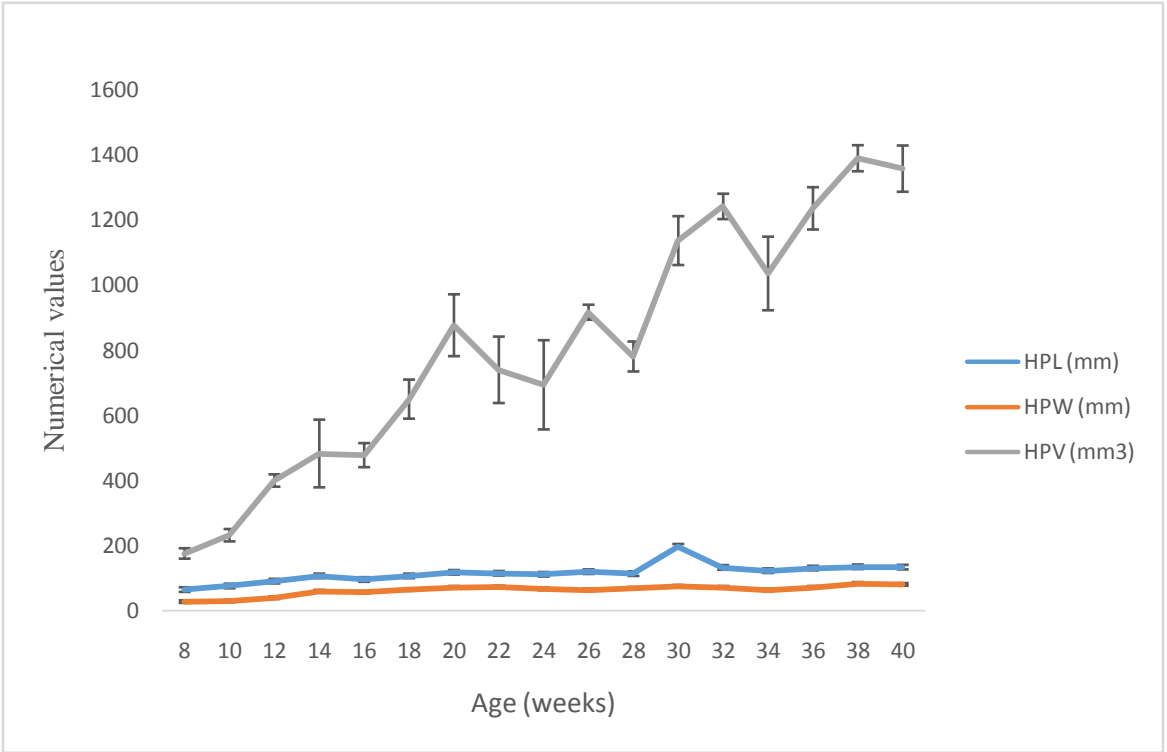


Figure 4.4: Variation of the hepatic ultrasound dimension with age.

KEY: HPL (Hepatic length), HPW (Hepatic width), HPV (Hepatic volume),

4.1.2 Biometry of the gallbladder

The parameters observed for the length (L), width (W), wall thickness (WT) and volume (V) of the gallbladder were presented in appendix (3a-3h). The mean values and the standard error of mean (\pm SEM) for the gall bladder length (GBL), width (GBW), wall thickness (GBWT) and volume (GBV) in the male puppies ranged from 12 ± 0.3 to 25 ± 0.7 mm, 6.4 ± 0.2 to 17 ± 0.2 mm, 0.7 ± 0.04 to 0.7 ± 0.13 mm and 0.19 ± 0.05 to 2.6 ± 0.44 cm³ respectively, while in the female puppies it ranged from 10 ± 1.8 to 17 ± 5.3 mm, 4.8 ± 1.2 to 14 ± 2.2 mm, 0.69 ± 0.13 to 0.67 ± 0.15 mm and 0.18 ± 0.03 to 1.7 ± 1 cm³ respectively (Figure 4.5; 4.6; 4.7; and 4.8). The overall mean values \pm SEM for the gall bladder length (GBL), width (GBW), wall thickness (GBWT) and volume (GBV) for the six puppies ranged from 11 ± 0.9 to 21 ± 2.9 mm, 5.6 ± 0.6 to 15 ± 1.1 mm, 0.7 ± 0.06 to 0.6 ± 0.08 mm and 0.18 ± 0.02 to 2.2 ± 0.54 cm³ respectively (Figure 4.9) .

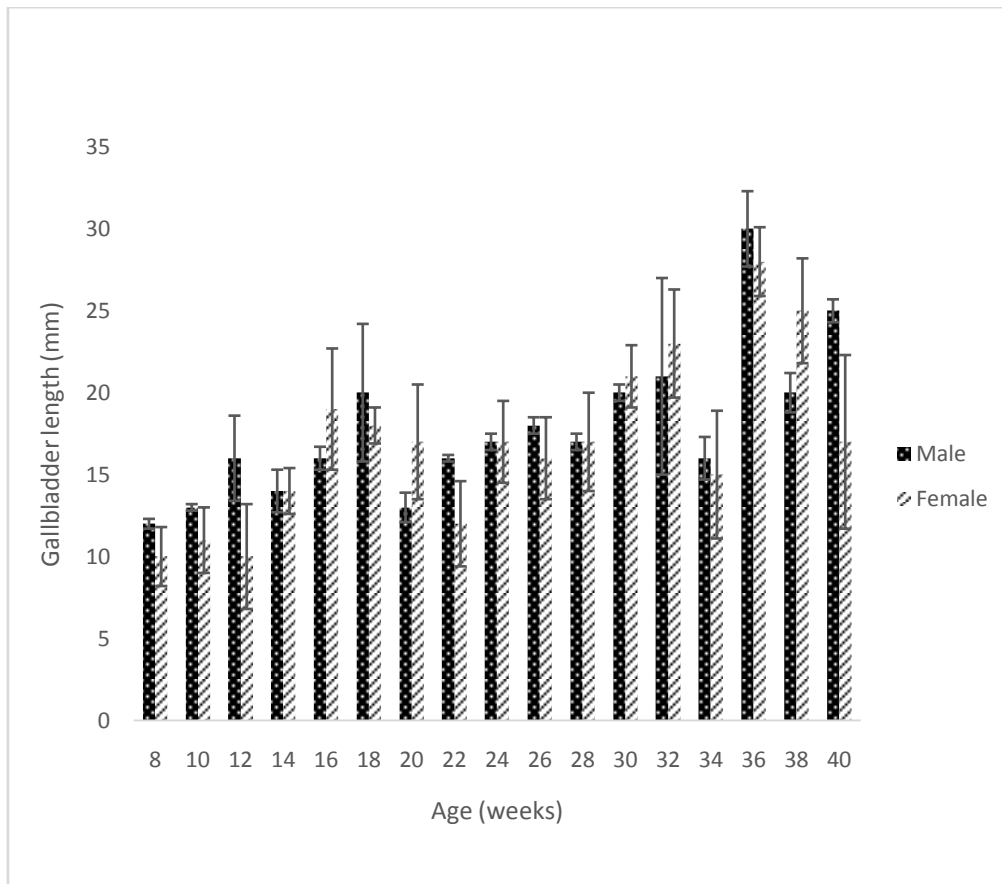


Figure 4.5: Mean values and SEM of the ultrasound gall bladder length dimension in male and female puppies.

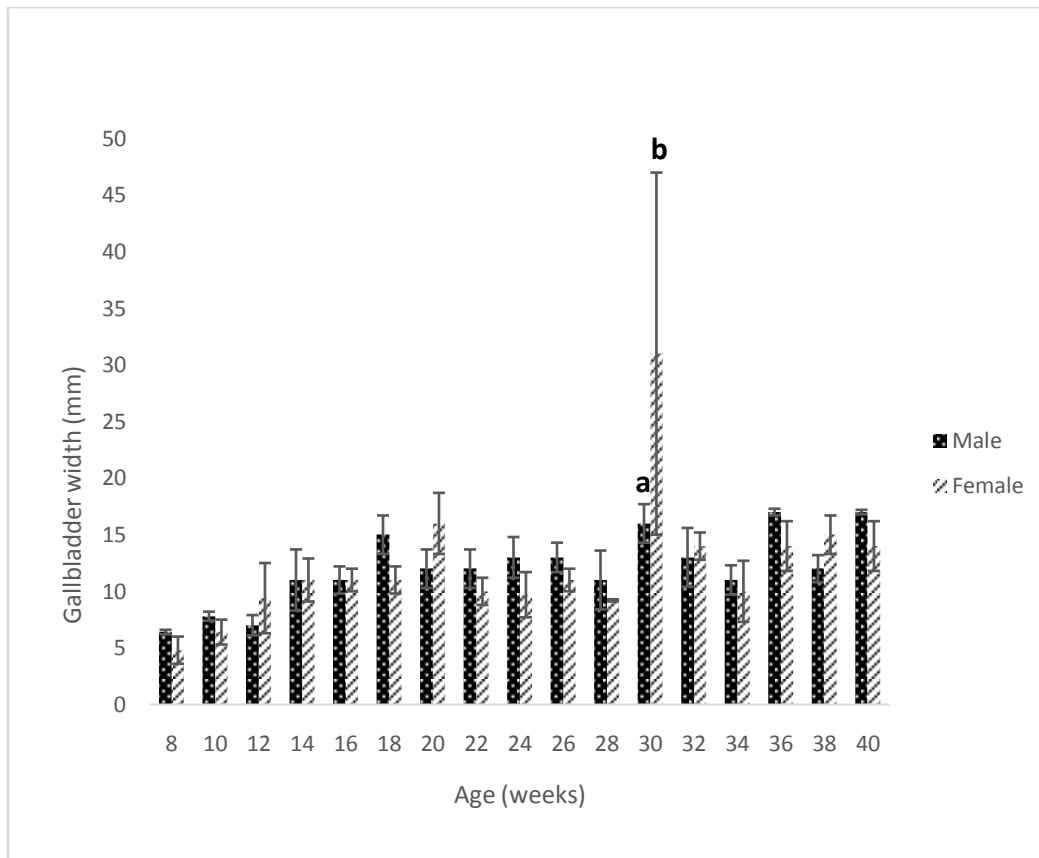


Figure 4.6: Mean values and SEM of the ultrasound gall bladder width dimension in male and female puppies

^{ab} Means in the same column with different superscript alphabets were significantly different ($p < 0.05$).

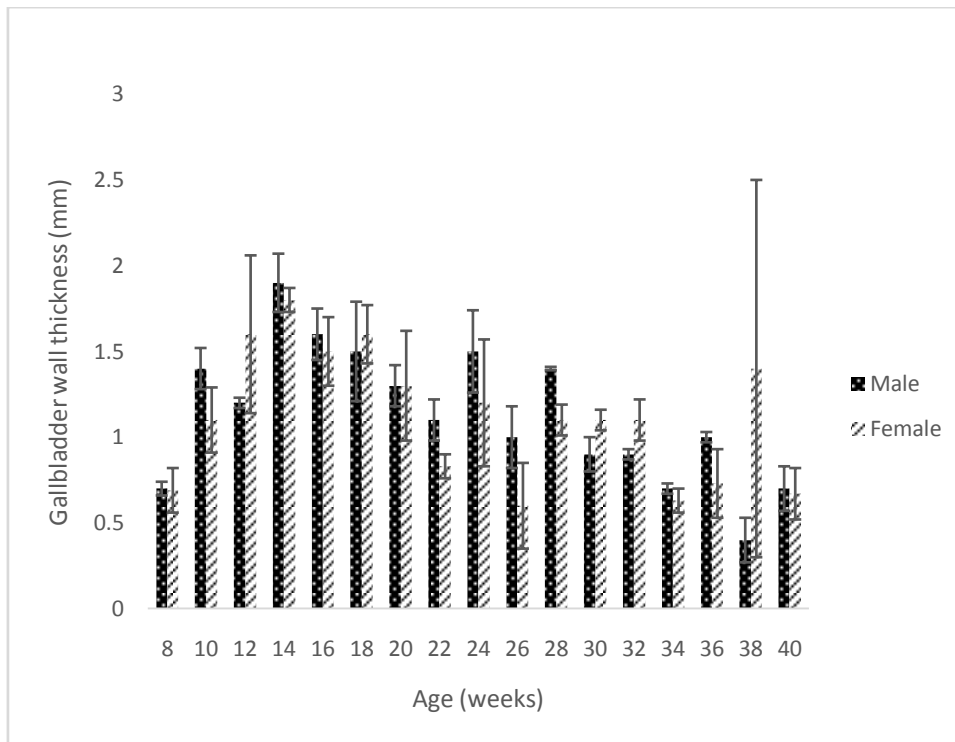


Figure 4.7: Mean values and SEM of the ultrasound gall bladder wall thickness dimension in male and female puppies

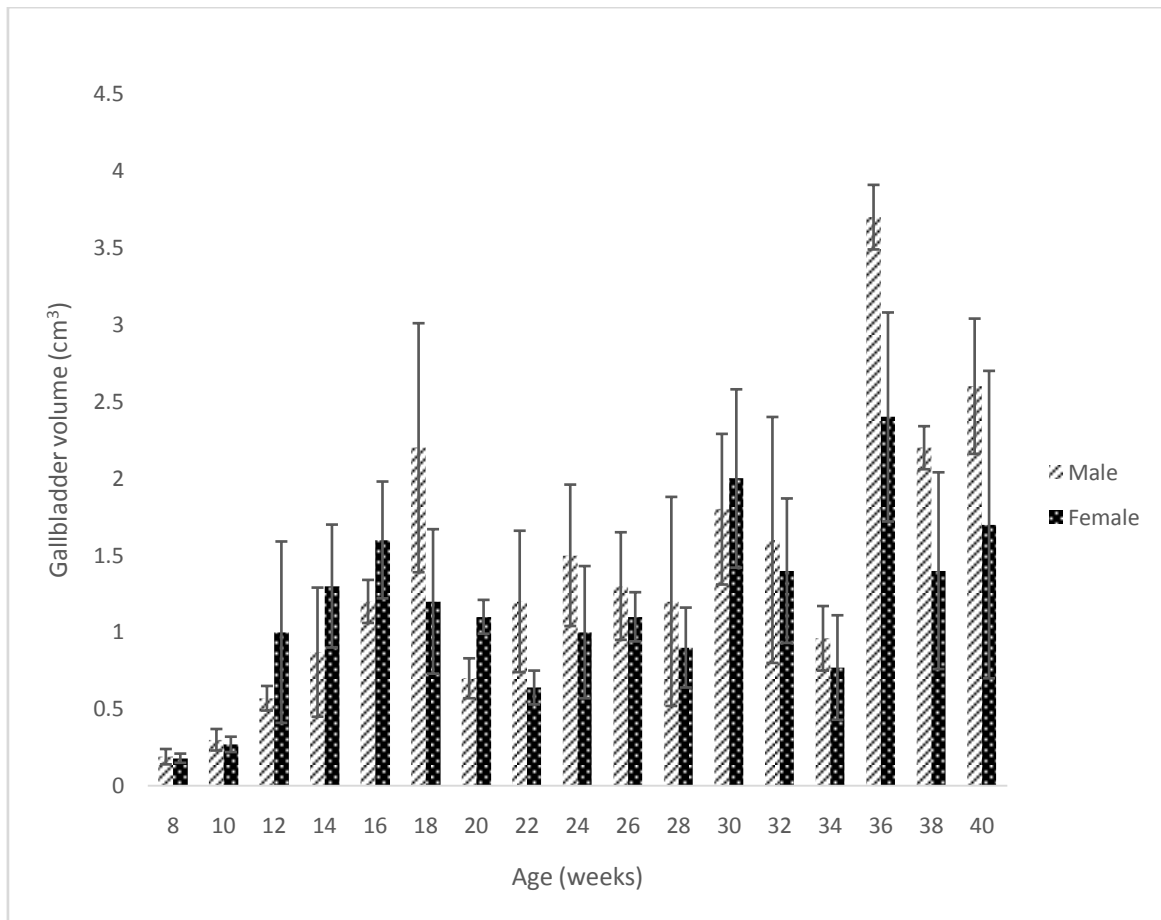


Figure 4.8: Mean values and SEM of the ultrasound gall bladder volume dimension in male and female puppies.

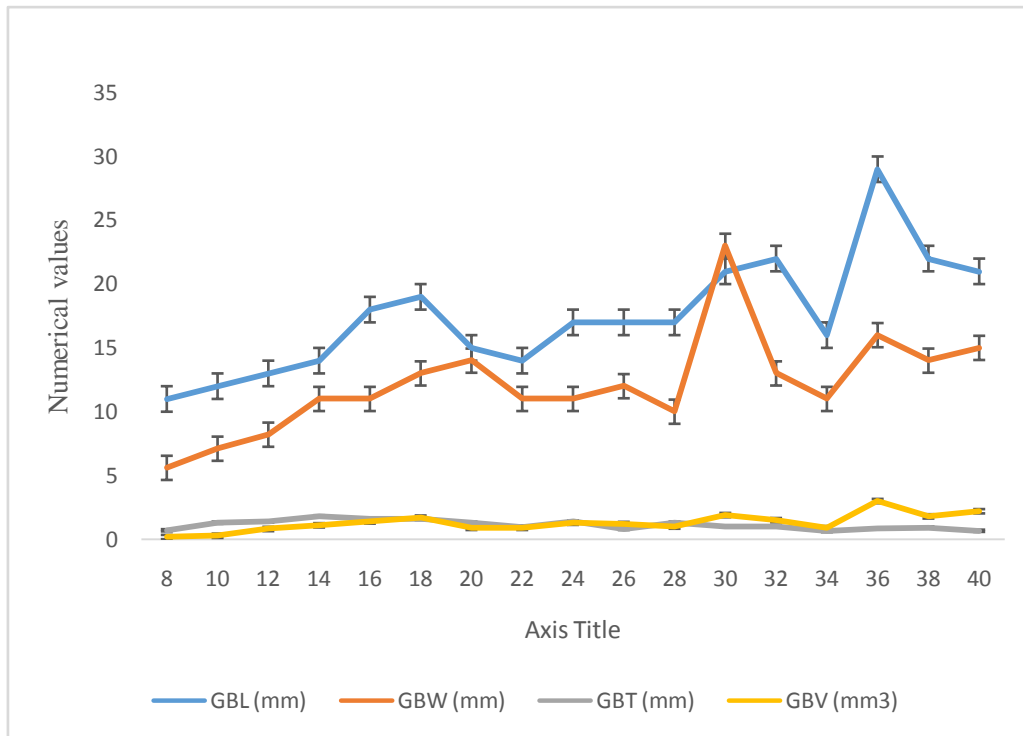


Figure 4.9 Variation of the ultrasound gall bladder dimension with age.

KEY: GBL (Gall bladder length), GBW (Gall bladder width), GBWT (Gallbladder wall thickness) GBV (Gallbladder Volume)

4.1.3 Echotexture of the liver and gall bladder

The liver parenchyma appeared as a loosely granular structure with homogenous and uniform echogenicity (Plate 4.1) and echotexture which was interrupted by short, highly echogenic paired parallel lines surrounding an anechoic lumen that represents the portal veins (4.3). The cranial border of the liver appeared as a curved hyper-echoic line that represents the diaphragm and it is the interface between the lungs and the liver (Plate 4.1 and 4.3). The gallbladder was observed as anechoic, round to oval structure just to the left of the midline of the puppies (right of the scanner) in most of the liver scanned (Plate 4.1). Measurements of the dimensions of the liver and gallbladder was presented in the Plate 4.2.



Plate 4.1: Longitudinal sonograph of the Nigerian Indigenous Puppy with homogenous isoechoic hepatic parenchyma (HP), anechoic circular area representing the gall bladder (GB) and curved hyper echoic line that represents the diaphragm (DPH).



Plate 4.2: Measurements of the dimensions of the liver: hepatic length (HL), hepatic width (HW) and gallbladder volume (GBV) in Nigerian Indigenous Puppy.

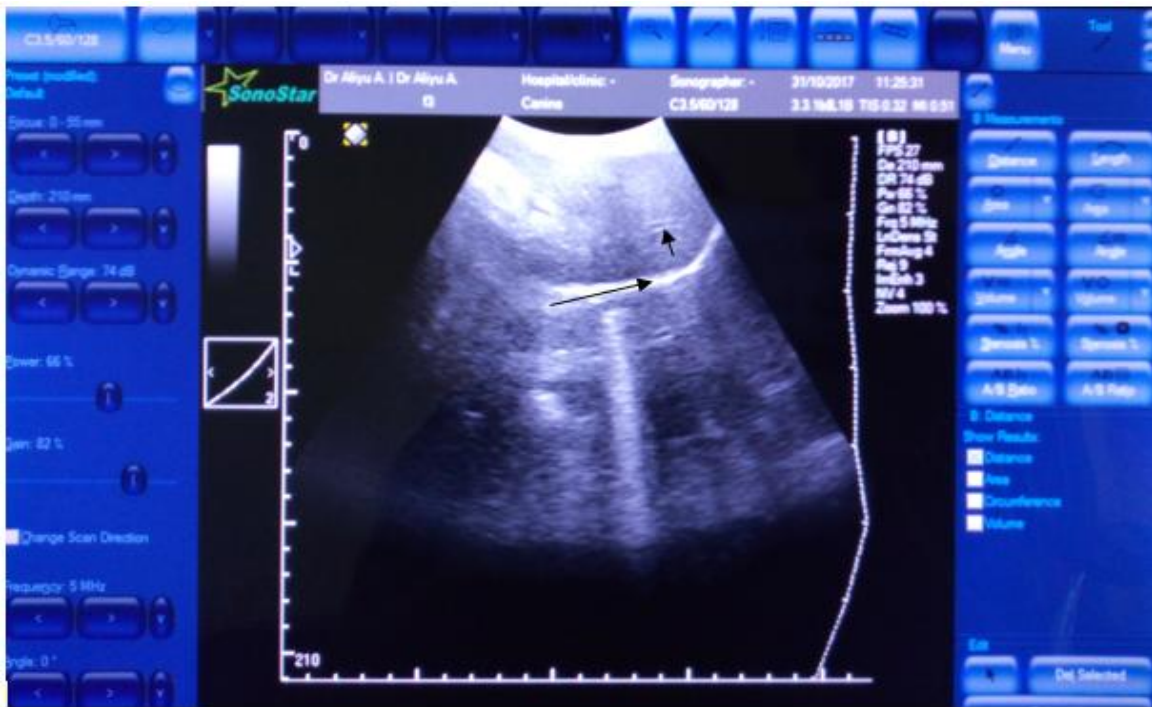


Plate 4.3: Echogenic paired parallel lines surrounding an anechoic lumen that represents the portal veins (short arrow) and curved hyper echoic line that represents the diaphragm (long arrow).

4.1.4 The correlation between the age and other demographic data and ultrasound hepatobiliary dimensions in the six puppies.

The age of the puppies correlated with the body demographic data ($r = 0.74$ to $r = 0.99$); hepatic ultrasound dimension ($r = 0.73$ to $r = 0.96$) and gall bladder ultrasound dimension ($r = 0.64$ to $r = 0.78$). However, it was significantly and negatively correlated with the gall bladder wall thickness ($r = -0.57$) (Table 4.1).

4.1.5 The correlation between the hepatic length (HL) with the demographic data and other ultrasound hepatobiliary dimensions.

Hepatic length (HL) was significant and highly correlated with the age ($r = 0.73$), weight ($r = 0.73$), body length ($r = 0.76$), height ($r = 0.78$), hepatic width ($r = 0.77$), hepatic volume ($r = 0.79$), gall bladder length, width and volume ($r = 0.64$ to $r = 0.95$). However, it was not significantly correlated with the portal vein diameter ($r = 0.29$) and gall bladder wall thickness ($r = -0.28$) (Table 4.2).

4.1.6 The correlation between the hepatic width (HW) with the demographic data and other ultrasound hepatobiliary dimensions.

The hepatic width was significantly and highly correlated with all the demographic data ($r = 0.76$ to $r = 0.93$) and the hepatobiliary parameters except portal vein diameter, cross sectional area and gall bladder wall thickness (Table 4.3).

Table. 4.1The correlation between the age other demographic data and ultrasound hepatobiliary dimensions in the six puppies (n = 6).

Parameter	Pearson r	P value summary	Is the correlation significant?	R squared
WT (kg)	0.99	***	Yes	0.97
BL (cm)	0.95	***	Yes	0.9
HT (cm)	0.94	***	Yes	0.89
BMI (Kg/m ²)	0.74	***	Yes	0.55
HL (mm)	0.73	***	Yes	0.53
HW (mm)	0.83	***	Yes	0.69
HV (cm ³)	0.96	***	Yes	0.93
PVD (mm)	-0.24	Ns	No	0.059
CSA (cm ²)	-0.24	Ns	No	0.057
GBL (mm)	0.78	***	Yes	0.61
GBW (mm)	0.64	**	Yes	0.41
GBWT (mm)	-0.57	*	Yes	0.33
GBV (cm ³)	0.72	**	Yes	0.52

*Correlation is significant at the 0.01 level (2-tailed), **Correlation is significant at the 0.001 level (2-tailed), ***Correlation is significant at the 0.0001 level (2-tailed), ns= not significant

KEY: WT (weight); BL (body length); HT (height); BMI (body mass index); HL (hepatic length); HW (hepatic width); HV (hepatic volume); PVD (portal vein diameter); CSA (cross sectional area); GBL (gall bladder length); GBW (gall bladder width); GBWT (gall bladder wall thickness); GBV (gall bladder volume).

Table. 4.2The correlation between the hepatic length with demographic data and other ultrasound hepatobiliary dimensions in the six puppies. (n = 6).

Parameter	Pearson r	P value summary	Is the correlation significant?	R squared
Age (weeks)	0.73	***	Yes	0.53
WT (kg)	0.73	***	Yes	0.53
BL (cm)	0.76	***	Yes	0.57
HT (cm)	0.78	***	Yes	0.61
BMI (Kg/m ²)	0.51	*	Yes	0.26
HW (mm)	0.77	***	Yes	0.6
HV (cm ³)	0.79	***	Yes	0.63
PVD (mm)	0.29	Ns	No	0.082
CSA (cm ²)	0.31	Ns	No	0.095
GBL (mm)	0.64	**	Yes	0.41
GBL (mm)	0.95	***	Yes	0.9
GBWT (mm)	-0.28	Ns	No	0.08
GBV (cm ³)	0.64	**	Yes	0.42

*Correlation is significant at the 0.01 level (2-tailed), **Correlation is significant at the 0.001 level (2-tailed), ***Correlation is significant at the 0.0001 level (2-tailed), ns= not significant

KEY: WT (weight); BL (body length); HT (height); BMI (body mass index); HL (hepatic length); HW (hepatic width); HV (hepatic volume); PVD (portal vein diameter); CSA (cross sectional area); GBL (gall bladder length); GBW (gall bladder width); GBWT (gall bladder wall thickness); GBV (gall bladder volume).

Table. 4.3The correlation between the hepatic width with demographic data and other ultrasound hepatobiliary dimensions in the six puppies. (n = 6).

Parameter	Pearson r	P value summary	Is the correlation significant?	R squared
Age (weeks)	0.83	***	Yes	0.69
WT (kg)	0.88	***	Yes	0.78
BL (cm)	0.93	***	Yes	0.86
HT (cm)	0.91	***	Yes	0.83
BMI(Kg/m ²)	0.76	***	Yes	0.58
HL (mm)	0.77	***	Yes	0.6
HV (cm ³)	0.87	***	Yes	0.76
PVD(mm)	0.08	Ns	No	0.0063
CSA(cm ²)	0.067	Ns	No	0.0045
GBL(mm)	0.69	**	Yes	0.47
GBW(mm)	0.74	***	Yes	0.55
GBWT(mm)	-0.19	Ns	No	0.037
GBV (cm ³)	0.7	**	Yes	0.49

*Correlation is significant at the 0.01 level (2-tailed), **Correlation is significant at the 0.001 level (2-tailed), ***Correlation is significant at the 0.0001 level (2-tailed), ns= not significant

KEY: WT (weight); BL (body length); HT (height); BMI (body mass index); HL (hepatic length); HW (hepatic width); HV (hepatic volume); PVD (portal vein diameter); CSA (cross sectional area); GBL (gall bladder length); GBW (gall bladder width); GBWT (gall bladder wall thickness); GBV (gall bladder volume).

4.1.7 Correlation between the hepatic volume (HV), demographic data and other ultrasound hepatobiliary dimensions.

The hepatic volume was significantly and highly correlated with all the demographic data and other ultrasound hepatobiliary dimension except portal vein diameter and cross sectional area (Table 4.4).

4.1.8 Correlation between the gallbladder length (GBL), demographic data and other ultrasound hepatobiliary dimensions.

The gall bladder was significant and highly correlated with all the demographic data and other ultrasound hepatobiliary dimension ($r = 0.64$ to $r = 0.95$) except the portal vein diameter and gall bladder wall thickness (Table 4.5).

4.1.9 Correlation between the gallbladder width (GBW), demographic data and other ultrasound hepatobiliary dimensions.

Gall bladder wall thickness was significant and highly correlated with all the demographic data and other ultrasound hepatobiliary dimension except the portal vein diameter and gall bladder wall thickness (Table 4.6).

4.1.10 Correlation between the gallbladder wall thickness (GBWT), demographic data and other ultrasound hepatobiliary dimensions.

The gall bladder wall thickness was significant and negatively correlated with the age ($r = -0.57$), weight ($r = -0.5$) and hepatic volume ($r = -0.52$) (Table 4.7).

Table. 4.4The correlations between the hepatic volume, demographic data and other ultrasound hepatobiliary dimensions in the six puppies. (n = 6).

Parameter	Pearson r	P value summary	Is the correlation significant?	R squared
Age (weeks)	0.96	***	Yes	0.93
WT (kg)	0.95	***	Yes	0.91
BL (cm)	0.93	***	Yes	0.86
HT (cm)	0.94	***	Yes	0.88
BMI (Kg/m ²)	0.7	**	Yes	0.49
HL (mm)	0.79	***	Yes	0.63
HW (mm)	0.87	***	Yes	0.76
PVD (mm)	-0.19	Ns	No	0.037
CSA (cm ²)	-0.19	Ns	No	0.038
GBL (mm)	0.8	***	Yes	0.64
GBW(mm)	0.74	***	Yes	0.54
GBWT(mm)	-0.52	*	Yes	0.27
GBV (cm ³)	0.74	***	Yes	0.55
BMI (Kg/m ²)	0.7	**	Yes	0.49

*Correlation is significant at the 0.01 level (2-tailed), **Correlation is significant at the 0.001 level (2-tailed), ***Correlation is significant at the 0.0001 level (2-tailed), ns= not significant

KEY: WT (weight); BL (body length); HT (height); BMI (body mass index); HL (hepatic length); HW (hepatic width); HV (hepatic volume); PVD (portal vein diameter); CSA (cross sectional area); GBL (gall bladder length); GBW (gall bladder width); GBWT (gall bladder wall thickness); GBV (gall bladder volume).

Table. 4.5The correlation between the gall bladder length, demographic data and other ultrasound hepatobiliary dimensions in the six puppies. (n = 6).

Parameter	Pearson r	P value summary	Is the correlation significant?	R squared
Age (weeks)	0.78	***	Yes	0.61
WT (kg)	0.79	***	Yes	0.63
BL (cm)	0.77	***	Yes	0.59
HT (cm)	0.75	***	Yes	0.56
BMI (Kg/m ²)	0.69	**	Yes	0.48
HL (mm)	0.64	**	Yes	0.41
HW (mm)	0.69	**	Yes	0.47
HV (cm ³)	0.8	***	Yes	0.64
PVD (mm)	-0.17	Ns	No	0.03
CSA (cm ²)	-0.17	Ns	No	0.029
GBW (mm)	0.71	**	Yes	0.5
GBWT(mm)	-0.27	Ns	No	0.071
GBV (cm ³)	0.95	***	Yes	0.9

*Correlation is significant at the 0.01 level (2-tailed), **Correlation is significant at the 0.001 level (2-tailed), ***Correlation is significant at the 0.0001 level (2-tailed), ns= not significant

KEY: WT (weight); BL (body length); HT (height); BMI (body mass index); HL (hepatic length); HW (hepatic width); HV (hepatic volume); PVD (portal vein diameter); CSA (cross sectional area); GBL (gall bladder length); GBW (gall bladder width); GBWT (gall bladder wall thickness); GBV (gall bladder volume).

Table. 4.6The correlation between the gall bladder width, demographic data and other ultrasound hepatobiliary dimensions in the six puppies. (n = 6).

Parameter	Pearson r	P value summary	Is the correlation significant?	R squared
Age (weeks)	0.64	**	Yes	0.41
WT (kg)	0.66	**	Yes	0.43
BL (cm)	0.68	**	Yes	0.47
HT (cm)	0.69	**	Yes	0.48
BMI (Kg/m ²)	0.52	*	Yes	0.27
HL (mm)	0.95	***	Yes	0.9
HW (mm)	0.74	***	Yes	0.55
HV (cm ³)	0.74	***	Yes	0.54
PVD (mm)	0.3	Ns	No	0.093
CSA (cm ²)	0.32	Ns	No	0.11
GBL (mm)	0.71	**	Yes	0.5
GBWT(mm)	-0.18	Ns	No	0.032
GBV (cm ³)	0.75	***	Yes	0.56

*Correlation is significant at the 0.01 level (2-tailed), **Correlation is significant at the 0.001 level (2-tailed), ***Correlation is significant at the 0.0001 level (2-tailed), Ns= not significant

KEY: WT (weight); BL (body length); HT (height); BMI (body mass index); HL (hepatic length); HW (hepatic width); HV (hepatic volume); PVD (portal vein diameter); CSA (cross sectional area); GBL (gall bladder length); GBW (gall bladder width); GBWT (gall bladder wall thickness); GBV (gall bladder volume).

Table. 4.7The correlation between the gall bladder wall thickness, demographic data and other ultrasound hepatobiliary dimensions in the six puppies. (n = 6).

Parameter	Pearson r	P value summary	Is the correlation significant?	R squared
Age (weeks)	-0.57	*	Yes	0.33
WT (kg)	-0.5	*	Yes	0.25
BL (cm)	-0.41	Ns	No	0.17
HT (cm)	-0.39	Ns	No	0.15
BMI (Kg/m ²)	-0.32	Ns	No	0.1
HL (mm)	-0.28	Ns	No	0.08
HW (mm)	-0.19	Ns	No	0.037
HV (cm ³)	-0.52	*	Yes	0.27
PVD(mm)	0.39	Ns	No	0.15
CSA (cm ²)	0.4	Ns	No	0.16
GBL (mm)	-0.27	Ns	No	0.071
GBW(mm)	-0.18	Ns	No	0.032
GBV (cm ³)	-0.17	Ns	No	0.027

*Correlation is significant at the 0.01 level (2-tailed), **Correlation is significant at the 0.001 level (2-tailed), ***Correlation is significant at the 0.0001 level (2-tailed), ns= not significant

KEY: WT (weight); BL (body length); HT (height); BMI (body mass index); HL (hepatic length); HW (hepatic width); HV (hepatic volume); PVD (portal vein diameter); CSA (cross sectional area); GBL (gall bladder length); GBW (gall bladder width); GBWT (gall bladder wall thickness); GBV (gall bladder volume).

4.1.11 Correlation between the gallbladder volume (GBV), demographic data and other ultrasound hepatobiliary dimensions.

The gall bladder volume was significant and highly correlated with all the demographic data and other ultrasound hepatobiliary dimension ($r = 0.69$ to $r = 0.75$) except with the portal vein diameter and gall bladder wall thickness (Table 4.8).

4.2 Evaluation of the Portal Vein in Six (6) Nigerian Indigenous Puppies

4.2.1 Biometry of the portal vein.

The mean values and SEM of the portal vein diameter and cross sectional area of the male puppies ranged from 2.1 ± 0.38 to 4.7 ± 0.09 mm and 2.7 ± 0.26 to 18 ± 0.75 cm² respectively (Figure 4.10 and 4.11; Appendix 4a). While that of the female ranged from 2.3 ± 0.09 to 4.8 ± 0.12 mm and 4 ± 0.61 to 18 ± 0.75 cm² respectively (Figure 4.10 and 11; Appendix 4a).

The overall mean values and standard error of mean of portal vein diameter ranged from 2.3 ± 0.1 to 4.8 ± 0.07 mm while the cross sectional area of the portal vein ranged from 4.25 ± 0.37 to 17.99 ± 0.53 cm² (Figure 4.10 and 11; Appendix 4b).

4.2.2 Correlation between the portal vein diameter (PVD), demographic data and ultrasound hepatobiliary dimensions.

The portal vein diameter was not significantly correlated with any of the demographic data and ultrasound hepatobiliary dimension (Table 4.9) studied. This was similarly observed for cross sectional area (Table 4.10).

Table. 4.8The correlation between the gall bladder volume, demographic data and other ultrasound hepatobiliary dimensions in the six puppies. (n = 6).

Parameter	Pearson r	P value summary	Is the correlation significant?	R squared
Age (weeks)	0.72	**	Yes	0.52
WT (kg)	0.74	***	Yes	0.54
BL (cm)	0.71	**	Yes	0.51
HT (cm)	0.69	**	Yes	0.47
BMI (Kg/m ²)	0.68	**	Yes	0.46
HL (mm)	0.64	**	Yes	0.42
HW (mm)	0.7	**	Yes	0.49
HV (cm ³)	0.74	***	Yes	0.55
PVD (mm)	-0.11	Ns	No	0.012
CSA (cm ²)	-0.11	Ns	No	0.011
GBL (mm)	0.95	***	Yes	0.9
GBW (mm)	0.75	***	Yes	0.56
GBWT (mm)	-0.17	Ns	No	0.027

*Correlation is significant at the 0.01 level (2-tailed), **Correlation is significant at the 0.001 level (2-tailed), ***Correlation is significant at the 0.0001 level (2-tailed), ns= not significant

KEY: WT (weight); BL (body length); HT (height); BMI (body mass index); HL (hepatic length); HW (hepatic width); HV (hepatic volume); PVD (portal vein diameter); CSA (cross sectional area); GBL (gall bladder length); GBW (gall bladder width); GBWT (gall bladder wall thickness); GBV (gall bladder volume).

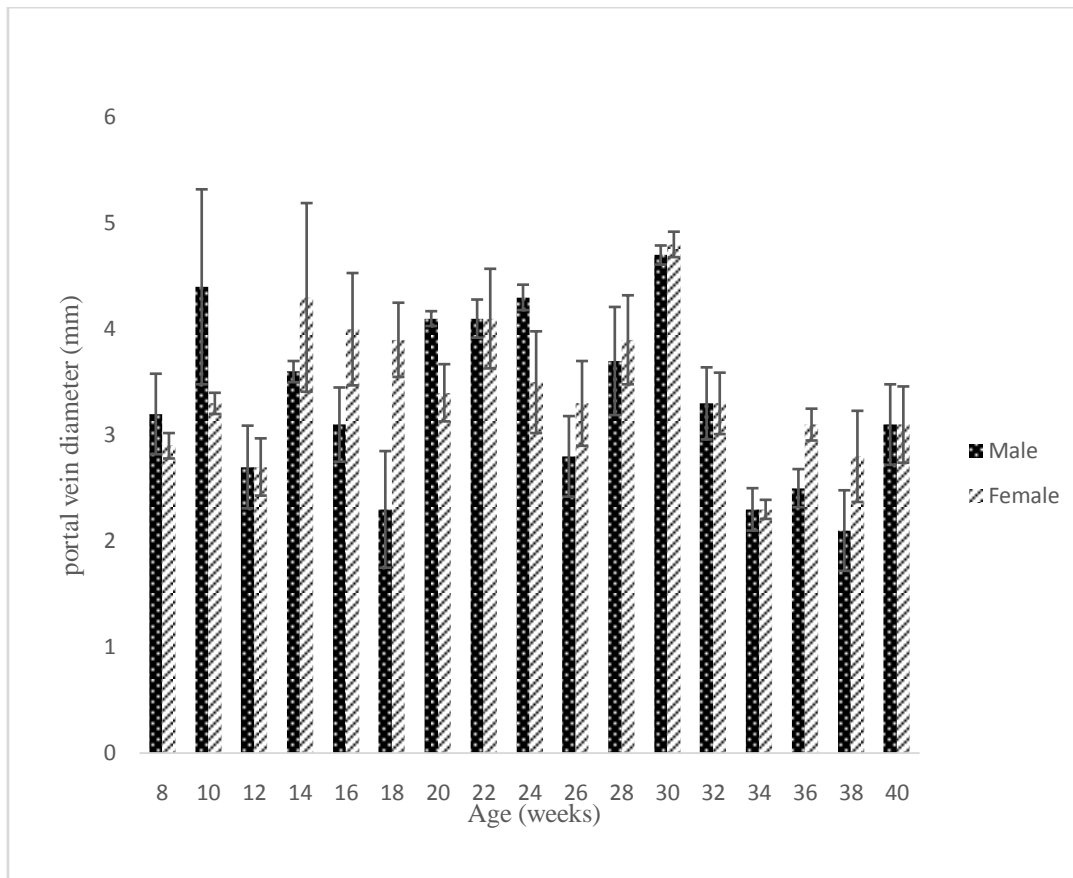


Figure 4.10: The mean and SEM of the portal vein diameter (PVD) and in male and female Nigerian Indigenous puppies.

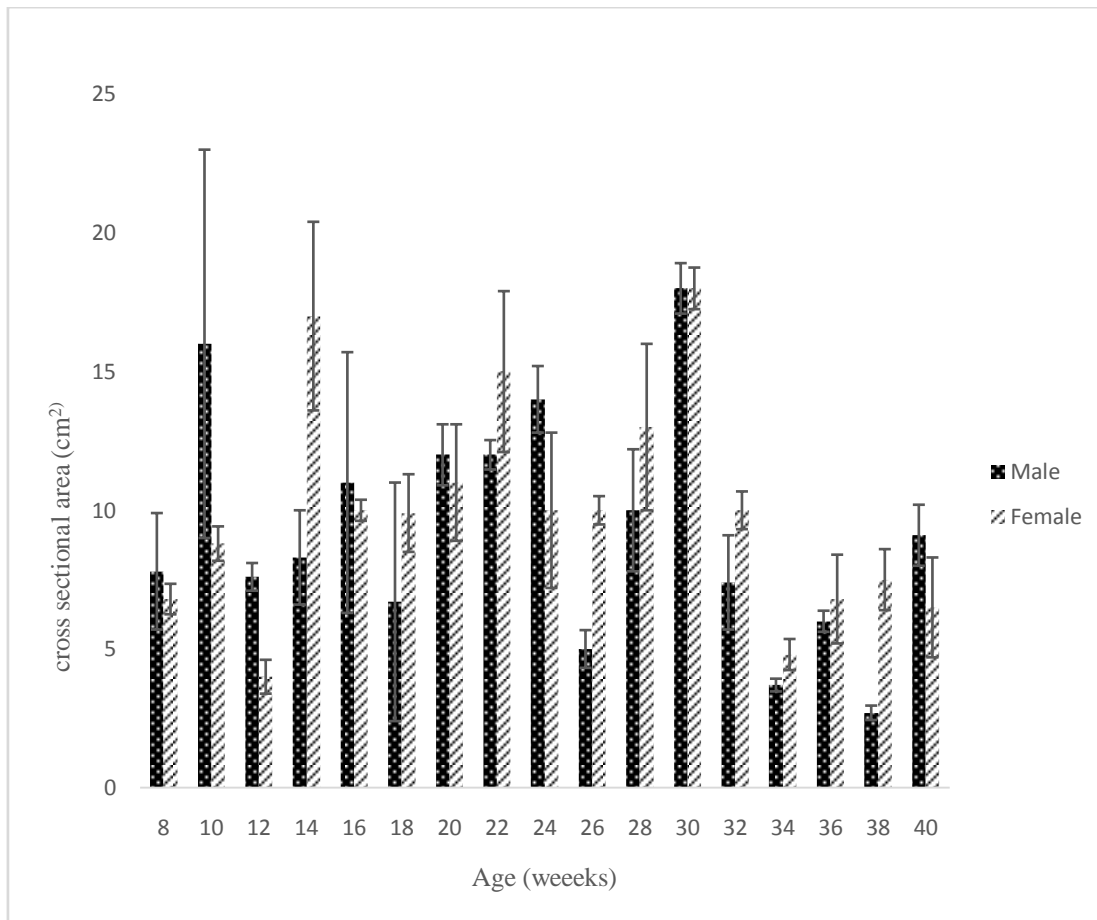


Figure 4.11: The mean and SEM of the cross sectional area (CSA) in male and female Nigerian Indigenous puppies.

Table 4.9 Correlation between the portal vein diameter, demographic data and ultrasound hepatobiliary dimensions in the six puppies. (n = 6).

Parameter	Pearson r	P value summary	Is the correlation significant?	R squared
Age (weeks)	-0.24	Ns	No	0.059
weight (kg)	-0.2	Ns	No	0.038
BL (cm)	-0.074	Ns	No	0.0055
HT (cm)	-0.077	Ns	No	0.0059
BMI (Kg/m ²)	-0.16	Ns	No	0.026
HL (cm)	0.29	Ns	No	0.082
HW (cm)	0.08	Ns	No	0.0063
HV (cm ³)	-0.19	Ns	No	0.037
CSA (cm ²)	0.99	***	Yes	0.99
GBL (cm)	-0.17	Ns	No	0.03
GBW (mm)	0.3	Ns	No	0.093
GBWT (mm)	0.39	Ns	No	0.15
GBV (cm ³)	-0.11	Ns	No	0.012
BMI (Kg/m ²)	-0.16	Ns	No	0.026

*Correlation is significant at the 0.01 level (2-tailed), **Correlation is significant at the 0.001 level (2-tailed), ***Correlation is significant at the 0.0001 level (2-tailed), ns= not significant

KEY: WT (weight); BL (body length); HT (height); BMI (body mass index); HL (hepatic length); HW (hepatic width); HV (hepatic volume); PVD (portal vein diameter); CSA (cross sectional area); GBL (gall bladder length); GBW (gall bladder width); GBWT (gall bladder wall thickness); GBV (gall bladder volume).

Table 4.10The correlation between the cross sectional area of the portal vein diameter, demographic data and ultrasound hepatobiliary dimensions in the six puppies. (n = 6).

Parameter	Pearson r	P value summary	Is the correlation significant?	R squared
Age (weeks)	-0.24	Ns	No	0.057
WT (kg)	-0.2	Ns	No	0.039
BL (cm)	-0.082	Ns	No	0.0067
HT (cm)	-0.082	Ns	No	0.0068
BMI (Kg/m ²)	-0.17	Ns	No	0.03
HL (mm)	0.31	Ns	No	0.095
HW (mm)	0.067	Ns	No	0.0045
HV (cm ³)	-0.19	Ns	No	0.038
PVD (mm)	0.99	***	Yes	0.99
GBL (mm)	-0.17	Ns	No	0.029
GBW (mm)	0.32	Ns	No	0.11
GBWT(mm)	0.4	Ns	No	0.16
GBV (cm ³)	-0.11	Ns	No	0.011

*Correlation is significant at the 0.01 level (2-tailed), **Correlation is significant at the 0.001 level (2-tailed), ***Correlation is significant at the 0.0001 level (2-tailed), ns= not significant

KEY: WT (weight); BL (body length); HT (height); BMI (body mass index); HL (hepatic length); HW (hepatic width); HV (hepatic volume); PVD (portal vein diameter); CSA (cross sectional area); GBL (gall bladder length); GBW (gall bladder width); GBWT (gall bladder wall thickness); GBV (gall bladder volume).

4.3 Biometry of the Pancreas

The pancreas could not be visualized in all the six puppies with the ultrasound machine used.

4.4 The Biochemical Assay of Alanine Aminotransferase (ALT), Aspartate Aminotransferase (AST) and Alkaline Phosphatase (ALP)

The mean and standard error of mean values obtained from the analysis of the serum for ALT, AST and ALP to evaluate the liver condition is presented in the Table 4.11.

Table 4.11. Mean values of the ALT, AST and ALP from the Nigerian Indigenous puppies. (n = 6).

Age (weeks)	AST(IU/L)	ALT(IU/L)	ALP(IU/L)
16	21 ± 3.6	25 ± 1.8	92 ± 15
24	20 ± 1.9	26 ± 2.9	79 ± 5.7
32	25 ± 2.3	24 ± 1.7	81 ± 4.9
40	27 ± 2.6	23 ± 1.9	84 ± 6.7
Reference values*	10-34	10-130	24-147

* (McAtee and Lidbury, 2017)

CHAPTER FIVE

5.0 DISCUSSION

It was observed that all the hepatic dimension including hepatic length (HPL), width (HPW) and volume (HPV) increased with age progressively with slight variation (Figure 4.4). This is to compensate for metabolic demand of the body as similarly explained by Siddiqui *et al.*, (2014). Progressive exponential growth of the HPL was observed throughout the study period (40weeks), though slight variation was recorded from various measurement (Figure 4.1). The variation was reported to be due to changes in the anatomic conformation after birth such as widening of the thorax that will allow repositioning of the liver and subsequent apparent reduction in the hepatic length and the volume (England, 1996). More so, Washabau (2012) reported that the liver was not always accessible to ultrasonographic scanning because a portion of it may be obscured by the overlying stomach. The hepatic length (HL) in male puppies ages 12 and 36 weeks were 90 ± 2.9 and 126 ± 3.4 mm respectively. This was higher than 65 ± 1.23 and 75 ± 0.88 mm observed in human of similar age by Dhingra *et al.*, (2010) respectively. Similarly, the hepatic length (HL) in female puppies at the age of 12 and 36 weeks were 92 ± 1.5 and 136 ± 1.3 mm respectively. This was higher than 62 ± 0.61 and 75 ± 0.92 mm observed in human of similar age by Dhingra *et al.*, (2010) respectively.

Although the hepatic length (HPL) of female was higher than that of the males at week 8 and 40, the difference was not significant (Figure 4.1). However, the HPL of male at the age of 30 weeks was significantly higher than that of the female puppies. There is hence no need to establish a separate reference value for both sex as similarly reported by several researchers (Sucena da Rocha *et al.*, 2009; Eze *et al.*, 2013 and Ozidikici, 2017).

It was also observed that all the gall bladder ultrasound dimension including gall bladder length (GBL) and width (GBW) increased progressively with age continuously with slight variation (Figure 4.9) except the gall bladder wall thickness (GBWT) in which the values does not follow any pattern. In this study, the observed mean values for male gall bladder dimension were not significantly different from that of the female. This was similar to the report by Adeyekun and Ikechukwu, (2013) who reported that there was no statistically significant difference between the male and female gall bladder dimension in human. In this study the observed GBL and GBW ranged from 11 ± 0.9 to 29.0 ± 1.4 mm and 5.6 ± 0.63 to 23 ± 7.9 mm respectively. This was different from the corresponding values of 11.4 to 95.7 mm and 15 to 48 mm observed by Adeyekun and Ikechukwu, (2013) in human. This was due to age and specie difference compared to our own study. The observed gall bladder volume in this study ranged from 0.18 ± 0.03 to 3.0 ± 0.42 cm³ while the gall bladder wall thickness ranged from 0.65 ± 0.03 to 1.8 ± 0.09 mm. This was similar to the mean gallbladder volume of 2.41ml (0.84–4.50ml) and gallbladder wall thickness of 0.9mm (0.6–1.2mm) observed in cats by Dominique *et al.*, (2010). This was however different from the corresponding range values of 6.96 to 108.1 cm³ and 1.6 to 4.2 mm observed by Adeyekun and Ikechukwu, (2013) in human. More so, higher GBWT of 1.7mm to 3mm has been reported by Cooperberg and Gibney, (1987); Wolson, (1990) and Mohammed *et al.*,

(2010) in human population. This was due to age and specie difference compared to our own study. Though a higher GBWT may be a nonspecific finding (Rall *et al.*, 1981), however, in children as well as matured human an increase GBWT may be a sign of disease (Mohammed *et al.*, 2010).

The liver parenchyma appeared as a loosely granular structure with homogenous and uniform echogenicity which was interrupted by short, highly echogenic paired parallel lines surrounding an anechoic lumen that represents the portal veins and anechoic linear structures that represents the hepatic veins (Plate 4.1). Nyland *et al.*, (2002) and Ivancic and Mai, (2008) had similarly reported the hepatic parenchyma to be homogeneous and uniform in echogenicity. However, Adeyekun and Ikechukwu, (2013) reported the hepatic parenchyma to be uniform hypoechoic echo texture which is coarsely echogenic in the puppies for the first 8 weeks of life. The cranial border of the liver appeared as a curved hyper-echoic line that represents the diaphragm which is the interface between the lungs and the liver as similarly reported by Nathalie, (2010) and Larson, (2013). The gallbladder was observed as anechoic, round to oval structure just to the left of the midline of the puppies (right of the scanner) in most of the liver scanned (Plate 4.2). This was similarly reported by several authors; Dominique *et al.*, 2010; Adeyekun and Ikechukwu, 2013 in normal cats and human population respectively.

In this study all the demographic data and hepatobiliary dimensions studied were found to increase significantly with age of the puppies. The growth pattern observed corresponds to the expected higher rate during the first year of life as similarly observed by Sucena da Rocha *et al.* (2009) and Eze *et al.* (2013) in healthy new born and children. In our study, it was also observed that HL was highly correlated with the age, weight, body length, and

height and moderately correlated with the BMI (Table 4.2). Significant increase in the liver dimension with increase in height and body weight has also been reported by several authors (Konus *et al.*, 1998; Soyupak *et al.*, 2002; Sucena da Rocha *et al.*, 2009; Eze *et al.*, 2013). Among the body parameters, height was found to have highest correlation coefficient hence best predictor of the HL as similarly reported by Eze *et al.*, (2013) in school age children. This signifies that height is the best predictor of HL among all the demographic data in different species. More so, BMI was found to be moderately correlated with HL which was similar to the report by Eze *et al.*, (2013) in children. There are few literature on the correlation of the HL with the hepatic width and volume, this study had found out that there was significantly high correlation among them. Furthermore, HL was found to be significantly correlated with GBL, GBW and GBV. This might be due to the fact that the liver, ventral pancreas and gall bladder have a common embryological tissue origin (posteroventral foregut endoderm) in early embryogenesis (Uemura *et al.*, 2015), hence same rate of development.

Similar to the HL, HW correlated significantly and strongly with all the demographic data and hepatobiliary dimensions studied. However, the relationship is stronger with the HW (Table 4.3). The relationship of the HW with the BMI is also stronger compared to what was observed with the HL. Unlike what was observed with the HL, body length had the highest correlation coefficient ($r = 0.93$), hence best predictor of the HW.

Similarly, HV correlated significant and strongly with all the demographic data and hepatobiliary dimensions studied, however, the relationship is stronger with the HV (Table 4.4). Unlike what was observed with the HL and HW, age and weight had the highest correlation coefficient ($r = 0.96$ and $r = 0.95$ respectively), hence weight is the best

predictor of the HV. So the higher the weight of a puppies the higher the hepatic volume. HV is however significant and negatively correlated with GBWT ($r = -0.52$).

In this study it was also observed that the GBL, GBW and GBV correlated significantly with all the demographic data and hepatobiliary dimensions studied, however, the relationship is stronger with the GBL and GBV (Table 4.5, 4.6 and 4.8). Among the demographic data, weight correlated best with the GBL and GBV ($r = 0.79$ and $r = 0.74$ respectively) while height correlated best with the GBW ($r = 0.69$). Adeyekun and Ikechukwu, (2013) has similarly reported in human subject that body weight correlated significantly with the GBW and GBV and not significantly with the GBL. In this study, BMI was significant and positively correlated with the GBL, GBW and GBV, however, Adeyekun and Ikechukwu, (2013) reported no significant relationship between the BMI with the GBL, GBW and GBV. Similar to our findings a strong positive correlation between gallbladder volume and the body weight of the dogs using ultrasonography has been reported by several authors in healthy dogs (Atalan *et al.*, 2007; Ramstedt *et al.*, 2008; Rahmani *et al.*, 2015), and humans (Kishk *et al.*, 1987) which indicated that the gallbladder volume increases with body weight. However, Finn-Bodner *et al.*, (1993) reported no relationship between the gallbladder volume and body weights of dog determined by an ellipsoid method. This may be due to differences in food with-holding intervals before measurements as well as the body weights of the dogs included in this study as similarly observed by Rahmani *et al.*, (2015).

GBWT was significant and negatively correlated with the age, weight and hepatic volume ($r = -0.57$, -0.5 and -0.52 respectively) and not significantly correlated with the BL, HT and BMI. This was different from the report of Mohammed *et al.*, (2010) and Adeyekun and

Ikechukwu, (2013) who found no correlation between the GBWT with the age and weight respectively. But similar to the finding of Mohammed *et al.*, (2010) in which body height does not correlated to the GBWT. This study showed that GBWT does not correlated with the BMI. However, Mohammed *et al.*, (2010) reported a strong positive correlation between GBWT and BMI.

Values obtained for portal vein diameter did not increase along with age (Figure 4.10) in our study, however, Siddiqui *et al.*, (2014) reported a significant increase in portal vein diameter with age. The values obtained from cross sectional area ranged from 0.04 to 0.13 cm². This was different from the values of 0.99 to 1.13 cm² observed by various authors in human (Moriyasu *et al.*, 1986; Tasu *et al.*, 2002; Chuo *et al.*, 2005; Aiyekomogbon *et al.*, 2014). This may be due to age or species difference from our study. There was no significant difference in the mean values of the portal vein diameter observed for both male and female. This was similarly reported by Kratzer *et al.*, (2003) and Siddiqui *et al.*, (2014). PVD does not correlate with any of the demographic data and hepatobiliary dimensions studied. This was different from the report by Shankar *et al.* (2011) and Siddiqui *et al.* (2014) who found that PVD correlated significantly and positively with the age and weight in human population (Shankar *et al.*, 2011; Siddiqui *et al.*, 2014).

The pancreas was not visible in all the six puppies with the ultrasound machine used. The inability to visualize the pancreas with the ultrasound machine was due to homogenous echogenicity with its adjacent fats and lack of well-defined capsule. Chaudhary and Bano (2011), reported that CT remains the most effective imaging modality for evaluation of the pancreas though MRI is increasingly used for further identification and characterization of pancreatic diseases. More so, Quenceret *et al.*, (2013) reported that ultrasound has a limited

role in pancreatic evaluation as the overlying gas from the transverse colon and stomach make visualizing pancreatic parenchyma difficult or even impossible.

The established normal parameters for the hepatic and gall bladder dimension is necessary in diagnosis of various clinical conditions as increase in the hepatic length and or volume would translate to hepatomegaly while decrease in the hepatic length and or volume compared to observed values at a specific age would translate to liver cirrhosis. Similarly, an increase in the gall bladder dimension compared to what was recorded in this study at a specific age could indicate some clinical conditions such as cholecystitis, gall stone, polyps and cancer.

CHAPTER SIX

6.0 CONCLUSION AND RECOMMENDATION

6.1 Conclusion

This study has established the following about the sonographic evaluation of the hepatobiliary system and pancreas in relation to the demographic data (age, body weight, height, length and body mass index) in clinically healthy puppies.

- i. The mean values and standard error of mean (\pm SEM) of the ultrasound measurement of the hepatic length (HL), hepatic width (HW) and hepatic volume (HV) for NIDs ranged from 65 ± 4.7 to 134 ± 3.6 mm, 28 ± 1.4 to 81 ± 3 mm and 176 ± 16 to 1358 ± 71 mm³ respectively.
- ii. The mean values \pm SEM for the gall bladder length (GBL), width (GBW), wall thickness (GBWT) and volume (GBV) for NIDs ranged from 11 ± 0.9 to 21 ± 2.9 mm, 5.6 ± 0.63 to 15 ± 1.5 mm, 0.71 ± 0.063 to 0.67 ± 0.088 mm and 0.18 ± 0.025 to 2.2 ± 0.54 mm³ respectively.
- iii. The hepatic length, width and volume correlated significantly and positively with all the demographic data (age, weight, height, body length and body mass index) with the height, body length and weight being the best predictor of the hepatic length, width and volume respectively.
- iv. The gall bladder length, width and volume correlated significant and positively with all the demographic data (age, weight, height, body length and body mass

index) with the weight being the best predictor of gall bladder length and volume while the height was the best predictor of gall bladder width.

- v. The gall bladder wall thickness correlated significant and negatively with the age ($r = -0.57$), weight ($r = -0.5$) and hepatic volume ($r = -0.52$).
- vi. The mean and standard error of mean for portal vein diameter ranged from 2.3 ± 0.1 to 4.8 ± 0.07 mm while the cross sectional area of the portal vein ranged from 4.25 ± 0.37 to 17.99 ± 0.53 mm² ; and PVD neither correlated with demographic data nor hepatobiliary dimensions studied.
- vii. The pancreas was not visible with the ultrasound machine employed for the study.

6.2 Recommendations

- i. The established normal parameters for the hepatic and gall bladder dimension should be incorporated in routine clinical examination of Nigerian Indigenous puppies towards diagnosis of hepatobiliary pathologic conditions.
- ii. The height, body length and weight being the best predictor of the hepatic length, width and volume respectively should be used in clinical diagnosis of hepatic diseases.
- iii. The weight being the best predictor of gall bladder length and volume could also be used in clinical diagnosis of diseases associated with the gall bladder organ.
- iv. Further studies be carried out on pancreas using CT and MRI.

6.3 Limitations

- i. The field coverage of ultrasound scan is minimal compared to that of CT and MRI.
- ii. The transducer was a single frequency probe and could not be adjusted to other frequencies.

REFERENCES

- Abby, C. (2010). Diagnostic Imaging: Liver Disease. *Veterinary Times*. Retrieved from <http://www.vettimes.co.uk/article/diagnostic-imaging-liver-disease/?format=pdf>. Accessed on 1/20/2016@ 15:59 GMT.
- Adeyekun, A. A. and Ikechukwu, O. U. (2013). Sonographic evaluation of gall bladder dimension in healthy adults in Benin City Nigeria. *West African Journal of Radiology*, 20(1): 4-8.
- Aguirre, A. (2010). Diseases of Gallbladder and Extrahepatic Biliary System. In: Ettinger, S., Feldman, E., eds. *Textbook of Veterinary Internal Medicine*. St. Louis, MO: Elsevier, Pp. 1689-1695.
- Aguirre, A. L., Center, S. A., Randolph, J. F., Yeager, A. E., Keegan, A. M., Harvey, H. J. and Erb, H. N. (2007). Gallbladder disease in Shetland Sheepdogs: 38 cases (1995–2005). *Journal of American Veterinary Medical Association*, 231: 79–88.
- Ahmed, R. M. E., Kandiel, M. M. M., Sosa, G. A., Abou El-Roos, M. E. A., Abdel-Ghaffar, A. E. and El-Azab, A. I. (2012). Ultrasound Imaging of the Testes and Accessory Sex Glands in Buffalo Bulls Treated with Gonadotrophic Releasing Hormone. *Journal of Reproduction and Infertility*, 3(1): 08-16
- Aiyekomogbon, J. O., Philip, O. I., Abdulkadir, M. T., Com, N. D., Rasheed, Y., Alfred, O. A., Kofo, S. and Igashi, J.B. (2014). Determination of normal portal vein congestive index on ultrasound scan among adults in Zaria, Nigeria. *Archives of International Surgery*, 4(3): 146-151.
- Allen, A.K. and Stone, L.R. (1990). Equine diagnostic ultrasonography-equipment selection and use. *Compendium of Continuing Education Practicing Veterinarian*, 12(9):1307-11.
- Anonymous1 (2006). The History of Ultrasound: A collection of recollections, articles, interviews and images. www.obgyn.net. Archived from the original on 5 August 2006. Retrieved
- Anonymous 2 (2013). [http://Zaria, en. Wikipedia. Org/Wiki/Zaria](http://Zaria.en.Wikipedia.Org/Wiki/Zaria). Retrieved on 25th April, 2016 at 21:00 GMT.
- Anonymous 3 (2015): The History of Ultrasound. Accessed from [www.ultrasoundSchools Guide.com](http://www.ultrasoundSchoolsGuide.com).
- Anonymous4 (2017). 1.7 M-mode. Available at <http://123sonography.com/content/17-mode>. Accessed on 14/02/17@20:43:18p:m
- Anonymous 5 (2005). Scientist fetch useful information from dog genome publications, cold spring laboratory, December 7, 2005; published online in Bio-medicine: “Phenotypic

variation among dog breeds whether be in size, shape, or behavior, is greater than another animal. Retrieved from www.wikipedia.com on the 17th July, 2018 at 20:01 GMT.

- Arowolo, R.O.A. (1999). *Protecting Our Livestock Resources*. 1995/96 Inaugural lecture, University Press, U.I. Ventures Ltd., Ibadan, pp. 5.
- Asadi, S., Molazem, M., Masoudifard, M., Jamshidi, S., Soroori, S. and Ghazale, N. (2011). Three-dimensional volumetric ultrasonography of enlarged adrenal gland in dog. *Iranian Journal of Veterinary Surgery*, 6: 31–35.
- Atalan, G., Barr, F. J. and Holt, P. E. (2007). Estimation of the volume of the gall bladder of 32 dogs from linear ultrasonographic measurements. *Veterinary Record*, 160: 118–122.
- Bailiff, N.L., Norris, C.R., Seguin, B., Griffey, S.M., Ling, G.V. (2004). Pancreatolithiasis and pancreatic pseudoblaster associated with pancreatitis in a cat. *Journal of American Animal Hospital Association*, 40(1):69–74.
- Barella, G., Lodi, M., Sabbadin, L. A. and Faverzani, S. (2012). A new method for ultrasonographic measurement of kidney size in healthy dogs. *Journal of Ultrasound*, 15: 186–191.
- Barthez, P.Y., Leveille, R. and Scriverani, P.V. (1997). Side lobes and grating lobes artifacts in ultrasound imaging. *Veterinary Radiology and Ultrasound*, 38:387–393.
- Best, E.J., Bush, D.J. and Dye, C. (2010). Suspected choledochal cyst in a domestic shorthair cat. *Journal of Feline Medicine and Surgery*, 12:814–817.
- Bonekamp, S., Kamel, I., Solga, S. and Clark, J. (2009). Can imaging modalities diagnose and stage hepatic fibrosis and cirrhosis accurately? *Journal of Hepatology*, 50:17–35.
- Boothe, H.W., Boothe, D.M., Komkov, A. and Hightower, D. (1992). Use of hepatobiliary scintigraphy in the diagnosis of extrahepatic biliary obstruction in dogs and cats: 25 cases (1982–1989). *Journal of American Veterinary Medical Association*, 201:134–141, 1992.
- Bosje, J. T., van den Ingh, T. S. and van der Linde-Sipman, J. S. (1998). Polycystic kidney and liver disease in cats. *Veterinary Quarterly*, 20:136–139.
- Braun, U., Nuss, K., Soldati, G. and Ossent, R. (2005). Clinical and ultrasonographic findings in four cows with liver tumours. *Veterinary Record*, 157(16): 482–4.
- Bukar-Kolo, Y. M., Mustapha, M., Zakariah, M., Allo, A. and Adamu, L. (2016). Relationships between zoometric measurements, coat colors and body condition scores of the Nigerian indigenous dogs in Maiduguri, Northeastern

- Carlisle, C. H., Wu, J. X. and Heath, T. J. (1995). Anatomy of the portal and hepatic veins of the dog: A basis for systematic evaluation of the liver by ultrasonography. *Veterinary Radiology and Ultrasound*, 36:227–233.
- Center, S. A. (1998). Nutritional support for dogs and cats with Hepatobiliary disease. *Journal of Nutrition*, 128: 2733-2746
- Center, S. A. (2009). Diseases of the Gallbladder and Biliary Tree. *Veterinary Clinic of North American Small Animal Practice*, 39:543-598.
- Cerri, G. G. and Vogueira, L. A. A. (2002). Ultra-sonografia em gastroenterologia. In: Mincis M. Gastroenterologia e hepatologia: diagnóstico e tratamento. 3^a ed. São Paulo, SP: Lemos Editorial pp. 45–53.
- Chammas, M. C., Marcelino, A. S. Z. and Saito, O. C. (2006). Vesícula biliar. Ductos biliares. In: Lopes AC. Tratado de clínica médica. São Paulo, SP: Roca; pp. 1217–32.
- Chaudhary, V. and Bano, S. (2011). Imaging of the pancreas: Recent advances. *Indian Journal of Endocrinology and Metabolism*, 15 (1): S25-S32.
- Choi, J., Keh, S., Kim, J. and Yoon, J. (2013). Radiographic liver size in Pekingese dogs versus other dog breeds. *Veterinary Radiology and Ultrasound*, 54(2): 103-6.
- Choong, C. C., Venkatesh, S. K. and Siew, E. P. (2012). Accuracy of routine clinical ultrasound for staging of liver fibrosis. *Journal of Clinical Imaging Science*, 2(1): 58.
- Christoph, F. D., Carla, S. and Maciej, J. (2012). Ultrasound of the liver. European Course Book. Available from <http://www.efsumb.org/ecb/ecb-01.asp>. Accessed on 28/07/2015 at 16:02 GMT.
- Chuo, L. S., Mahmud, R., and Salih, Q. A. (2005). Colour dopplerultrasound examination of the main portal vein and inferior vena cava in normal Malaysian adult population: A fasting and postprandial evaluation. *The Internet Journal of Cardiovascular Research*, 2.
- Coltera, M. (2010): Ultrasound physics in a nutshell. *Otolaryngologic Clinics of North America*, 43(6):1149–59.
- Contran, R. S., Kumar, V. and Robbins, S. L. (2005). Robbins: pathologic basis of disease. 7th edition. Philadelphia, PA: Elsevier Saunders. 2005. Pp. 1325-1419
- Cooperberg, P. L. and Gibney, R. G (1987). Imaging of the gall bladder. *Radiology*, 163: 605-613.

- Cornell, K. (2012). Pancreas. In: Tobias, K.M., Johnston, S.A. (eds.). *Veterinary Surgery: Small Animal*. St. Louis, Elsevier, Saunders. 97(2): 1659-1673.
- Covey, J. L., Degner, D. A., Jackson, A. H., Hofeling, A. D. and Walshaw., R.. (2009). Hilar liver resection in dogs. *Veterinary Surgery*, 38:104–111.
- Cruz-Arambulo, R, Wrigley, R. and Powers, B. (2004). Sonographic features of histiocytic neoplasms in the canine abdomen. *Veterinary Radiology and Ultrasound*, 45:554–558.
- Cuccovillo, A. and Lamb, C.R. (2002). Cellular features of sonographic target lesions of the liver and spleen in 21 dogs. *Veterinary Radiology and Ultrasound*, 43:275–278
- Cullen, J. M. (2009). Summary of the World Small Animal Veterinary Association standardization committee guide to classification of liver disease in dogs and cats. *Veterinary Clinics of North America: Small Animal Practice*, 39: 395-418
- Cullen, J. M., van den Ingh, T., Bunch, S. E., Rothuizen, J., Washabau, R. J. and Desmet, V. J. (2006). Morphological classification of circulatory disorders of the canine and feline liver. In: *Standards for Clinical and Histological Diagnosis of Canine and Feline Liver Diseases*, ed. Rothuizen *et al.*, pp. 41-59, Saunders Elsevier, Philadelphia
- d' Anjou, M. A. and Penninck, D. (2015). Liver. In: Penninck, D., d'Anjou, M.A. (eds). *Atlas of Small Animal Ultrasonography*. ed. 2 Ames, Ia, Wiley-Blackwell Publishing. Pp. 183-238
- d'Anjou, M. A. (2007). The sonographic search for portosystemic shunts. *Clinical Techniques in Small Animal Practice*, 22:104–114.
- d'Anjou, M. A. (2008). Liver. In Penninck, D., d'Anjou, M.A., editors: *Atlas of Small Animal Ultrasonography*. 1st ed. Ames, Ia., Wiley-Blackwell Publishing. pp 339-364
- d'Anjou, M. A., Penninck, D., Cornejo, L. and Pibarot, P. (2004). Ultrasonographic diagnosis of portosystemic shunting in dogs and cat. *Veterinary Radiology of Ultrasound*, 45:424–437.
- Dähnert, W. (2001). Radiologia: manual de revisão. 3^a ed. Rio de Janeiro, RJ: Revinter.
- Daniela, G. (2011). Physical principles: In: *British Small Animal Veterinary Association Manual of Canine and Feline Ultrasonography*. Ed. Barr. F and Gaschen. Pp 15-16. British Small Animal Veterinary Association Publication Gloucester
- Dhingra, B., Suvasini, S., D., Evendra, M., Reema, K., Ravindra, M. P. and Shailendra, A. (2010). Normal values of liver and spleen by ultrasonography in Indian Children. *Indian Pediatrics*, 47: 487-492.

- Diana, A., Guglielmini, C., Specchi, S., Di Tommaso, M., Pietra, M., Baron Toaldo, M. and Cipone, M. (2012). Ultrasonographic evaluation of preprandial and postprandial gallbladder volume in healthy cats. *American Journal of Veterinary Research*, 73:1583–1588.
- Dominique, G. P., Jennifer, O. B. and Cynthia, R. L. W. (2010). Sonographic assessment of gallbladder volume in normal cats. *Veterinary Radiology and Ultrasound*, 51 (6): 665–666.
- Dyce, K. M., Sack, W. O. and Wensing, C. J. G. (1987). Editors: *Textbook of Veterinary Anatomy*, ed 1, Philadelphia, Saunders, pp 130–133.
- Elbagir, S, Mohamed, Y., and Bushra, A. (2014). Role of CT scan and Ultrasound Imaging in Characterization of Common Liver Diseases. *Indian Journal of Applied Research*.
- El Sharkawy, E., Faris, R., Grumbach, K., Edelman, R., Clemens, T., Rao, M., Darwish, M. (1997). Ultrasonographic measurement of the normal liver and spleen among Egyptians 10-50 years old. *Journal of Egyptians Public Health Association*, 72(3-4):257-83.
- England, G. C. W. (1996). Renal and hepatic ultrasonography in the neonatal dog. *Veterinary Radiology and Ultrasound*, 37 (5): 374-382.
- Etue, S. M., Penninck, D. G., Labato, M. A., Pearson, S. and Tidwell, A. (2001). Ultrasonography of the normal feline pancreas and associated anatomic landmarks: a prospective study of 20 cats, *Veterinary Radiology and Ultrasound*,42:330
- Evans, H. E. (1993). The digestive apparatus and abdomen. In Evans HE, editor: *Miller's Anatomy of the Dog*, ed 3, Philadelphia, 1993, Saunders, pp 385–463.
- Eze, C. U., Kenneth, K. A., Daniel, N. E. and Ann, E. A. (2013). Sonographic biometry of liver size among Ibo school age children of South-East, Nigeria. *Radiography*, 19,: 228-233.
- Feldman, M.K., Katyal, S. and Blackwood, M.S. (2009). Ultrasound artifacts. *Radiographics* ,29:1179.
- Finn-Bodner, S. T., Park, R. D., Tyler, J. W., Twedt, D. C. and Curtis, C. R. (1993). Ultrasonographic determination, in vitro and in vivo, of canine gallbladder volume, using four volumetric formulas and stepwise-regression models. *American Journal of Veterinary Research*, 54: 832–835.
- Forman, M. A., Marks, S. L., De Cock, H. E., Hergesell, E. J., Wisner, E. R., Baker, T. W., Kass, P. H., Steiner, J. M. and Williams, D. A. (2004). Evaluation of serum feline pancreatic lipase immunoreactivity and helical computed tomography versus conventional testing for the diagnosis of feline pancreatitis. *Journal of Veterinary Internal Medicine*, 18: 807-815

- Frances, B. and Lorrie, G. (2011). British Small Animal Veterinary Association Manual of Canine and Feline ultrasonography. Retrieved from <http://www.British Small Animal Veterinary Association.com>. Accessed on 11/22/2015@ 16:27 G.M.T
- Franchi-Teixeira, A. R., Antoniali, F. and Boin, I. F. S .F. (1997). Icterícia obstrutiva: diagnóstico laboratorial e de imagem. *Medicina (Ribeirão Preto)*, 30:198–208.
- Gaillot, H. A., Penninck, D. G., Webster, C. R. and Crawford, S. (2007). Ultrasonographic features of extrahepatic biliary obstruction in 30 cats. *Veterinary Radiology and Ultrasound* 48:439–447.
- Gerhardt, A., Steiner, J. M., Williams, D. A. Kramer, S., Fuchs, C., Janthur, M., Hewicker-Trauntwein, M., and Nolte, I. (2001). Comparison of the sensitivity of different diagnostic tests for pancreatitis in cats. *Journal of Veterinary Internal Medicine*, 15, 329-333
- Godshalk, C. P., Badertscher, R. R. and Rippey, M. K. (1988). Qualitative ultrasonic assessment of liver size in the dog, *Veterinary Radiology*, 29:162.
- Goel, S., Rustagi, S.M., Saha, S., Mehta, V., Suri, R. K. and Rath, G. (2015). Aberrant Pancreatic ductal Organisation : a case report. *Surgical and Radiological Anatomy*, 37 (5): 543-546
- Guillot, M., d'Anjou, M.A., Alexander, K., Bédard, C., Desnoyers, M., Beauregard, G. and Del Castillo, J. (2009) Can sonographic findings predict the results of liver aspirates in dogs with suspected liver disease? *Veterinary Radiology of Ultrasound*, 50:513–518
- Gunderman, R.B. (2007). Fundamentos de radiologia: apresentação clínica, fisiopatologia, técnicas de imagens. In: R. J. Guanabara Koogan. 2ª ed. Rio de Janeiro.
- Hall, E. J. and German, A. J. (2005). Laboratory evaluation of hepatic disease. In *British Small Animal Veterinary Association Manual of Canine and Feline Clinical Pathology*. Villiers. E and Blackwood, L. Eds., pp. 184–206, British Small Animal Veterinary Association, Gloucester, UK, 2nd edition.
- Hangiandreou, N. J. (2003). AAPM/RSNA physics tutorial for residents: Topics in US: B-mode US: basic concepts and new technology, *Radiographics*, 23:1019.
- Hansson, K., Haggstrom, J., Kwart, C. and Lord, P. (2002). Left atrial to aortic root indices using two-dimensional and M-mode echocardiography in Cavalier King Charles spaniels with and without left atrial enlargement. *Veterinary Radiology and Ultrasound*, 43:568–575.
- Harbin, W. P., Robert, N. J. and Ferrucci Jr, J. T. (1980). Diagnosis of cirrhosis based on regional changes in hepatic morphology: a radiological and pathological analysis. *Radiology*, 135(2): 273-283.

- Harran, N., d'Anjou, M. A., Dunn, M. and Beauchamp, (2011). Gallbladder sludge on ultrasound is predictive of increased liver enzymes and total bilirubin in cats. *Canadian Veterinary Journal*, 52:999–1003
- Harran, N., d'Anjou, M.A. and Dunn, M. (2009). Gallbladder sludge in cats: Prevalence and association with elevated serum liver parameters. *2009 Annual Scientific Meeting of the American College of Veterinary Radiology*. Memphis, TN. P 31.
- Hashimoto, S., Goto, H., Hirooka, Y., Itoh, A., Ishiguro, Y., Kojima, S., Hirai, T., Hayakawa, T. and Naitoh, Y. (1999). An evaluation of three-dimensional ultrasonography for the measurement of gallbladder volume. *American Journal of Gastroenterology*, 94: 3492–3496.
- Head, L. L. and Daniel, G. B. (2005). Correlation between hepatobiliary scintigraphy and surgery or post-mortem examination findings in dogs and cats with extrahepatic biliary obstruction, partial obstruction or patency of the biliary system: 18 cases (1995–2004). *Journal of American Veterinary Medical Association*, 227:1618–1624.
- Hecht, S. and Henry, G. (2007). Sonographic evaluation of normal and abnormal pancreas: *Clinical techniques in Small Animal Practice*, 22(3): 115-21
- Hecht, S., Penninck, D. G., Mahony, O. M., King, R. and Rand, W. M. (2006). Relationship of pancreatic duct dilation to age and clinical findings in cats. *Veterinary Radiology and Ultrasound*, 47: 287–294.
- Heller, M. T. and Tublin, M. E. (2014). The role of ultrasonography in the evaluation of diffuse liver disease. *Radiologic Clinics of North America*, 52(6), 1163-117.
- Heng, H. G. and Widmer, W. R. (2010). Appearance of common ultrasound artifacts in conventional vs. spatial compound imaging. *Veterinary Radiology and Ultrasound*, 51:621–627.
- Hess, R. S., Saunders, H. M., Van Winkle, T. J., Shofer, S. F., Washabau, R. J. (1998). Clinical, clinicopathologic, radiographic and ultrasonographic abnormalities in dogs with fatal acute pancreatitis: 70 cases (1986-1995). *Journal of the American Veterinary Medical Association*, 213:665-670
- Hetch, S. and Baron, M., (2011). Pancrease. In: Frances, B., Lorrie, G (eds). *British Small Animal Veterinary Association Manual of Canine and Feline Ultrasonography*. Retrieved from <http://www.British Small Animal Veterinary Association.com>. Accessed on 11/12/2015@ 16:27 G.M.T
- Hindi, A., Paterson, C. and Barr, R. G. (2013). Artifacts in diagnostic ultrasound. *Reports in Medical Imaging*, 6:29–48.

- Hinkle Schwartz, S. G., Mitchell, S. L., Keating, J. H. and Chan, D. L. (2006). Liver lobe torsion in dogs: 13 cases (1995–2004). *Journal of American Veterinary Medical Association*, 228:242–247.
- Hittmair, K.M, Vielgrader, H. D. and Loupal, G. (2001). Ultrasonographic gallbladder wall thickness in cats. *Veterinary Radiology and Ultrasound*,42:149-155.
- Hornbuckle, W. E. and Kleine, L. J. (1980).Medical management of prostatic disease. In: *Current Veterinary Therapy: Small Animal Practice*. Kirk, K.W., editor. (Vol. VII). W.B. Saunders Co., Philadelphia, PA.1146-1150.
- Huber, A., Ebner, L., Heverhagen, J. T. and Christe, A. (2015). State-of-the-art imaging of liver fibrosis and cirrhosis: A comprehensive review of current applications and future perspectives. *European Journal of Radiology open*, 2: 90-100.
- Hudson, L. C. and Hamilton, W. P. (1993). *Atlas of Feline Anatomy for Veterinarians*. 1st edition. Philadelphia: WB Saunders, pp. 287
- Huwart, L., Sempoux, C. and Salameh, N. (2007). Liver fibrosis: noninvasive assessment with MR elastography versus aspartate aminotransferase- to-platelet ratio index. *Radiology*,245:458-466.
- Huwart, L., Sempoux, C., Vicaut, E.,Salameh, N., Annet, L., Danse, E., Peeters, F., ter Beek, L. C., Rahier, J., Sinkus, R., Horseman, Y. and van Beers, B. E. (2008). Magnetic resonance elastography for the noninvasive staging of liver fibrosis. *Gastroenterology*, 135:32-40.
- Igado, O. O. (2011). Neurometrics and neurocraniometry of the Nigerian local dog (*Canis lupus familiaris*). *Journal of Veterinary Anatomy*, 4(2):99-109.
- Ivancic, M. and Mai, W. (2008). Qualitative and quantitative comparison of renal vs. hepatic ultrasonographic intensity in healthy dogs. *Veterinary Radiology and Ultrasound*,49:368.
- Jaeger, J.O. Mattoon, J.S.,Bateman S.W. and Morandi, F. (2003). Combined use of ultrasonography and contrast enhanced computed tomography to evaluate acute necrotizing pancreatitis in two dogs. *Veterinary Radiology and Ultrasound*,44:72-79
- Jazrawi, R. P. (2003). Measurement of gallbladder motor functions: an overview. *Digestive and Liver Diseases*,35Suppl. 3: S51–S55.
- Jonderko, K., Ferre, J. P. and Bueno, L. (1994). Noninvasive evaluation of kinetics of gallbladder emptying and filling in the dog. A real-time ultrasonographic study. *Digestive Diseases and Sciences*,39: 2624–2633.
- Jonkers, I. J., Smelt, A. H., Ledeboer, M., Hollum, M. E., Biemond, I., Kuipers, F., Stellaard, F., Boverhof, R., Meinders, A. E., Lamers, C. H. and Masclee, A. A. (2003). Gall bladder dysmotility: a risk factor for gall stone formation in

hypertriglyceridaemia and reversal on triglyceride lowering therapy by bezafibrate and fish oil. *Gut*,52: 109–115.

- Kirberger, R. M. (1995). Imaging artifacts in diagnostic ultrasound-a review. *Veterinary Radiology of Ultrasound*, 36:297–306.
- Kishk, S. M., Darweesh, R. M., Dodds, W. J., Lawson, T. L., Stewart, E. T., Kern, M. K. and Hassanein, E. H. (1987). Sonographic evaluation of resting gallbladder volume and postprandial emptying in patients with gallstones. *American Journal of Roentgenology*, 148: 875–879.
- Konus, O. L., Ozdemir, A., Akkaya, A., Erba, G., Celik, H. and Isik, S. (1998). Normal liver, spleen and kidney dimension in neonates, infants and children: evaluation with sonography. *American Journal of Roentgenology*, 171: 1693- 8.
- Kratzer, W., Fritz, V., Mason, R. A., Haenle, M. M. and Kaechele, V. (2003). Factors Affecting Liver Size: A Sonographic Survey of 2080 Subjects. *Journal of Ultrasound in Medicine*, 22: 1155–1161.
- Kremkau, F.W. (1993). *Diagnostic ultrasound: Principles and instruments*. 4th ed. Philadelphia, WB Saunders, pp. 411
- Kremkau, F.W. (2011a). Artifacts. In Kremkau FW, editor: *Sonography: principles and instruments*, ed 8, St. Louis, Elsevier Saunders, p 176.
- Kremkau, F.W. (2011b). Instruments. In: Kremkau, F.W, editor: *Sonography: principles and instruments*, ed 8, St. Louis, Elsevier Saunders, p 69.
- Kremkau, F.W. (2011c). Introduction. In: Kremkau FW, editor: *Sonography: principles and instruments*, ed 8, St. Louis, Elsevier Saunders, p 1.
- Kudo, M., Zheng, R. Q., Kim, S. R., Okabe, Y., Osaki, Y., Iijima, H. and Usuki, N. (2008). Diagnostic accuracy of imaging for liver cirrhosis compared to histologically proven liver cirrhosis. *Intervirolgy*, 51(Suppl. 1):17-26.
- Kumari, S., Luthra, R. A., Chandolia, R. K., Kumar, S., Kumar, P., Devender, Kumar, A., Bishnoi, N. and Bishnoi, S. (2016). Study on development of accessory sex glands in prepubertal kids using two-dimensional ultrasonography, *Veterinary World*, 9(4): 346-350.
- Lamb, C. R. (1990). Abdominal ultrasonography in small animals: examination of the liver, spleen, and pancreas. *Journal of Small Animal Practice*, 31:6.
- Lamb, C. R. (1991). Ultrasonography of the liver and biliary tract. *Problem Vet Medicine*, 3:555–73.

- Lamb, C. R. (1996). Ultrasonographic diagnosis of congenital portosystemic shunts in dogs: Results of a prospective study. *Veterinary Radiology and Ultrasound*, 37:281–288.
- Lamb, C. R. and Mahoney, P. N. (1994). Comparison of three methods for calculating portal blood flow velocity in dogs using duplex-Doppler ultrasonography. *Veterinary Radiology and Ultrasound*, 35:190–194.
- Lamb, C. R., Forster-van Hijfte, M. A., White, R. N., McEvoy, F. J. and Rutgers, H. C. (1996a). Ultrasonographic diagnosis of congenital portosystemic shunt in 14 cats. *Journal of Small Animal Practice*, 35:205–209.
- Lamb, C. R., Hartzband, L. E., Tidwell, A. T. and Pearson, S. H. (1991). Ultrasonographic findings in hepatic and splenic lymphosarcoma in dogs and cats. *Veterinary Radiology and Ultrasound*, 32:117–120.
- Lamb, C. R., Simpson, K. W., Boswood, A. and Matthewman, L. A. (1995). Ultrasonography of pancreatic neoplasia in the dog: A retrospective review of 16 cases. *Veterinary Records*, 37:65–68.
- Larson, M. M. (2013). The Liver and Spleen. In: Thrall, D.E. (Ed). *Textbook of Veterinary Diagnostic Imaging*. ed. 6. St. Louis, Elsevier. Pp. 686-689
- Larson, M. M., Panciera, D. L., Ward, D. L., Steiner, J. M. and Williams, D. A. (2005). Age-related changes in the ultrasound appearance of the normal feline pancreas. *Veterinary Radiology and Ultrasound*, 46: 238–242.
- Last, R. D., Hill, J. M., Roach, M., Kaldenberg T. (2006). Congenital dilatation of the large and segmental intrahepatic bile ducts (Caroli's disease) in two Golden retriever littermates. *Journal of South African Veterinary Association* 77(4): 210–214.
- Lavoue, R., Geffre, A., Braun, J. P., Peeters, D., Granat, F., Bourges-Abella, N., Trumel, C. (2014). Breed-specific haematologic reference intervals in healthy adult Dogues de Bordeaux. *Veterinary Clinical Pathology*, 43: 352–361.
- Lee, E. S. and Lee, J. M. (2014). Imaging diagnosis of pancreatic cancer: a state of the art review. *World Journal of Gastroenterology*, 20: 7864–7877.
- Léveillé, R., Biller, D. S. and Shiroma, J. T. (1996). Sonographic evaluation of the common bile ducts in cats. *Journal of Veterinary Internal Medicine*, 10:296–299.
- Levine, H. III. (2010). *Medical Imaging*. Santa Barbara, California: ABC-CLIO, LLC. p. 62
- Lim, S. Y., Nakamura, K., Morishita, K., Sasaki, N., Murakami, M., Osuga, T., Ohta, H., Yamasaki, M. and Takiguchi, M. (2013). Qualitative and quantitative contrast enhanced ultrasonography of the pancreas using bolus injection and continuous

- infusion methods in normal dogs. *Journal of Veterinary Medical Science*,75: 1601–1607.
- Lipinski, M. J. Foenicke, L., Baysac, K. C., Leutenegyer, C. M., Levy, A. M., Longeri, M., Niini, T., Ozpinar, H., Slater, M.R., Pedersen, N. C. and Lyon, L. A. (2008). The ascent of cat breeds: Genetic evaluations of breeds and worldwide random breed Populations.*Genomics*, 91(1): 12-21. Doi: 10.1016/j. ygeeno.10.009
- Liptak, J. M., Darnell, W. S., Monnet, E., Powers, B. E., Bachand, A. M., Kenny, J. G., and Withrow, S.J. (2004). Massive Hepatocellular Carcinoma in Dogs: 48 cases (1992-2002). *Journal of American Veterinary Medical Association*, 225: 1225-12230
- Loomba, R., Wolfson, T., Ang, B., Hooker, J., Behling, C., Peterson, M., Valasek, M., Lin, G., Brenner, D., Gamst, A. and Ehman, R. (2014). Magnetic resonance elastography predicts advanced fibrosis in patients with nonalcoholic fatty liver disease: a prospective study. *Hepatology*, 60:1920- 1928.
- Mareschal, A., Anjou, M. A., Moreau, M., Alexander, K. and Beauregard, G. (2007). Ultrasonographic measurement of kidney to-abdominal aorta ratio as a method of estimating renal size in dogs. *Veterinary Radiology and Ultrasound*,48: 434–438.
- Markowitz, J., Rappaport, A. and Scott, A. C. (1949). The function of the hepatic artery in the dog. *American Journal of Digestive Disease*, 16:344–348.
- Marolf, A. J., Leach, L., Gibbons, D. S., Bachand, A., and Twedt, A. (2012). Ultrasonographic findings of feline cholangitis. *Journal American Animal Hospital Association* 48:36–42.
- Marzio, L., Capone, F., Neri, M., Mezzetti, A., De Angelis, C. and Cuccurullo, F. (1988). Gallbladder kinetics in obese patients. Effect of a regular meal and low-calorie meal. *Digestive Diseases and Sciences*,33: 4–9.
- Matsumoto, T, Sushil, K, Condon, R. (1988). Canine gallbladder cyclic motor activity. *American Journal of Physiology*, 255:G409-G416.
- McAtee, B. B and Lidbury, J. A. (2017). Continuing education: Liver enzyme interpretation and liver function test. *Today's Veterinary Practice*, 7: 3.
- Mehler, S. and Bennet, R. (2009). Canine Extrahepatic biliary tract diseases and Surgery. *Compendium*. Pp. 302-314.
- Mendonça, D. S., Moron, R. F., Maldonado, A. L., Araujo Junior, E., Nardoza, L. M. and Moron, A. F. (2012). Assessment of renal volume by three-dimensional ultrasonography in pregnant bitches: an experimental study using virtual organ computer aided analysis. *Biomedical Central Veterinary Research*,8: 102

- Mills, P., Saverymuttu, S., Fallowfield, M., Nussey, S. and Joseph, A. E. (1990). Ultrasound in the diagnosis of granulomatous liver disease. *Clinical Radiology*, 41:113–115.
- Mohammed, S, Tahir, A., Ahidjo, A, Mustapha, Z., Franza, O., Okoye, I. and Shugaba, A. (2010). Sonographic gall bladder wall thickness in normal adult population in Nigeria. *Journal of Radiology*, SA: 84-86.
- Monnet, E. and Twedt, D. C. (2003). Laparoscopy. *Veterinary Clinics of North America: Small Animal Practice*, 33(5): 1147–1163.
- Morita, Y., Takiguchi, M., Yasuda, J., Eom, K.D. and Hashimoto, A. (1998). Endoscopic ultrasonographic findings of the pancreas after pancreatic duct ligation in the dog. *Veterinary Radiology of Ultrasound*, 39:557–562.
- Moriyasu, F., Nishida, O., Ban, N., Nakamura, T, Sakai, M. and Miyake, T. (1986). Congestion index of portal vein. *American Journal of Roentgenology*, 146: 735-9.
- Mundt, M. W., Hausken, T., Smout, A. J. and Samsom, M. (2005). Relationships between gastric accommodation and gastrointestinal sensations in healthy volunteers. A study using the barostat technique and two- and three-dimensional ultrasonography. *Digestive Disease and Science*, 50: 1654–1660.
- Murakami, T., Feeney, D. A. and Bahr, K. L. (2012). Analysis of clinical and ultrasonographic data by use of logistic regression models for prediction of malignant versus benign causes of ultrasonographically detected focal liver lesions in dogs. *American Journal of Veterinary Research*, 73:821–829.
- Murtaugh, R. J., Herring, D. S., Jacobs, R. M. and Dehoff, W. D. (1985). Pancreatic ultrasonography in dogs with experimentally induced acute pancreatitis. *Journal of Veterinary Radiology*, 26: 27–32.
- Nathalie, R. (2010). Liver: In: *British Small Animal Veterinary Association Manual of Canine and Feline Ultrasonography*. Ed. Barr. F and Gaschen. Pp 86. British Small Animal Veterinary Association Publication Gloucester.
- Neer, T. (1992). A Review of Disorders of the Gallabdder and Extrahepatic Biliary Tract in the Dog and Cat. *Journal of Veterinary Internal Medicine*, 6:186-192.
- Newell, S. M., Selcer, B. A., Girard, E., Roberts, G. D., Thompson, J. P. and Harrison, J. M. (1998). Correlations between ultrasonographic findings and specific hepatic diseases in cats: 72 cases (1985–1997). *Journal of American Veterinary Medical Association*, 213:94–98.
- Newell, S.M., Selcer, B.A., Roberts, R.E., Cornelius, L.M and Mahaffey, E.A. (1996). Hepatobiliary scintigraphy in the evaluation of feline liver disease. *Journal of Veterinary Internal Medicine*, 10:308–315.

- Nielsen, L., Kjelgaard-Hansen, M., Jensen, A. L., Kristensen, A. T. (2010). Breed-specific variation of haematologic and biochemical analytes in healthy adult Bernese Mountain dogs. *Veterinary Clinical Pathology*, 39: 20–28.
- Nyland, T. G and Fisher, P. E. (1990). Evaluation of experimentally induced canine hepatic cirrhosis using duplex Doppler ultrasound. *Journal of Veterinary Radiology*, 31: 189-194.
- Nyland, T. G. and Matton, J. S. (1995). *Veterinary Diagnostic Ultrasound*. Philadelphia: WB Saunders. 143-265.
- Nyland, T. G., Barthez, P.Y., Ortega, T. M. and Davis, C. R. (1996). Hepatic ultrasonographic and pathologic findings in dogs with canine superficial necrolytic dermatitis. *Journal of Veterinary Radiology and Ultrasound*, 37:200–205.
- Nyland, T. G., Koblik, P. D. and Tellyer, S. E. (1999). Ultrasonographic evaluation of biliary cystadenomas in cats. *Veterinary Radiology and Ultrasound*, 40:300–306.
- Nyland, T. G., Mattoon, J. S., Herrgesell, E. J. and Wisner, E. R. (2002). Liver. In Nyland, T.G., Mattoon, J.S., editors: *Small Animal Diagnostic Ultrasound*, 2nd ed., Philadelphia, Saunders, pp 93–127.
- Nyland, T. G., Mattoon, J. S., Herrgesell, E. J., Fígado (2005). In: Nyland, T.G., Mattoon, J.S. *Ultra-som diagnostic em pequenos animais*. 2^a ed. São Paulo, SP: Roca. p. 95–130.
- Nyland, T.G. and Gillett, N.A. (1982). Sonographic evaluation of experimental bile duct ligation in the dog. *Veterinary Radiology and Ultrasound*, 23:252–260.
- Nyland, T.G. and Hager, D.A. (1985). Sonography of the liver, gallbladder, and spleen. *Veterinary Clinic North American: Small Animal Practice*, 15:1123–48.
- Nyman, H. T., Kristensen, A. T., Flagstad, A. and McEvoy, F. J. (2004). A review of the sonographic assessment of tumor metastases in liver and superficial lymph nodes. *Veterinary Radiology and Ultrasound*, 45:438–448.
- O'Brien, R.T., Iani, M., Delaney, F. and Young, K. (2004). Contrast harmonic ultrasound of spontaneous liver nodules in 32 dogs. *Veterinary Radiology of Ultrasound*, 45:547–553.
- Olayemi, F. O., Azeez, I. O., Ogunyemi, A. and Ighagbon, F. O. (2009). Study on erythrocyte values of the nigerian indigenous dog. *Folia Veterinaria*, 53(2):65-7.
- Ozidikici, M. (2017). Normal values of liver by ultrasonography in children in the Eastern Anatolia region. *Revista Argentina Anatomia*, 8(1): 19-22.

- Park, R. D., Nyland, T. G., Lattimer, J. C., Miller, C. W. and Lebel, J. L. (1981). B-mode grayscale ultrasound: imaging artifacts and interpretation principles, *Veterinary Radiology*,22:204.
- Patrick, R. K. (2010). Equipment: In: *British Small Animal Veterinary Association Manual of Canine and Feline Ultrasonography*. Ed. Barr. F and Gaschen. Pp 15-16. British Small Animal Veterinary Association Publication Gloucester
- Penninck, D. and d' Anjou, M. A., (2015). Pancreas. In: Penninck, D., d'Anjou, M.A. (eds). *Atlas of Small Animal Ultrasonography*. ed. 2 Ames, Ia, Wiley-Blackwell Publishing. Pp. 309-329
- Penninck, D. G. (2002). Artifacts. In Nyland TG, Mattoon JS, editors: *Small Animal Diagnostic Ultrasound*, ed 2, Philadelphia, Saunders, p 19.
- Penninck, D. G. and Berry, C. (1997). Diagnostic imaging of the feline liver. *Seminars in Veterinary Medical Surgery (Small Animals) Journal: Feline Liver Disease* 12:10–21.
- Penninck, D. G., Zeyen, U., Taeymans, O. N. and Webster, C. R. (2013). Ultrasonographic measurement of the pancreas and pancreatic duct in clinically normal dogs. *American Journal of Veterinary Research*,74: 433–437.
- Penninck, D., Brisson, J.O. and Webster, C.R. (2010). Sonographic assessment of gallbladder volume in cats. *Veterinary Radiology and Ultrasound*, 51:665–666.
- Penninck, D.G., Zeyen, U., Taeymans, O. and Webster, C. R. (2013). Ultrasonographic measurement of the pancreas and pancreatic duct in clinically normal dogs. *American Journal of Veterinary Research*. 74:433–437.
- Peter, A.T., Pierson, R.A. and Jakovljevic, S. (1992) Use of real-time ultrasonography in bovine and equine reproduction. *Compendium on Continuing Education for the Practising Veterinarian*, 14(8): 1116-1124.
- Pierson, R. A. and Adams, G. P. (1995) Computer-assisted image analysis, diagnostic ultrasonography and ovulation induction: Strange bed fellows. *Theriogenology*, 43: 105-112.
- Piyasena, P., Mohareb, E., McKellar, R.C. (2003). Inactivation of microbes using ultrasound: a review, *International Journal of Food Microbiology*, 87: 207–216.
- Porter, M. (1991). Therapeutic ultrasound. *Journal of Equine Veterinary Science*,11: 357-62.
- Portincasa, P., Moschetta, A., Colecchia, A., Festi, D. and Palasciano, G. (2003). Measurements of gallbladder motor function by ultrasonography: towards standardization. *Digestive and Liver Disease*,35(3): S56–S61.

- Powis, R. L. (1986). Ultrasound Science for the Veterinarian. *Veterinary Clinic North American: Equine Practice*, 2(1): 3-27.
- Powis, R. L. (1993). The saga of the lingering transducer. *Journal of Equine Veterinary Science*, 13(6): 323-4.
- Quencer, K., Kambadakone, A., Sahani, D., and Guimaraes, A. S. R. (2013). *Imaging of the pancreas: Part 1. Applied Radiology*, 42(9): 14-2.
- Rahmani, V., Molazem, M., Jamshid, S., Vali, Y and Hanifeh, M. (2015). Evaluation of gallbladder volume and contraction index with three-dimensional ultrasonography in healthy dogs. *Journal of Veterinary Medical Science*, 77(9): 1157–1161.
- Rall, P. W., Quinn, M. F. and Juttner, H. U. (1981). Gall bladder wall thickening: Patients without intrinsic gall bladder disease. *American Journal of Roentgenology*, 13: 65-68.
- Ramstedt, K. L., Center, S. A., Randolph, J. F., Yeager, A. E., Erb, H. N. and Warner, K. L. (2008). Changes in gallbladder volume in healthy dogs after food was withheld for 12 hours followed by ingestion of a meal or a meal containing erythromycin. *American Journal of Veterinary Research*, 69: 647–651.
- Rivers, B.J., Walther, P.A., Johnston, G.R, Merkel, L.K. and Hardy, R.M. (1997). Acalculous cholecystitis in four canine cases: ultrasonographic findings and use of ultrasonographic-guided, percutaneous cholecystocentesis in diagnosis, *Journal of American Animal Hospital Association*, 33: 207.
- Robben, J.H., Pollak, Y.W., Kirpensteijn, J., Borofika, S.A., van den Ingh, T.S, Teske, E. and Voorhout, G. (2005). Comparison of ultrasonography, computed tomography, and single-photon emission computed tomography for the detection and localization of canine insulinoma. *Journal of Veterinary Internal Medicine* 19: 15-22
- Rocha, S. M. S, Oliveira, I. R. S and Widman, A. (2003). Hepatometria ultra-sonográfica em crianças: proposta de novo método. *Radiologia Brasileira*, 36:63–70.
- Romański, K. W. and Siembieda, J. (2002). Validation of the methods estimating gallbladder volume. *Bulletin. Veterinary Institute Pulawy*, 46: 95–104.
- Santiago, I., Loureiro, R., Curvo-Semedo, L., Marques, C, Guila, F.T., Matos, C. and Casiero-Alves, F. (2012). Congenital cystic lesions of the biliary tree. *American Journal of Roentgenology* 198:825–835.
- Sato, A. and Solano, M. (2004). Ultrasonographic findings in abdominal mast cell disease: A retrospective study of 19 patients. *Veterinary Radiology of Ultrasound*, 45:51–57.
- Saunders, H. M. (1991). Ultrasonography of the pancreas. *Problems in Veterinary Medicine*, 3: 583–603.

- Scampini, J. (2017). Overview of Ultrasound Imaging System and Electrical components required for main Subfunction. Available at <http://www.maximintegrated.com/en/app-notes/index.mvp/id/4696>. Accessed on 30/1/2017@ 12:51 GMT.
- Scheffer, R. C., Gooszen, H. G., Wassenaar, E. B. and Samsom, M. (2004). Relationship between partial gastric volumes and dyspeptic symptoms in fundoplication patients: a 3D ultrasonographic study. *American Journal of Gastroenterology*, 99: 1902–1909.
- Schwarz, L.A., Penninck, D.G. and Leveille-Webster, C. (1998). Hepatic abscesses in 13 dogs: A review of the ultrasonographic findings, clinical data and therapeutic options. *Veterinary Radiology of Ultrasound*, 39:357–365.
- Shankar, R., Shetty, G. S., Srinath, M. G. and Kulkarni, R. (2011). Estimation of Portal Vein Diameter in co – Relation with the Age, Sex and Height of an Individual. *Anatomica Karnataka*, 5(2): 13-16.
- Sharkey, L., Gjevre, K., Hegstad-Davies, R., Torres, S., Munoz-Zanzi, C. (2009). Breed-associated variability in serum biochemical analytes in four large-breed dogs. *Veterinary Clinical Pathology*, 38: 375–380.
- Sharon, A., and Center, B.C., (2016). Imaging in Hepatic Disease in Small Animals. In: Sharon.A., Center, B.C. (eds). *MSD Veterinary Manual*. Kenilworth, N.J. U.S.A
- Siddharth, S., Goyal, A. (2007). The origin of echocardiography. *Texas Heart Institute Journal*, 34(4): 431-438.
- Siddiqui, T. R., Hassan, N. and Gul, P. (2014). Impact of anthropometrical parameters on portal vein diameter and liver size in a subset of Karachi based population. *Pakistan Journal of Medical Sciences*, 30(2): 384-388.
- Soyupak, S. K., Nari, I. N., Yapicioglu, H., Satar, M. and Sungur, E. H. (2002). Sonographic measurements of the liver, spleen and kidney dimensions in the healthy term and preterm new borns. *European Journal of Radiology*, 43: 73-8.
- Spaulding, K. A. (1993). Ultrasound corner: Gallbladder wall thickness. *Veterinary Radiology of Ultrasound*, 34:270-272.
- Steiss, J. E.(2000). Physical therapy modalities: therapeutic ultrasound and phonophoresis. *Compendium on Continuing Education for the Practicing Veterinarian*, 22: 690-693.
- Stonewater, J. L., Lamb, C., Shelling, S. H. (1990). Ultrasonographic features of canine hepatic nodular hyperplasia. *Veterinary Radiology of Ultrasound*, 31:268–272.
- Sucena de Rocha, S. M., Ana, P. S. F., Ilka, R. S., Azzo, W., Maria, C. C., Luiz, A. N. and Giovanni, G. C (2009). Sonographic determination of liver size in healthy newborns, infant and children under 7 years of age. *Radiologia Brasileria*, 42(1).

- Sullivan, L. M. O. and Fígado, O. (2000). sistema biliar e o pâncreas. In: Juhl, J.H., Crummy, A.B., Kuhlman, J.E., editores. Paul & Juhl: interpretação radiológica. 7ª ed. Rio de Janeiro, RJ: Guanabara Koogan. p. 433–63.
- Sullivan, S., Krasner, N. and Williams, R. (1976). The clinical estimation of liver size: a comparison of techniques and an analysis of the source of error. *British Medical Journal*, 30:1042–3.
- Szatmari, V., Rothuizen, J., van den Ingh, G.A., van Sluijs, F.J., Voorhout, G. (2004). Ultrasonographic findings in dogs with hyperammonemia: 90 cases (2000–2002). *Journal of American Veterinary Medical Association*, 224:717–727.
- Tantary, H. A., Soodan, J. S., Chirag, S., Ansari, M. M., Kumar, S. and Imtiyaz, T. (2014). Diagnostic studies in dogs with hepatic disorders. *International Journal of Veterinary Science*, 3(4): 210-215.
- Tasu, J. P., Rocher, L., Pelectier, G., Kuoch, V., Kulh, E. and Miquel, A. (2002). Hepatic venous pressure gradient by duplex Doppler ultrasound. *Clinical Radiology*, 57: 746- 52.
- Tchelepi, H., Ralls, P. W., Radin, R. and Grant, E. (2002). Sonography of diffuse liver disease. *Journal of Ultrasound in Medicine*, 21(9): 1023-1032.
- Tobias, K. M. and Rawlings, C. A. (1996). Surgical techniques for extravascular occlusion of intrahepatic shunts. *Compendium on Continuing Education for Practicing Veterinarians*, 18:745–755.
- Torres, A. R., Cassle, S. E., Haymore, M., Hill, R. C. (2014). Haematologic differences between Dachshunds and mixed breed dogs. *Veterinary Clinical Pathology*, 43: 519–524.
- Tsai. S. (2011). The role of Imaging in Diagnosing Pancreatitis. Available at <http://www.angell.org/diagnosticimaging>. Accessed on 3/16/2016 @ 20:22 GMT
- Tsukagoshi, T., Ohno, K., Tsukamoto, A., Fukushima, K., Takahashi, M., Nakashima, K., Fujino, Y. and Tsujimoto, H. (2012). Decreased gallbladder emptying in dogs with biliary sludge or gallbladder mucocele. *Veterinary Radiology and Ultrasound*, 53(1): 84–91.
- Uemura, M., Igarashi, H., Ozawa, A., Tsunekwa, N., Kurohmaru, M., Kanai-Azuma, M and Kanai, Y. (2015). Fate mapping of gallbladder progenitors in posteroventral foregut endoderm of mouse early somite-stage embryos. *Journal of Veterinary Medical Sciences*, 77: 587-91. PMID: 25648459
- Uršič, M., Ravnik, D., Hribernik, M., Pecar, J., Butinar, J. and Fazarinc, G. (2007). Gross anatomy of the portal vein and hepatic artery ramifications in dogs: corrosion cast study. *Anatomy, Histology, Embryology*, 36 (2): 83–87.

- Venkatesh, S. K., Yin, M., Takahashi, N., Glockner, J. F., Talwalkar, J. A. and Ehman, R. L. (2015). Non-invasive detection of liver fibrosis: MR imaging features vs. MR elastography. *Abdominal Imaging*, 40:766-775.
- Venkatesh, S.K., Wang, G., Lim, S.G. and Wee, A. (2014). Magnetic resonance elastography for the detection and staging of liver fibrosis in chronic hepatitis B. *European Radiology*, 24:70-78.
- Vignoli, M., and Saunders, J. (2011): Image-guided interventional procedures in the dog and cat. *The Veterinary Journal*, 187: 297–303.
- Vosough, D., Masoudifard, M., Vajhi, A., Molazem, M. and Veshkini, A. (2008). Use of three-dimensional ultrasonography of the eye and measurement of optical long axis in dog. *Iranian Journal Veterinary Research*, 2: 92–94.
- Wang, K. W., Panceria, D. L., Al-Rukibat, R. K. and Radi, A. Z. (2004). Accuracy of ultrasound-guided fine-needle aspiration of the liver and cytologic findings in dogs and cats: 97 cases (1990–2000). *Journal of American Veterinary Medical Association*, 224:75–78.
- Washabau, P. J. (2012). Liver. In: *Canine and Feline Gastroenterology*, 1e. pp: 849-957. Saunders publication.
- Washabau, R. (2013). Diseases of the Gastrointestinal Tract: Liver. *Canine and Feline Gastroenterology*. St. Louis, MO: Elsevier, 853-855.
- Watson, P. J. (2003). Exocrine pancreatic insufficiency as an end stage pancreatitis in four dogs. *Journal of Small Animal Practice*, 44:306–312.
- Weissman, A., Penninck, D., Wester, C., Hecht, S., Keating, J. and Craig, L. E. (2012). Ultrasonographic and clinicopathological features of feline gastrointestinal eosinophilic sclerosing fibroplasia in 4 cats. *Journal of Feline Medicine and Surgery*, 15: 148–154.
- Whiteley, M. B., Feeney, D. A., Whiteley, L. O. and Hardy, R. M. (1989). Ultrasonographic appearance of primary and metastatic canine hepatic tumors: A review of 48 cases. *Ultrasound Medicine*, 8:621–630.
- Wolson, A. H. (1990). Ultrasound measurement of the gall bladder. In: Goldberg, B. B., Kurtz, A. B., eds. *Atlas of ultrasound measurement*. Chicago. Year Book Medical Publishers, pp 108-109.
- Worthen, N. J. and Beabeau, D. (1982). Normal pancreatic echogenicity: relation to age and body fat. *American Journal of Radiology*, 139:1095.
- Wu, J. X. and Carlisle, C. H. (1995). Ultrasonographic examination of the canine liver based on recognition of hepatic and portal veins, *Veterinary Radiology of Ultrasound*, 36:234.

- Yin, M., Talwalkar, J. A., Glaser, K. J., Manduca, A., Grimm, R. C., Rossman, P. J. and Ehman, R. L. (2007). Assessment of hepatic fibrosis with magnetic resonance elastography. *Clinical Gastroenterology and Hepatology*, 5(10): 1207-1213.
- Zeissman, H. A. (2014). Hepatobiliary Scintigraphy in 2014. *Journal of Nuclear Medicine*. 55:967-975. DOI: 10.2967/jnumed.113.131490
- Zhang, Y., Zhang, X. M., Prowda, J. C., Zhang, H. L., Sant'Anna Henry, C., Shih, G. and Prince, M. R. (2009). Changes in hepatic venous morphology with cirrhosis on MRI. *Journal of Magnetic Resonance Imaging*, 29(5): 1085-1092.
- Zhou, Y. C., Wang, J., Zhang, B., Su, Y. Q. (2002). Ultrasonic immunization of sea bream, *Pagrus major*, with a mixed vaccine against *Vibrio alginolyticus* and *V. anguillarum*. *Journal of Fish Diseases*, 25: 325-31.
- Zwiebel, W. J. (1995). Sonographic diagnosis of diffuse liver disease. *Seminar Ultrasound Computed Tomography and Magnetic Resonance Imaging*, 16:8–15.
- Zwingenberger, A.L., McLear, R. C. and Weisse, C. (2005). Diagnosis of arterioportal fistulae in four dogs using computed tomographic angiography. *Veterinary Radiology of Ultrasound*. 46: 427-477.

APPENDICES

Appendix 1: Demographic data of 6 Nigerian Indigenous Puppies Appendix 1a: Animal ID 1 (Male)

Age (weeks)	Weight (kg)	BL (cm)	HT (cm)	BMI (kg/m ²)
8	1.9	33	22	0.00392562
10	2.8	36	29	0.00332937
12	3.6	36	31	0.0037461
14	5.5	46	34	0.00475779
16	7.6	59	38	0.00526316
18	8.7	60	41	0.00517549
20	9.2	60	46	0.00434783
22	9.6	62	47	0.00434586
24	10.1	63	47	0.00457221
26	11.1	65	49	0.00462307
28	11.5	67	50	0.0046
30	12.2	68	51	0.0046905
32	12.9	68	52	0.00477071
34	13.6	71	53	0.00484158
36	14.1	73	53	0.00501958
38	14.5	74	54	0.00497257
40	14.9	74	54	0.00510974

Appendix 1b: Animal ID 2 (Male) (n=6)

Age (weeks)	Weight (kg)	BL (cm)	HT (cm)	BMI (kg/m²)
8	1.9	31.8	21.9	0.0039616
10	2.6	33	29	0.0030916
12	3.2	36	32	0.003125
14	5.3	48	33	0.0048669
16	7.3	51	39	0.0047995
18	7.5	54	43	0.0040562
20	8.5	62	48	0.0036892
22	9.2	64	47	0.0041648
24	10.6	65	48	0.0046007
26	11.3	67	50	0.00452
28	11.5	70	52	0.004253
30	12.8	70	52	0.0047337
32	13.2	71	53	0.0046992
34	14.1	72	54	0.0048354
36	14.9	74	54	0.0051097
38	15.2	74	54	0.0052126
40	15.5	74	54	0.0053155

Appendix 1c: Animal ID 3 (Male) (n=6)

Age (weeks)	Weight (kg)	BL (cm)	HT (cm)	BMI (kg/m²)
8	2.1	34.6	21.8	0.00441882
10	2.4	38	30	0.00266667
12	3.3	42	34	0.00285467
14	4.7	43	36	0.00362654
16	6.6	55	40	0.004125
18	7.8	56	41	0.0046401
20	8.4	58	44	0.00433884
22	9.1	61	45	0.00449383
24	10	61	45	0.00493827
26	11.5	63	50	0.0046
28	11.6	65	51	0.00445982
30	12	65	52	0.00443787
32	13.1	66	52	0.00484468
34	14.8	67	53	0.00526878
36	15.2	73	54	0.00521262
38	15.8	74	55	0.00522314
40	16	74	56	0.00510204

Appendix 1d: Animal ID 4 (Female) (n=6)

Age (weeks)	Weight (kg)	BL (cm)	HT (cm)	BMI (kg/m²)
8	2	35.1	22.1	0.0040949
10	2.9	33	30	0.0032222
12	3.8	40	34	0.0032872
14	5.6	48	35	0.0045714
16	8.2	57	38	0.0056787
18	8.5	58	43	0.0045971
20	8.8	62	46	0.0041588
22	9.5	67	46	0.0044896
24	10.5	68	48	0.0045573
26	12	69	51	0.0046136
28	12.2	70	52	0.0045118
30	13	71	53	0.004628
32	13.5	71	53	0.004806
34	14.3	73	53	0.0050908
36	15.4	77	53	0.0054824
38	16.3	78	54	0.0055898
40	16.7	79	55	0.0055207

Appendix 1e: Animal ID 5 (Female) (n=6)

Age (weeks)	Weight (kg)	BL (cm)	HT (cm)	BMI (kg/m²)
8	2.1	34.5	22	0.00433884
10	2.8	39	30	0.00311111
12	3.2	38	35	0.00261225
14	5.8	48	37	0.00423667
16	8.2	53	38	0.00567867
18	8.4	57	40	0.00525
20	8.6	58	44	0.00444215
22	9	61	44	0.00464876
24	9.5	62	46	0.0044896
26	11.2	64	49	0.00466472
28	11.5	71	51	0.00442138
30	12	71	52	0.00443787
32	12.8	72	52	0.00473373
34	13.5	73	53	0.00480598
36	14	74	54	0.0048011
38	14.3	74	54	0.00490398
40	15.3	74	54	0.00524691

Appendix 1f: Animal ID 6 (Female)

Age (weeks)	Weight (kg)	BL (cm)	HT (cm)	BMI (kg/m²)
8	1.8	34.5	21.7	0.00382255
10	2.5	39	29	0.00297265
12	3.5	40	34	0.00302768
14	5.5	49	37	0.00401753
16	7.5	54	39	0.00493097
18	8.2	57	42	0.00464853
20	9.5	62	47	0.00430059
22	10.1	67	47	0.00457221
24	10.5	67	47	0.00475328
26	11.5	50	50	0.0046
28	12	70	51	0.00461361
30	12.2	70	52	0.00451183
32	12.4	71	53	0.00441438
34	14.9	71	54	0.00510974
36	15.5	73	56	0.0049426
38	15.9	73	57	0.00489381
40	16.3	74	57	0.00501693

Appendix 2: Biometry of the liver and the Hepatic portal vein diameter in six (6) Nigerian Indigenous Puppies

Appendix 2a: Animal ID 1 (Male) (n=6)

Age (weeks)	HL (mm)	HW (mm)	HV (mm³)	PVD (mm)	CSA (mm²)
8	52	27.6	171.127	3.9	11.947455
10	71	29.8	187.964	6.2	30.19462
12	94.2	40.5	437.83	3.2	8.04352
14	65.2	51.73	145.018	3.4	9.08038
16	99	49.8	576.666	2.5	4.909375
18	108.2	64.1	668.054	1.8	2.54502
20	131.5	68.2	1190.113	4	12.568
22	137.2	71.2	1140.525	3.8	11.34262
24	150.1	78.3	1247.443	4.1	13.204255
26	120.9	53.6	925.615	2.2	3.80182
28	108.8	72.6	673.676	3.4	9.08038
30	293.962	73.85	1079.48	4.6	16.62118
32	132.3	63.1	1213.355	2.6	5.30998
34	118.8	57.1	1039.2	2.1	3.464055
36	125.4	67.4	1234.645	2.6	5.30998
38	125.4	79.2	1352.34	1.7	2.270095
40	122.4	78.7	1210.345	3.1	7.548655

Appendix 2b Animal ID 2 (Male) (n=6)

Age (weeks)	HL (mm)	HW (mm)	HV (mm³)	PVD (mm)	CSA (mm²)
8	53.8	26.2	181.472	2.6	5.30998
10	74.6	27.3	217.507	3.4	9.08038
12	90.6	45.5	389.818	2.9	6.606055
14	191.6	71.6	876.774	3.7	10.753495
16	101.4	50.9	545.136	3.2	8.04352
18	93.7	64.7	430.993	1.7	2.270095
20	126.5	79.6	1061.167	4.2	13.85622
22	91.1	61.9	406.795	4	12.568
24	103.9	70.6	406.795	4.5	15.906375
26	114.6	65.1	877.381	2.8	6.15832
28	110.6	73.8	685.392	3	7.0695
30	251.764	77.4	1132	4.7	17.351695
32	131.1	84.4	1233.871	3.7	10.753495
34	123.1	59.2	1077.9	2.1	3.464055
36	132.5	71.3	1304.696	2.8	6.15832
38	133.1	83	1417.6	1.8	2.54502
40	127.4	81.9	1259.08	3.8	11.34262

Appendix 2c: Animal ID (Male). (n=6)

Age (weeks)	HL (mm)	HW (mm)	HV (mm³)	PVD (mm)	CSA (mm²)
8	57.9	30.1	101.563	3	7.0695
10	84.7	34.8	318.112	3.5	9.622375
12	84.4	32.5	314.442	1.9	2.835655
14	83.4	47.4	302.224	3.7	10.753495
16	97.5	61.2	484.604	3.7	10.753495
18	113.9	63.2	773.918	3.4	9.08038
20	111.9	81.9	734.377	4.2	13.85622
22	108.1	75.2	661.496	4.4	15.20728
24	122.1	61.7	953.481	4.2	13.85622
26	123.5	65	985.453	3.5	9.622375
28	123.5	78	974.236	4.7	17.351695
30	141.5	80.7	1483.566	4.9	18.859855
32	136.2	70.6	1322.44	3.5	9.622375
34	138.4	75.9	1386.636	2.7	5.726295
36	121	75.9	934.362	2.2	3.80182
38	141.3	81.4	1476.035	2.9	6.606055
40	137.4	70.9	1356.798	2.5	4.909375

Appendix 2d: Animal ID 4 (Female) (n=6)

Age (weeks)	HL (mm)	HW (mm)	HV (mm³)	PVD (mm)	CSA (mm²)
8	72.3	33.3	196.67	2.8	6.15832
10	73.1	35.3	204.621	3.4	9.08038
12	94.6	41.2	443.717	3.2	8.04352
14	103.5	64.9	576.44	2.5	4.909375
16	84.8	50.5	319.336	5.1	20.43086
18	116.4	73.9	825.745	4.4	15.20728
20	114.4	65.8	784.844	3.6	10.18008
22	118.9	77.1	879.997	3.7	10.7535
24	103.5	81.8	580.648	3.9	11.94746
26	120.9	68.7	925.615	2.5	4.909375
28	112.2	69.5	739.039	4.3	14.5239
30	255.698	78.7	1150.266	5	19.6375
32	127.1	56.5	1073.826	2.8	6.15832
34	129.3	62.2	1131.413	2.3	4.155295
36	137	73.7	1348.478	2.9	6.606055
38	142.7	89.1	1520.22	2	3.142
40	137.3	88.3	1356.56	3.3	8.554095

Appendix 2e: Animal ID 5 (Female) (n=6)

Age (weeks)	HL (mm)	HW (mm)	HV (mm³)	PVD (mm)	CSA (mm²)
8	80.1	27.1	219.148	2.7	5.726295
10	75.6	29.4	226.518	3.1	7.548655
12	92.9	42.7	419.196	2.5	4.909375
14	102.9	57	571.222	5	19.6375
16	94.8	57.6	446.084	3.5	9.622375
18	100.7	53.3	534.611	4	12.568
20	121.5	77.6	938.663	3.8	11.34262
22	106.3	74.9	628.952	5	19.6375
24	92.9	58.9	419.922	2.5	4.909375
26	122.2	68.1	956.486	3.6	10.18008
28	114.2	60.4	779.882	4.4	15.20728
30	122.7	62.5	966.685	4.9	18.859855
32	136.7	72.8	1338.713	3.8	11.34262
34	100.8	57.4	536.245	2.5	4.909375
36	133.7	74.5	1215.685	3.4	9.08038
38	135	78.9	1302.909	3.5	9.622375
40	147.9	91	1695.542	2.4	4.52448

Appendix 2f: Animal ID 6 (Female) (n=6)

Age (weeks)	HL (mm)	HW (mm)	HV (mm³)	PVD (mm)	CSA (mm²)
8	70.9	22.9	186.938	3.1	7.548655
10	76.8	23.3	236.987	3.4	9.08038
12	89.4	39.3	394.698	2.3	4.155295
14	93.5	67.9	428.141	5.3	22.064695
16	98.2	73.8	495.806	3.5	9.622375
18	108.4	68.4	666.725	3.2	8.04352
20	101.7	59.8	551.27	2.9	6.606055
22	128.8	74.9	719.693	3.5	9.622375
24	101.9	53.5	554.373	4	12.568
26	116.5	66.3	828.865	3.8	11.34262
28	116.7	62	833.051	3.1	7.548655
30	124.5	74.7	1010.312	4.6	16.62118
32	134.4	84.5	1267.258	3.4	9.08038
34	125.5	70	1045.354	2.2	3.80182
36	138	70	1376.5	3.1	7.548655
38	134.4	91.9	1269.937	2.8	6.15832
40	134.3	76.8	1269.563	3.6	10.18008

Appendix 2g: Mean values and SEM of the hepatic ultrasound dimension in male (n = 3) and female (n = 3) puppies.

Age (weeks)	HL (mm)		HW (mm)		HV (cm ³)	
	Male	Female	Male	Female	Male	Female
8	55 ± 1.7	74 ± 2.9	28 ± 1.1	28 ± 3.0	151 ± 25	201 ± 9.5
10	77 ± 4.1	75 ± 1.1	31 ± 2.2	29 ± 3.5	241 ± 39	223 ± 9.5
12	90 ± 2.9	92 ± 1.5	40 ± 3.8	41 ± 1.0	381 ± 36	419 ± 14
14	113 ± 3.9	100 ± 3.2	57 ± 7.5	63 ± 3.3	441 ± 222	525 ± 49
16	99 ± 1.1	93 ± 4.0	54 ± 3.6	61 ± 6.9	535 ± 47	420 ± 53
18	105 ± 6.0	109 ± 4.5	64 ± 0.4	65 ± 6.2	624 ± 101	676 ± 84
20	123 ± 5.9	113 ± 5.8	77 ± 4.2	68 ± 5.2	995 ± 136	758 ± 113
22	112 ± 13	118 ± 6.5	69 ± 3.9	76 ± 0.7	736 ± 215	743 ± 73
24	125 ± 13	99 ± 3.3	70 ± 4.8	65 ± 8.7	869 ± 246	518 ± 50
26	120 ± 2.6	120 ± 1.7	61 ± 3.8	68 ± 0.7	929 ± 31	904 ± 38
28	114 ± 4.6	114 ± 1.3	75 ± 1.6	64 ± 2.8	778 ± 98	784 ± 27
30	229 ± 45 ^a	168 ± 44 ^b	77 ± 2.0	72 ± 4.9	1232 ± 127	1042 ± 55
32	133 ± 1.5	133 ± 2.9	73 ± 6.2	71 ± 8.1	1257 ± 33	1227 ± 79
34	127 ± 5.9	119 ± 8.9	64 ± 5.9	63 ± 3.7	1168 ± 110	904 ± 186
36	126 ± 3.4	136 ± 1.3	72 ± 2.5	73 ± 1.4	1158 ± 114	1314 ± 50
38	133 ± 4.6	137 ± 2.7	81 ± 1.1	87 ± 4.0	1415 ± 36	1364 ± 50
40	129 ± 4.4	140 ± 4.1	77 ± 3.3	85 ± 4.4	1275 ± 43	1441 ± 130

^{ab} Means in the same row with different superscript alphabets were significantly different (p < 0.05).

KEY: HL (Hepatic length), HW (Hepatic width), HV (Hepatic volume).

Appendix 2h: Overall mean values and SEM of the hepatic ultrasound dimension in puppies (n=6).

Age (weeks)	Parameters		
	HL (mm)	HW (mm)	HV (cm ³)
8	65 ±4.7	28±1.4	176 ± 16
10	76 ±1.9	30±1.9	232 ± 19
12	91 ±1.6	40±1.8	400 ± 19
14	107±18	60±3.9	483 ±104
16	96 ±2.4	57±3.8	478 ± 37
18	107±3.4	65±2.8	650 ± 60
20	118±4.4	72±3.6	877 ± 95
22	115±6.8	73±2.3	740 ±102
24	112±8.5	67±4.6	694 ±137
26	120±1.4	64±2.3	917 ± 23
28	114±2.2	69±2.8	781 ± 46
30	198± 31	75±2.6	1137± 75
32	133±1.5	72±4.6	1242± 39
34	123±5.1	64±3.1	1036±113
36	131±2.7	72±1.3	1236± 65
38	135±2.5	84±2.2	1390± 40
40	134±3.6	81±3.0	1358± 71

KEY: HL (Hepatic length), HW (Hepatic width), HV (Hepatic volume), CSA (Cross sectional area)

Appendix 3: Biometry of the gallbladder of six Nigerian Indigenous Puppies

Appendix 3a: Animal ID 1 (Male) (n=6)

Age (weeks)	GBL (mm)	GBW (mm)	GBWT (mm)	GBV (mm³)
8	12.3	6.4	0.65	0.286
10	13.6	7.7	1.2	0.412
12	15.9	8.8	1.2	0.57
14	11.3	8.3	1.6	0.408
16	16.4	11.5	1.4	1.259
18	11.8	13	1	1.023
20	15.1	8.2	1.1	0.518
22	15.1	8.5	1.1	0.54
24	16.5	9.2	1.2	0.59
26	16.8	9.9	1.1	0.611
28	16.3	8.7	1.4	0.502
30	19.8	17.5	1	2.279
32	11.4	9	0.9	0.487
34	17.2	12.1	0.6	1.154
36	26.6	16.4	1	3.381
38	18.1	11	0.3	2.0264
40	24.8	16.3	0.8	2.366

Appendix 3b: Animal ID 2 (Male) (n=6)

Age (weeks)	GBL (mm)	GBW (mm)	GBWT (mm)	GBV (mm³)
8	11.9	6.1	0.8	0.121
10	13	8.5	1.6	0.166
12	11.9	5.6	1.2	0.419
14	13.9	16.4	2.2	1.704
16	15.2	13.3	1.9	1.377
18	24.2	13	2	1.807
20	12.7	11.5	1.3	0.643
22	15.8	13.3	1.3	2.07
24	18	14.1	1.4	2.01
26	17.9	13.5	1.3	1.648
28	16.5	8.6	1.42	0.51
30	20.8	17	1	2.391
32	19.3	12.8	1	1.147
34	17.9	12.5	0.7	1.192
36	28.1	17.4	1	3.528
38	19	11.5	0.3	2.124
40	25.8	16.9	0.8	3.501

Appendix 3c: Animal ID 3 (Male) (n=6)

Age (weeks)	GBL (mm)	GBW (mm)	GBWT (mm)	GBV (mm³)
8	11.1	6.6	0.7	0.156
10	12.8	7.1	1.3	0.325
12	21	6.5	1.3	0.712
14	15.7	8.4	1.9	0.505
16	17.7	9	1.6	0.923
18	24.5	18	1.6	3.751
20	12.1	17.1	1.5	0.951
22	15.8	13.9	0.9	0.879
24	17.7	15.2	2	1.905
26	18.6	14.2	0.7	1.682
28	18	16.5	1.4	2.543
30	18.9	12.1	0.7	0.854
32	32	18	0.9	3.154
34	13.6	8.5	0.7	0.548
36	34	16.4	0.9	4.064
38	22.2	14.9	0.7	2.488
40	23.3	16.4	0.4	2.034

Appendix 3d: Animal ID 4 (Female) (n=6)

Age (weeks)	GBL (mm)	GBW (mm)	GBWT (mm)	GBV (mm³)
8	8.6	3.4	0.51	0.232
10	9	7.1	0.9	0.306
12	12.8	13.1	1	2.125
14	11.4	10.5	1.9	1.329
16	26.4	12.8	1.5	2.268
18	16.8	12.1	1.9	0.91
20	13	15.6	1	1.05
22	9.3	9	0.9	0.613
24	20.1	13.6	0.9	1.866
26	10.5	9	1.1	0.989
28	12.1	9.3	1.3	0.469
30	21.2	17.3	1.1	2.429
32	27.1	15.8	0.9	2.3
34	18.8	13.2	0.7	1.252
36	29.1	18	1.1	3.639
38	20.4	12.4	0.4	2.278
40	27.9	18.3	0.9	3.773

Appendix 3e: Animal ID 5 (Female) (n=6)

Age (weeks)	GBL (mm)	GBW (mm)	GBWT (mm)	GBV (mm³)
8	8.1	3.9	0.62	0.148
10	9	4.3	1	0.171
12	14.2	11.8	1.3	0.925
14	16.4	14.6	1.7	1.915
16	14.5	10.2	1.9	0.987
18	17.7	13.1	1.3	2.102
20	14.6	20.7	0.9	0.939
22	9.3	8.7	0.7	0.473
24	17.7	8	1.9	0.656
26	18.6	11.5	0.4	1.388
28	22.4	9.3	1	1.383
30	24.8	62.5	1	2.747
32	16.4	11.5	1.1	0.679
34	18.8	13.1	0.7	0.929
36	30.1	14.6	0.7	2.383
38	30.9	18.3	3.5	0.125
40	11.6	11.5	0.4	0.653

Appendix 3f: Animal ID 6 (Female) (n=6)

Age (weeks)	GBL (mm)	GBW (mm)	GBWT (mm)	GBV (mm³)
8	13.75	7.15	0.95	0.159
10	14.9	7.8	1.5	0.318
12	4	3.2	2.5	0.092
14	13.8	8.1	1.7	0.521
16	16.7	9.4	1.2	1.42
18	20.6	9	1.6	0.557
20	24.2	11.5	1.9	1.322
22	17	12.4	0.9	0.835
24	11.8	7.5	0.7	0.486
26	17.4	12.1	0.3	0.874
28	17.3	9	1.1	0.856
30	18.3	13	1.2	0.872
32	24.8	13.3	1.3	1.362
34	7.1	5	0.5	0.116
36	23.4	10.5	0.4	1.292
38	22.6	15.5	0.3	1.697
40	12.4	12.1	0.7	0.762

Appendix 3g: Mean values and SEM of the ultrasound gall bladder dimension in male (n = 3) and female (n = 3) puppies.

Age (weeks)	GBL (mm)		GBW (mm)		GBWT (mm)		GBV (cm ³)	
	Male	Female	Male	Female	Male	Female	Male	Female
8	12 ± 0.3	10 ± 1.8	6.4 ± 0.2	4.8 ± 1.2	0.7 ± 0.04	0.69 ± 0.13	0.19 ± 0.05	0.18 ± 0.03
10	13 ± 0.2	11 ± 2.0	7.8 ± 0.4	6.4 ± 1.1	1.4 ± 0.12	1.10 ± 0.19	0.30 ± 0.07	0.27 ± 0.05
12	16 ± 2.6	10 ± 3.2	7.0 ± 0.9	9.4 ± 3.1	1.2 ± 0.03	1.60 ± 0.46	0.57 ± 0.08	1.0 ± 0.59
14	14 ± 1.3	14 ± 1.4	11 ± 2.7	11 ± 1.9	1.9 ± 0.17	1.80 ± 0.07	0.87 ± 0.42	1.3 ± 0.40
16	16 ± 0.7	19 ± 3.7	11 ± 1.2	11 ± 1.0	1.6 ± 0.15	1.50 ± 0.20	1.20 ± 0.14	1.6 ± 0.38
18	20 ± 4.2	18 ± 1.1	15 ± 1.7	11 ± 1.2	1.5 ± 0.29	1.60 ± 0.17	2.20 ± 0.81	1.2 ± 0.47
20	13 ± 0.9	17 ± 3.5	12 ± 1.7	16 ± 2.7	1.3 ± 0.12	1.30 ± 0.32	0.70 ± 0.13	1.1 ± 0.11
22	16 ± 0.2	12 ± 2.6	12 ± 1.7	10 ± 1.2	1.1 ± 0.12	0.83 ± 0.07	1.20 ± 0.46	0.64 ± 0.11
24	17 ± 0.5	17 ± 2.5	13 ± 1.8	9.7 ± 2.0	1.5 ± 0.24	1.20 ± 0.37	1.50 ± 0.46	1.0 ± 0.43
26	18 ± 0.5	16 ± 2.5	13 ± 1.3	11 ± 1.0	1.0 ± 0.18	0.60 ± 0.25	1.30 ± 0.35	1.1 ± 0.16
28	17 ± 0.5	17 ± 3.0	11 ± 2.6	9.2 ± 0.1	1.4 ± 0.01	1.10 ± 0.09	1.20 ± 0.68	0.9 ± 0.26
30	20 ± 0.5	21 ± 1.9	16 ± 1.7 ^a	31 ± 16 ^b	0.9 ± 0.10	1.10 ± 0.06	1.80 ± 0.49	2.0 ± 0.58
32	21 ± 6.0	23 ± 3.3	13 ± 2.6	14 ± 1.2	0.9 ± 0.03	1.10 ± 0.12	1.60 ± 0.80	1.4 ± 0.47
34	16 ± 1.3	15 ± 3.9	11 ± 1.3	10 ± 2.7	0.7 ± 0.03	0.63 ± 0.07	0.96 ± 0.21	0.77 ± 0.34
36	30 ± 2.3	28 ± 2.1	17 ± 0.3	14 ± 2.2	1.0 ± 0.03	0.73 ± 0.20	3.70 ± 0.21	2.4 ± 0.68
38	20 ± 1.2	25 ± 3.2	12 ± 1.2	15 ± 1.7	0.4 ± 0.13	1.40 ± 1.10	2.20 ± 0.14	1.4 ± 0.64
40	25 ± 0.7	17 ± 5.3	17 ± 0.2	14 ± 2.2	0.7 ± 0.13	0.67 ± 0.150	2.60 ± 0.44	1.7 ± 1.0

^{ab} Means in the same row with different superscript alphabets were significantly different (p < 0.05).

KEY: GBL (Gall bladder length), GBW (Gall bladder width), GBWT (Gallbladder wall thickness) GBV (Gallbladder Volume)

Appendix 3h: Overall mean values and SEM of the ultrasound gall bladder dimension in the puppies (n=6).

Parameters	GBL (mm)	GBW (mm)	GBWT (mm)	GBV (cm ³)
8	11 ±0.9	5.6±0.6	0.7 ±0.06	0.18±0.02
10	12 ±1.0	7.1±0.6	1.3 ±0.11	0.28±0.03
12	13 ±2.3	8.2±1.5	1.4 ±0.22	0.81±0.29
14	14 ±0.8	11 ±1.5	1.8 ±0.08	1.10±0.27
16	18 ±1.8	11 ±0.7	1.6 ±0.11	1.40±0.20
18	19 ±2.0	13 ±1.2	1.6 ±0.15	1.70±0.47
20	15 ±1.8	14 ±1.9	1.3 ±0.15	0.90±0.12
22	14 ±1.4	11 ±1.0	0.9 ±0.08	0.90±0.24
24	17 ±1.1	11 ±1.4	1.4 ±0.21	1.30±0.30
26	17 ±1.3	12 ±0.8	0.8 ±0.17	1.20±0.18
28	17 ±1.4	10 ±1.3	1.3 ±0.07	1.0 ±0.33
30	21 ±0.9	23 ±7.9	1.0 ±0.07	1.90±0.34
32	22 ±3.1	13 ±1.3	1.0 ±0.06	1.50±0.42
34	16 ±1.9	11 ±1.3	0.6 ±0.03	0.87±0.18
36	29 ±1.4	16 ±1.1	0.8 ±0.11	3.0 ±0.42
38	22 ±1.9	14 ±1.1	0.9 ±0.52	1.80±0.35
40	21 ±2.9	15 ±1.1	0.6 ±0.08	2.20±0.54

KEY: GBL (Gall bladder length), GBW (Gall bladder width), GBWT (Gallbladder wall thickness) GBV (Gallbladder Volume)

Appendix 4a: The mean and SEM of the portal vein diameter (PVD) and cross sectional area (CSA) in male (n=3) and female (n=3) Nigerian Indigenous puppies.

AGE (weeks)	PVD (mm)		CSA (cm ²)	
	Male	Female	Male	Female
8	3.2 ± 0.38	2.9 ± 0.12	7.8 ± 2.1	6.8 ± 0.55
10	4.4 ± 0.92	3.3 ± 0.10	16 ± 7.0	8.8 ± 0.62
12	2.7 ± 0.39	2.7 ± 0.27	7.6 ± 0.5	4.0 ± 0.61
14	3.6 ± 0.10	4.3 ± 0.89	8.3 ± 1.7	17 ± 3.40
16	3.1 ± 0.35	4.0 ± 0.53	11 ± 4.7	10 ± 0.38
18	2.3 ± 0.55	3.9 ± 0.35	6.7 ± 4.3	9.9 ± 1.40
20	4.1 ± 0.07	3.4 ± 0.27	12 ± 1.10	11 ± 2.10
22	4.1 ± 0.18	4.1 ± 0.47	12 ± 0.53	15 ± 2.90
24	4.3 ± 0.12	3.5 ± 0.48	14 ± 1.20	10 ± 2.80
26	2.8 ± 0.38	3.3 ± 0.40	5.0 ± 0.68	10 ± 0.51
28	3.7 ± 0.51	3.9 ± 0.42	10 ± 2.20	13 ± 3.0
30	4.7 ± 0.09	4.8 ± 0.12	18 ± 0.91	18 ± 0.75
32	3.3 ± 0.34	3.3 ± 0.29	7.4 ± 1.70	10 ± 0.68
34	2.3 ± 0.20	2.3 ± 0.09	3.7 ± 0.23	4.8 ± 0.56
36	2.5 ± 0.18	3.1 ± 0.15	6.0 ± 0.38	6.8 ± 1.60
38	2.1 ± 0.38	2.8 ± 0.43	2.7 ± 0.26	7.5 ± 1.10
40	3.1 ± 0.38	3.1 ± 0.36	9.1 ± 1.10	6.5 ± 1.80

^{ab} Means in the same row with different superscript alphabets were significantly different (p < 0.05).

KEY: PVD (portal vein diameter), CSA (cross sectional area).

Appendix 4b: The overall mean values and standard error of mean (\pm SEM) of the portal vein diameter (PVD) and Cross sectional area (CSA) of six (6) Nigerian Indigenous puppies.

Age (weeks)	Parameters	
	PVD (mm)	CSA (mm ²)
8	3.0 \pm 0.19	7.30 \pm 0.99
10	3.8 \pm 0.48	12.43 \pm 3.56
12	2.7 \pm 0.21	5.766 \pm 0.88
14	3.9 \pm 0.43	12.87 \pm 2.69
16	3.6 \pm 0.35	10.56 \pm 2.14
18	3.1 \pm 0.46	8.29 \pm 2.13
20	3.8 \pm 0.20	11.4 \pm 1.12
22	4.1 \pm 0.22	13.19 \pm 1.51
24	3.9 \pm 0.29	12.07 \pm 1.54
26	3.1 \pm 0.27	7.67 \pm 1.27
28	3.8 \pm 0.30	11.8 \pm 1.81
30	4.8 \pm 0.07	17.99 \pm 0.53
32	3.3 \pm 0.20	8.71 \pm 1.00
34	2.3 \pm 0.10	4.25 \pm 0.37
36	2.8 \pm 0.17	6.42 \pm 0.74
38	2.5 \pm 0.30	5.06 \pm 1.19
40	3.1 \pm 0.23	7.84 \pm 1.12

KEY: PVD (portal vein diameter), CSA (cross sectional area).

Appendix 5. Assay of serum ALT, AST and ALP

RESULTS OF BIOCHEMICAL ANALYSIS 4th MONTH

S/N	AST(IU/L)	ALT(IU/L)	ALP(IU/L)
1	10	17	72
2	23	24	71
3	36	28	89
4	15	29	80
5	23	26	74
6	21	23	168

RESULTS OF BIOCHEMICAL ANALYSIS 6TH MONTH

S/N	AST(IU/L)	ALT(IU/L)	ALP(IU/L)
1	19	38	56
2	22	27	76
3	27	21	89
4	13	19	91
5	20	30	71
6	17	21	90

RESULTS OF BIOCHEMICAL ANALYSIS 8TH MONTH

S/N	AST(IU/L)	ALT(IU/L)	ALP(IU/L)
1	18	31	63
2	26	24	81
3	24	22	94
4	28	22	70
5	33	25	88
6	19	19	89

RESULTS OF BIOCHEMICAL ANALYSIS 10TH MONTH

S/N	AST(IU/L)	ALT(IU/L)	ALP(IU/L)
1	21	28	75
2	23	24	71
3	36	28	95
4	30	20	63
5	21	19	103
6	32	17	97

Appendix 6: Ethical clearance certificate

**AHMADU BELLO UNIVERSITY, ZARIA**
DIRECTORATE OF ACADEMIC PLANNING & MONITORING

Vice Chancellor Prof. Ibrahim Garba, B.Sc. (Hons) Geology, M.Sc. (Mineral Exploration) ABU, Ph.D. Geology (London), D.I.C., F.S.M.G.S.
Director: Prof. M.F. Ishiyaku, D.Sc. (Hons) Botany (ABU), M.Sc. Plant Breeding (Unidos), Ph.D. Agriculture (University of Reading, U.K.), M.A.S.H., M.B.S.N.

Tel. Zaria + 234-069-581912 Fax, 234 (069) 550022 Telegram: UAHBELL0 Zaria e-mail: dapm@abu.edu.ng

Appl No.: ABUCAUC/2018/Veterinary Surg. & Radiology/007 13th June, 2018
Approval No: ABUCAUC/2018/007

Prof. C.A. Awasum
Department of Veterinary Surgery and Radiology,
Faculty of Veterinary Medicine,
Ahmadu Bello University,
Zaria.

Sir,

APPROVAL OF RESEARCH STUDY 'ULTRASONOGRAPHIC EVALUATION OF THE HEATOBILIARY SYSTEM AND PANCREAS OF NIGERIAN INDIGENOUS DOGS'

This is to convey the approval of the ABUCAUC to you for the aforesaid study domiciled in the Department of Veterinary Surgery and Radiology. The approval is predicated on the assumption that you shall maintain and care for the Experimental Animals as approved after the visitation of the Committee.

Monitoring of the Research by spot checks, invitations or any other means the Committee deems fit shall be undertaken at the convenience of the Committee.

This approval can and shall be revoked should a significant breach in the terms and condition of the approval occur. It is hence your responsibility to ensure that the agreed terms are maintained to the end of the Study.

The said approval shall be posted on the ABUCAUC Page on the University's website.
Note upon completion of the research, ethical clearance certificate will be issued.


U.D. Abdullahi
For: Chairman, ABUCAUC.

Cc. Director, DAPM
Director, IC & ICT
Dean, Veterinary Medicine
HOD, Veterinary Surgery and Radiology
Prof. C.A. Kudi